

POLITECNICO DI TORINO

Collegio di Ingegneria Meccanica, Aerospaziale, dell'Autoveicolo e della
Produzione

**Corso di Laurea Magistrale
in Automotive Engineering**

Tesi di Laurea Magistrale

MODELLING AND FUEL CONSUMPTION EVALUATION FOR A VARIABLE COMPRESSION RATIO SYSTEM



Relatori

Prof.ssa Daniela Misul

Prof. Giovanni Belingardi

Prof. Brian P. Sangeorzan

Candidato

Luca Barazzoni

A.A. 2017/2018

Acknowledgements

This work ends my studies at Politecnico di Torino, thus i want to thank everyone that helped and supported me during, not only the development of my thesis, but for the last two years, through advices, constructive criticism and observations.

I would like to say special thanks to Professor Daniela Misul and Professor Giovanni Belingardi, my advisors at Politecnico di Turin, for their disponibility and for the help that they offered me during my all thesis work. They continuously supported me even if the distance and the time zone seemed to be an insurmountable obstacle.

Then, i would like to thank my American advisors, Professor Brian Sangeorzan and Professor Daniel DelVescovo from Oakland University, for actively following my during my work and actively guiding me step by step in the development of my work. I would like to acknowledge also Asim Iqbal and Ken Hardman from FCA for their support to the project and all the precious advices that they gave me.

I would like to thank also Professor Sayed Nassar, responsible of Project Fiat-Chrysler at Oakland University, for the help and support that he gave me during my permanence in Michigan.

Finally, I must express my very profound gratitude to my family and to my friends for providing me with unfailing support and continuous encouragement throughout my years of study and through the process of researching and writing this thesis. This accomplishment would not have been possible without them. Thank you.

Abstract

Given increasingly stringent emission targets, engine efficiency has become of foremost importance. While increasing engine compression ratio can lead to efficiency gains, it also leads to higher in-cylinder pressure and temperatures, thus increasing the risk of knock. One potential solution is the use of a Variable Compression Ratio system, which is capable of exploiting the advantages coming from high compression ratio while limiting its drawbacks by operating at low engine loads with a high compression ratio, and at high loads with a low compression ratio, where knock could pose a significant threat. This study describes the design of a model for the evaluation of fuel consumption for an engine equipped with a VCR system over representative drive cycles and aims to analyze how its effectiveness is affected by various powertrain and vehicle parameters.

As an initial step, the compression ratio switching time was assumed to be constant independently from the engine working conditions. Successively, an engine speed-load dependent switch time was introduced based on reported values for a real VCR system. Then, the effect of transients during compression ratio changes was accounted for through the introduction of a worsening percentage applied to the mass of fuel injected. After that, the impact of the vehicle characteristics were evaluated by analyzing four vehicles, each belonging to a different segment. Separately, the influence of vehicle mass and final drive ratio were also analyzed. Also, simulations were run on five different drive cycles from the EPA and European Commission, in order to assess the role of the drive cycle characteristics on VCR performance. Finally, the possible advantages coming from the usage of a 3-stage VCR system were evaluated.

Results showed improvements between 0.3% and 0.7% in fuel economy over a static 10:1 compression ratio, depending on the selected vehicle and drive cycle. However, the analysis on the effect of transients demonstrated that an increase of about the 2% in the mass of fuel injected during changes in compression ratio can counter balance all the benefits coming from the adoption of a VCR system. Furthermore, it was showed that the VCR system effectiveness increased under lower power demand conditions where a higher compression ratio could be utilized over a wider range of the drive cycle. Thus, lighter vehicles and drive cycles with milder accelerations and lower vehicle speeds are more suitable for this type of system. Additionally, a 3-stage VCR system is more effective in terms of increasing fuel economy than a 2-stage VCR system.

Sommario

Dati obbiettivi di emissione crescentemente stringenti, l'efficienza del motore è diventata di primaria importanza. Accrescere il rapporto di compressione può portare a crescite di efficienza, portando però anche ad avere più alte temperature e pressioni in camera, accrescendo perciò il rischio di knock. Una possibile soluzione è l'utilizzo di un sistema a rapporto di compressione variabile, il quale è in grado di sfruttare i vantaggi ottenibili da un rapporto di compressione alto contemporaneamente limitando i suoi svantaggi operando a bassi carichi con un rapporto di compressione alto e, ad alti carichi con un rapporto di compressione basso, dove il knock costituisce una importante minaccia. Questo studio descrive lo sviluppo di un modello per il calcolo dei consumi di benzina per un motore equipaggiato con un sistema VCR sopra cicli di guida rappresentativi e punta ad analizzare come la sua efficienza è influenzata da vari parametri relativi al propulsore e al veicolo.

Come primo passo, il tempo necessario al cambio di rapporto di compressione è stato assunto costante indipendentemente dalle condizioni operative del motore. Successivamente, un tempo dipendente da velocità-carico motore è stato introdotto basandosi su valori misurati su un sistema VCR reale. Poi, l'effetto di transitori durante i cambi di rapporto di compressione è stato considerato attraverso l'introduzione di una percentuale peggiorativa applicata alla massa di benzina iniettata. Dopodiché, l'impatto delle caratteristiche del veicolo è stato valutato considerando quattro veicoli, ognuno appartenente ad un diverso segmento. Separatamente, l'influenza della massa del veicolo e del rapporto del differenziale è stata anche analizzata. Inoltre, simulazioni sono state eseguite su cinque diversi cicli di guida dell'EPA e della Commissione Europea, così da determinare il ruolo delle caratteristiche del ciclo di guida sulle performance di un sistema a rapporto di compressione variabile. Infine, i possibili vantaggi ottenibili dall'utilizzo di un sistema VCR a tre rapporti di compressione sono stati valutati.

I risultati hanno mostrato miglioramenti tra il 0.3% e il 0.7% nei consumi di carburante rispetto a un rapporto di compressione statico di 10:1, in base a veicolo e ciclo di guida scelto. Tuttavia, l'analisi sull'effetto dei transitori ha dimostrato che una crescita di circa il 2% nella massa di benzina iniettata durante cambi di rapporto di compressione può controbilanciare tutti i vantaggi derivanti dall'adozione di un sistema VCR. Inoltre, è stato dimostrato che l'efficacia di un sistema VCR cresce in condizioni di bassa potenza richiesta, dove un alto rapporto di compressione può essere utilizzato su buona parte di un ciclo di guida. Perciò, veicoli leggeri e cicli di guida con accelerazioni più gentili e velocità del veicolo più basse sono più adatti a questo tipo di sistema. In aggiunta, un sistema VCR a tre rapporti di compressione è più efficiente nel ridurre i consumi che uno a soli due rapporti di compressione.

Table of contents

Acknowledgements.....	3
Abstract.....	4
Sommario.....	5
List of figures.....	8
List of tables.....	11
Chapter 1	12
Introduction.....	12
1.1 The Effects of Increasing Compression Ratio.....	12
1.2 Variable Compression Ratio Engines.....	14
1.3 Types of Variable Compression Ratio Mechanisms	16
<i>1.3.1 Multi-link mechanisms</i>	<i>16</i>
<i>1.3.2 Variable Conrod Length Systems.....</i>	<i>18</i>
1.4 Objective of the dissertation	19
Chapter 2	20
Code inputs and assumptions.....	20
2.1 Engine maps.....	20
<i>2.1.1 Identification of the switch line.....</i>	<i>22</i>
2.2 Vehicle data.....	26
2.3 Drive cycle.....	28
2.4 Assumptions	33
Chapter 3	34
Evaluation of the engine operating points	34
2.1 Vehicle with continuously variable transmission	34
<i>3.1.1 Assumptions</i>	<i>34</i>
<i>3.1.2 Procedure.....</i>	<i>35</i>
3.2 Vehicle with discrete transmission.....	37
<i>3.2.1 Assumptions</i>	<i>38</i>
<i>3.2.2 Procedure.....</i>	<i>38</i>
3.3 Compression Ratio Switching logic	40
Chapter 4	46
Impact of the switching time	46
4.1 Impact of switching time on fuel consumption.....	46
4.2 Impact of the switch time on the number of incomplete switches	48
Chapter 5	50
Speed-Load Dependent Switch time.....	50

5.1	Implementation of a Speed-Load Dependent Switch time	50
5.2	Impact of a LDS time on fuel consumption	52
5.3	Impact of a SLDS time on the number of incomplete switches.....	53
5.4	Impact of the “switch multiplier”	54
Chapter 6		57
Impact of the transients.....		57
6.1	Methodology for the study of transients.....	57
6.2	Results.....	57
Chapter 7		61
Impact of the vehicle characteristics and of the drive cycle.....		61
7.1	Impact of the vehicle characteristics	61
7.2	Impact of the mass and of the final drive ratio.....	70
7.3	Impact of the drive cycle.....	73
7.4	Conclusions	75
Chapter 8		77
3-stage VCR.....		77
8.1	Engine maps.....	77
8.2	Results validation	84
8.3	Fuel savings: 2-stage VCR vs. 3-stage VCR.....	89
Conclusions		93
Future developments.....		94

List of figures

Figure 1 – Classification of CR mechanisms as described in [15]	16
Figure 2 – Scheme of the ore convenient multi-link mechanism layout [15].....	17
Figure 3 – Picture of a multi-link mechanism for a VCR system [16]	18
Figure 4 – Scheme of a variable length connecting rod [4].....	19
Figure 5 - Points at which data were collected for CR=10 pistons.....	21
Figure 6 - Points at which data were collected for the CR=11.4 pistons.....	22
Figure 7 - BSFC map for the 10 : 1 CR.....	23
Figure 8 - BSFC map for the 11.4 : 1 CR.....	23
Figure 9 – Plot of the differential map Δ BSFC and detail of the switching line	25
Figure 10 – Plot of blended fuel map	25
Figure 11 – Picture of the Ford Escape	26
Figure 12 – FTP speed profile	29
Figure 13 – HWFET speed profile	29
Figure 14 – US06 speed profile	30
Figure 15 – NEDC speed profile	30
Figure 16 – WLTP speed profile	31
Figure 17 – Cycle characterization for the CVT.....	32
Figure 18 – Cycle characterization for the MT.....	32
Figure 19 – Plot of the constant power lines over the BSFC map.....	37
Figure 20 – Detail of the changing BSFC during an instantaneous switch	43
Figure 21 – Detail of the BSFC changing during a non-instantaneous completed switch	44
Figure 22 - Detail of the BSFC changing during a non-instantaneous not completed switch.....	44
Figure 23 – Bar plot of the fuel economy for a vehicle equipped with a CVT for various VCR switching times (magenta), and two fixed CR cases (cyan)	47
Figure 24 – Bar plot of the fuel economy for a vehicle equipped with a DT for various VCR switching times (magenta), and two fixed CR cases (cyan).....	47
Figure 25 – Bar plot for the number of switches from HCR to LCR for the CVT for various switching times	48
Figure 26 – Bar plot for the number of switches from LCR to HCR for the CVT for various switching times	48
Figure 27 – Bar plot for the number of switches from HCR to LCR for the DT	49
Figure 28 – Bar plot for the number of switches from LCR to HCR for the DT	49
Figure 29 – Surface plot of the number of engine cycles required for a switch from low to high compression ratio as a function of engine speed and load, mapped to the baseline engine map discussed in Chapter 3.....	51
Figure 30 – Bar plot for the comparison of the consumptions for a vehicle equipped with a CVT using a SLDS time or a fixed time.....	52
Figure 31 – Bar plot for the comparison of the consumptions for a vehicle equipped with a DT using a SLDS time or a fixed time.....	52
Figure 32 – Bar plot of the number of switches from LCR to HCR for a CVT	53
Figure 33 – Bar plot of the number of switches from HCR to LCR for a CVT	53
Figure 34 – Bar plot of the number of switches from LCR to HCR for a DT	54
Figure 35 – Bar plot of the number of switches from HCR to LCR for a DT	54
Figure 36 – Bar plot of the number of switches for a varying switch multiplier for a CVT.	55
Figure 37 – Bar plot of the number of switches for a varying switch multiplier for a DT.....	56
Figure 38 – Bar plot for the evaluation of the impact of the transients, neglecting the increased FMEP, for a vehicle equipped with a CVT.	58

Figure 39 – Bar plot for the evaluation of the impact of the transients, including the increased FMEP, for vehicle equipped with a CVT.	58
Figure 40 – Bar plot for the evaluation of the impact of the transients, neglecting the increased FMEP, for a vehicle equipped with a DT.	59
Figure 41 – Bar plot for the evaluation of the impact of the transients, including the increased FMEP, for vehicle equipped with a DT.	59
Figure 42 – Bar plot for the fuel economy of the different vehicles, considering a CVT.	63
Figure 43 – Bar plot for the fuel economy of the different vehicles, considering a DT.	63
Figure 44 – Plot of the lines representing the relative fuel consumption of the LCR with respect to the VCR (red) and of the HCR with respect to the VCR (blue), considering a Ford Escape equipped with a CVT.	64
Figure 45 – Plot of the lines representing the relative fuel consumption of the LCR with respect to the VCR (red) and of the HCR with respect to the VCR (blue), considering a Ford Transit equipped with a CVT.	65
Figure 46 – Plot of the lines representing the relative fuel consumption of the LCR with respect to the VCR (red) and of the HCR with respect to the VCR (blue), considering a Ford Fusion equipped with a CVT.	65
Figure 47 – Plot of the lines representing the relative fuel consumption of the LCR with respect to the VCR (red) and of the HCR with respect to the VCR (blue), considering a Ford Fiesta equipped with a CVT.	66
Figure 48 – Plot of the lines representing the relative fuel consumption of the LCR with respect to the VCR (red) and of the HCR with respect to the VCR (blue), considering a Ford Escape equipped with a DT.	67
Figure 49 – Plot of the lines representing the relative fuel consumption of the LCR with respect to the VCR (red) and of the HCR with respect to the VCR (blue), considering a Ford Transit equipped with a DT.	67
Figure 50 – Plot of the lines representing the relative fuel consumption of the LCR with respect to the VCR (red) and of the HCR with respect to the VCR (blue), considering a Ford Fusion equipped with a DT.	68
Figure 51 – Plot of the lines representing the relative fuel consumption of the LCR with respect to the VCR (red) and of the HCR with respect to the VCR (blue), considering a Ford Fiesta equipped with a DT.	68
Figure 52 – Detail of the oscillations in the relative fuel consumption for the Ford Fusion.	69
Figure 53 – Differential map Δ BSFC with operating points corresponding to the peaks highlighted in Figure 52	69
Figure 54 – Bar plot for the fuel economy considering different test masses, considering a CVT and the FTP-75 as drive cycle.	71
Figure 55 – Bar plot for the fuel economy considering different test masses, considering a DT and the FTP75 as drive cycle.	71
Figure 56 – Bar plot for the fuel economy considering different final drive ratios, considering a CVT and the FTP-75 as drive cycle.	72
Figure 57 – Bar plot for the fuel economy considering different final drive ratios, considering a DT and the FTP-75 as drive cycle.	73
Figure 58 – Bar plot for the comparison between drive cycles, considering a vehicle equipped with a CVT.	74
Figure 59 – Bar plot for the comparison between drive cycles, considering a vehicle equipped with a CVT.	74
Figure 60 – Plot showing the location of the experimental points and of the additional points for the 10.5:1 CR.	78
Figure 61 – Plot showing the location of the experimental points and of the additional points for the 12.5:1 CR.	78
Figure 62 – Plot showing the location of the experimental points and of the additional points for the 14.5:1 CR.	79
Figure 63 – BSFC map for the 10.5:1 CR.	80
Figure 64 – BSFC map for the 12.5:1 CR.	81
Figure 65 – BSFC map for the 14.5:1 CR.	81
Figure 66 – Plot of the differential map Δ BSFC between LCR and MCR and detail of the switching line.	82
Figure 67 – Plot of the differential map Δ BSFC between LCR and HCR and detail of the switching line.	82

Figure 68 – Operating points of the engine over the performance map in the case of a 3-stage VCR, for a vehicle equipped with a CVT, driven along the FTP-75.	84
Figure 69 – Operating points of the engine over the performance map in the case of a 2-stage VCR, for a vehicle equipped with a CVT, driven along the FTP-75.	85
Figure 70 – Operating points of the engine over the performance map in the case of a 2-stage VCR, for a vehicle equipped with a CVT, driven along the FTP-75.	85
Figure 71 – Operating points of the engine over the performance map in the case of a 3-stage VCR, for a vehicle equipped with a CVT, driven along the US06.	86
Figure 72 – Operating points of the engine over the performance map in the case of a 3-stage VCR, for a vehicle equipped with a DT, driven along the FTP-75.	87
Figure 73 – Operating points of the engine over the performance map in the case of a 2-stage VCR, for a vehicle equipped with a CVT, driven along the FTP-75.	88
Figure 74 – Operating points of the engine over the performance map in the case of a 2-stage VCR, for a vehicle equipped with a CVT, driven along the FTP-75.	88
Figure 75 – Bar plot of the fuel economy for a vehicle equipped with a CVT for various VCR configurations (magenta), and three fixed CR cases (cyan) over the FTP-75.	89
Figure 76 – Bar plot of the fuel economy for a vehicle equipped with a CVT for various VCR configurations (magenta), and three fixed CR cases (cyan) over the US06.	90
Figure 77 – Bar plot of the fuel economy for a vehicle equipped with a DT for various VCR configurations (magenta), and three fixed CR cases (cyan) over the FTP-75.	91
Figure 78 – Plot of the engine operating points causing a decreased efficiency for the VCR system applied to a vehicle equipped with a DT.	92

List of tables

Table 1 – EPA vehicle characteristics	27
Table 2 – Gear ratios for the manual transmission equipped on the selected vehicle	27
Table 3 – Drive cycle characteristics	28
Table 4 – EPA vehicles characteristics.....	62
Table 5 – Gear ratios for the manual transmission equipped on the selected vehicles	62
Table 6 – Results of the analysis of the impact of the vehicle characteristics and of the drive cycles for vehicle equipped with a CVT	75
Table 7 – Results of the analysis of the impact of the vehicle characteristics and of the drive cycles for vehicle equipped with a DT	76

Chapter 1

Introduction

From the standpoint of resolving global environmental issues, government agencies worldwide are introducing new and more demanding legislations in an effort to reduce CO₂ and other pollutant emissions. While electrification of powertrain systems is one potential pathway for pollutant emissions reductions, these systems still face significant challenges with regard to widespread market penetration. Hence, in the interim, increasing engine efficiency continues to be one of the most relevant topics worldwide. In general, the easiest pathway towards increasing engine thermal efficiency in Spark Ignition (SI) engines is to increase the engine Compression Ratio (CR), though this approach comes with its share of challenges.

1.1 The Effects of Increasing Compression Ratio

Focusing on Spark Ignition (SI) engines, in order to better understand the effect of the CR on the engine efficiency, it is possible to look at the work of Smith and Heywood [1]. In their study, the ideal gas constant-volume combustion cycle was used as a framework to analyze the effect of the CR on the engine efficiency. The cycle consists of isentropic compression, constant volume heat addition, isentropic expansion and constant volume heat rejection processes. The efficiency of this cycle is influenced by the CR according to the relationship:

$$\eta_{f,ig} = 1 - \frac{1}{CR^{\gamma-1}} \quad (1)$$

where $\eta_{f,ig}$ is the indicated gross fuel conversion efficiency and γ is the ratio of specific heats. This model, even though it is based on an ideal cycle, gives a simple relationship between CR and engine efficiency, which shows that any increase in compression ratio will result in a corresponding increase in thermal efficiency.

Other studies have analyzed more in detail how, in a real engine cycle, the CR impacts on the efficiency. In particular, referring to the study of Ayala and Gerty [2], it is possible to decompose the gain in efficiency into heat transfer, pumping loss, expansion work, and burn duration effects. The absolute pumping loss increases at higher compression ratio, indeed with a higher thermal efficiency, in order to keep the same indicated mean effective pressure (IMEP), higher throttling has to be applied, to reduce the flow rate of both fuel and air. The absolute heat transfer also increases at higher compression ratio, due to higher in-cylinder temperatures, but also due to the higher surface area to volume ratio [3], decreasing the efficiency benefits. Burn duration effects are highly dependent on the air-fuel ratio λ , but the change in burn duration due to changes in compression ratio are negligible at stoichiometric operation. The majority of the thermal efficiency increase from increasing geometric

Introduction

compression ratio is due to the thermodynamic effect of having a larger volume expansion ratio. In addition, the usage of a high compression ratio can improve combustion stability, even under unfavorable thermodynamic conditions, for example in operation with high amount of residuals or high relative air fuel ratio, such that the idle speed can be reduced, valve overlap increased and, if applicable, lean burn limits extended [4].

The possibility of increasing the compression ratio is not limited only to SI engines, but is applicable also to Compression Ignition (CI) engines [4]. The compression ratio typically used for a passenger car diesel engine lies in the range between 15 and 16.5. A higher CR would result in better combustion stability and an attendant reduction in CO and HC emission in the low-load range, especially at low engine and ambient temperatures. However, a higher CR would result in less favorable particulate/NOX trade-off, which is due to a shorter ignition delay and a concomitant decrease in pre-mix combustion. In addition, there are significant disadvantages in respect of full load behavior, as the higher CR at a constant permissible peak pressure needs to be balanced by a later start of injection or a reduced boost pressure. Moreover, it is not possible to demonstrate a better start-up behavior of high-CR systems at very low ambient temperatures, since at these conditions, fuel ignition is largely due to the glow plug and not to the compression-induced heat, which is CR-dependent.

Regarding SI engines, the most important limitation related to an increase in CR is the onset of knock. Knock is fundamentally a chemical process, initiated by preflame reactions, leading to the rapid autoignition of the unburned charge. Increasing the CR at a given manifold pressure increases the maximum cylinder pressure and the temperature of the unburned mixture, increasing the likelihood of knock at high loads. Indeed there is a natural limit on how high the CR can be raised if an engine is to be operated at fixed compression ratio in all the speed and load ranges. Moreover, compression ratio has to be limited also to avoid severely compromised torque output [5].

Various methods, including variable valve timing and direct fuel injection, can be exploited to reduce knock insurgence. Retarding the intake valve closure reduces the effective compression ratio of the engine, while preserving the higher expansion ratio for improved efficiency, while Direct Injection (DI) takes advantage of the liquid fuel vaporization process to reduce the charge temperature. Another possible solution to avoid knock is to apply a spark retard from the Maximum Brake Torque (MBT) timing, however this will result in a reduction in engine efficiency [1]. The most effective enabling technology for the usage of a higher compression ratio are fuels with high octane rating, which is a measure of its resistance to knock.

The chosen type of fuel can have a profound impact on knock insurgence through its chemical properties. High octane gasoline and alcohol fuels have proven to be capable of reducing the knock probability through their molecular structure [6]. Furthermore, preflame reactions that typically lead

Introduction

to knock are highly depending on temperature, hence alcohol-based fuels, thanks to their high heat of vaporization, can exploit evaporative cooling, blocking at the root one knock onset mechanism [7]. Finally, the usage of a high compression ratio has a negative impact on pollutants emissions also for SI engines. Considering gasoline DI engines, increasing the CR increases the peak temperature during combustion, favoring the formation of NO_x . Increases in engine compression ratio can also increase HC emissions, since a higher CR increases the relative importance of crevice volumes which trap unburned hydrocarbons, and leads to a decrease in the temperature at the end of the expansion stroke, making the oxidation of unburned hydrocarbons in exhaust catalysts more difficult.

Thus, the large scale adoption of high octane fuels would allow automotive manufacturers to increase compression ratio and engine efficiency. Nevertheless, nowadays fuels with different octane ratings are used throughout the world. For example, in the United States, regular fuels have a content of 10% ethanol, while in Europe no fuel is alcohol added [8].

1.2 Variable Compression Ratio Engines

Given the absence of uniformity in fuel octane ratings across the world, other solutions for the usage of higher compression ratios in normal engines have to be found. Variable Compression Ratio (VCR) systems seem to be the perfect solution, being capable of coupling the advantages coming from the usage of a high compression ratio, while, at the same time, avoiding knock.

As mentioned before, the insurgence of knock limits the compression ratio that may be used in naturally aspirated engines, or the compression ratio and the boost level in turbocharged engines. If the compression ratio is chosen to avoid knock at high loads then, especially at light loads, the engine may lack torque [9]. The perfect solution would be being able to adapt the compression ratio to the working conditions, which is exactly what is done by VCR systems. These systems exploit a lower CR at full load to avoid knock and contemporarily lower the temperatures and the pressure at the end of the compression stroke, allowing the engine to operate at a more optimal combustion phasing than would be possible at a higher compression ratio, thus improving efficiency. A higher compression ratio is instead exploited at part load where, without knock limitations, and the subsequent need to retard combustion, it is always beneficial in terms of efficiency and thus fuel consumption [10].

Through the use of a VCR system, it is also possible to run an engine following the Atkinson cycle [9,11,12]. An Atkinson cycle engine is basically an engine in which the strokes have different lengths. In particular, the power and exhaust stroke are longer than the intake and compression strokes in order to try to achieve a pressure at the end of the power stroke equal to the atmospheric pressure. When this occurs, all the available energy has been obtained from the combustion process, allowing the Atkinson cycle engine to achieve a greater efficiency with respect to an engine following the Otto

Introduction

cycle. The main disadvantage of the Atkinson cycle with respect to the Otto cycle is a reduction in power density. Because of the shorter compression stroke, an Atkinson cycle engine is not able to trap as much fresh charge as an analogous Otto cycle engine.

A Variable Compression Ratio system is also perfectly suited to be used together with other technologies for emissions and fuel consumption reduction. In order to operate an engine at higher loads and thus higher efficiency, “downsizing and turbocharging” is becoming more and more popular. Between 1975 and 2013, average engine displacement decreased by about 39%, but average vehicle weight remained basically the same [13]. An obvious problem related to this technology is that the compression ratio has to be reduced to mitigate knock insurgence, indeed high boost levels and correspondingly increased engine loads are required to compensate for the power reduction due to the reduced displacement. It has been already discussed how VCR systems can mitigate the risks of knocking while maintaining high engine efficiency, and thus these systems are an obvious compliment to further engine downsizing and boosting, though naturally aspirated engines could also make use of VCR systems for efficiency gains.

Another technical challenge is related to the transient behavior of turbocharging systems. The greater the degree of downsizing, the lower the torque that the engine can develop under naturally aspirated operations, leading to greater dependency on intake boosting. Thus, short response time turbochargers are required for transient operations. From a technical point of view, it is difficult to design turbochargers for high power density engines, which demand minimal turbo lag and high torque output at low engine speeds. VCR systems could reduce the turbo lag under these conditions simply by reducing the compression ratio, such that the exhaust gas enthalpy available to the turbocharger turbine is increased. Reasoning in the opposite way, at high loads, a VCR system could be used to reduce the exhaust temperatures, making it possible to use more sophisticated and more delicate turbochargers [14]. A VCR system could also provide optimized catalyst control through parameters like the exhaust temperature. When the engine is cold, the VCR system could be used to increase exhaust gas temperatures at the expense of engine efficiency, thereby reducing the catalyst light off time [14].

1.3 Types of Variable Compression Ratio Mechanisms

The different types of variable compression ratio mechanisms can be classified by the component that actually varies the compression ratio [15]. The actuation can be obtained through components that are normally moving under steady state operations or through stationary components. Referring to **Figure 1**, the former types act on either the piston crown (a), the piston pin (b) or the crank pin (c) to adjust the compression ratio. The latter exert an action on parts such as the control shaft, often referred to as multi-link mechanisms, (d), the cylinder head (e), the structure supporting the crankshaft main bearings (f), or part of the combustion chamber (g). Of particular interests are multi-link mechanisms and systems with variable conrod length obtainable through an eccentrically mounted piston pin.

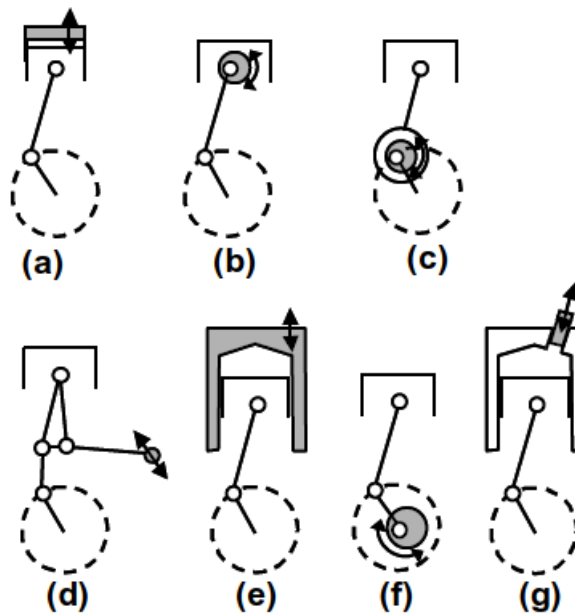


Figure 1 – Classification of CR mechanisms as described in [15]

1.3.1 Multi-link mechanisms

Multi-link mechanism systems offer the advantage of stable and continuous compression ratio control. This class involves the actuation of a component that is stationary during steady state operation of the engine, which simplifies the task of controlling its position. For this reason, these systems are often referred to as Continuous VCR, since they allow for the use of several CRs between two limit compression ratios. Multi-link mechanisms connect the piston pin and the crank pin through a series of multiple links. By varying the inclination of the different links it is possible to obtain a different stroke, and therefore a different geometric CR. These systems can assume different layouts, but the most convenient is the one showed in **Figure 2**. This particular layout is advantageous because, locating the control point at a downward oblique angle from the crankshaft, it can be applied

Introduction

to standard engines with few modifications, indeed there is no need for an increase in width of the engine.

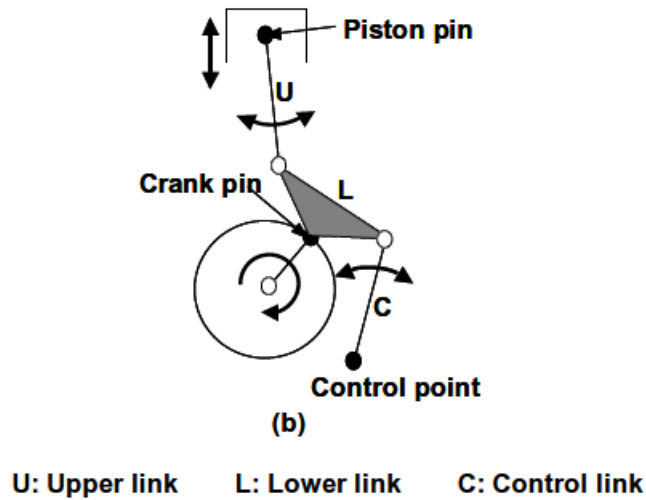


Figure 2 – Scheme of the ore convenient multi-link mechanism layout [15]

The piston pin and crankpin are connected by means of the upper and lower links. The control link motion is governed by a control shaft, which is provided with eccentric journals. The control link is connected at one end to the eccentric journal and at the other end to the lower link, which swings and revolves accordingly to the control shaft rotation. Because the lower link is connected to the crank pin, it pivots around the control pin while revolving together with the crank pin. The upper link is connected to the piston, so it pivots around the piston pin while moving up and down together with the piston. The control link pivots around the eccentric journal of the control shaft, moving together with the horizontal motion of the lower link, which, in turn, acts on the lower and upper link. Varying the inclination of angle of these two, which are connected to the piston pin and to the crank pin, it is possible to change the piston position at the Top Dead Center (TDC) and therefore the compression ratio. Moreover, by optimizing the link geometry, it is possible to minimize the 2nd order vibrations and to reduce the piston-side thrust load, making it possible to reduce the engine frictional losses associated with the extra linkages, thereby providing no net increase in frictional losses. However, the high cost and complexity of these systems are still a deterrent to its application on a broad scale. Despite this, several manufacturers have designed and tested multi-link mechanisms for compression ratio control, including the example shown in **Figure 3**, which shows a multi-link mechanism for a variable compression ratio engine developed by Nissan [16].

Introduction



Figure 3 – Picture of a multi-link mechanism for a VCR system [16]

1.3.2 Variable Conrod Length Systems

In general, all the systems that achieve a variable compression ratio through a variation of the conrod length require less modifications to the base engine architecture. In their study, Kleeberg and Tomazic [10] showed that, in principle, it is possible to incorporate a conrod with variable length in an engine with a bore of only 70 mm, without the need of extensive modifications. The main issue of this type of system is that the actuation force to vary the CR has to come from outside the system via some additional mechanism. The need to use some means of remote control, such as hydraulic pressure, makes it difficult to achieve stable control of the compression ratio in every cylinder. For this reason, these systems are not suitable to achieve a continuous CR control, hence they are normally referred to as 2-stage VCR, since they allow the engine to switch between only two discrete CRs [15].

Among all these systems, the one with variable connecting rod length by an eccentrically mounted piston pin is superior with regard to integration and production costs. Its working principle is well described in the work of Wittek and Tiemann [4]. The eccentric bearing is subject to a moment, generated by the combined action of gas forces and inertia forces, which allows for adjustment of the conrod length. No power consuming actuators are needed, providing a cost effective solution. The eccentric moment takes on positive as well as negative values during a combustion cycle, making adjustments in compression ratio in both directions possible. The moment acting on the eccentric is supported via linkages by hydraulic pistons, highlighted in **Figure 4**. The two support chambers are provided with a valve each to connect them to the oil circuit and with a check valve, which provides an open passage from the chamber to the crankcase. Thus, by discharging oil from a chamber, the corresponding piston will move downward in its support chamber. At the same time, the other support

Introduction

chamber is filled with oil, and the corresponding piston is pushed upward. The combined motion of the two pistons will lead the motion of the eccentric, which, by rotating, adjusts the length of the conrod. The adjustment process takes several working cycles to conclude; the number of cycles required for the adjustment depends on the operating point as well as the hydraulic resistance. The hydraulic resistance can be adjusted through orifices to be able to complete the change in length in the desired time. On the other hand, the adjustment time must not be too short, so as to avoid cavitation of oil at the check valve, or high impact loads on the support mechanism when the end stops are reached.

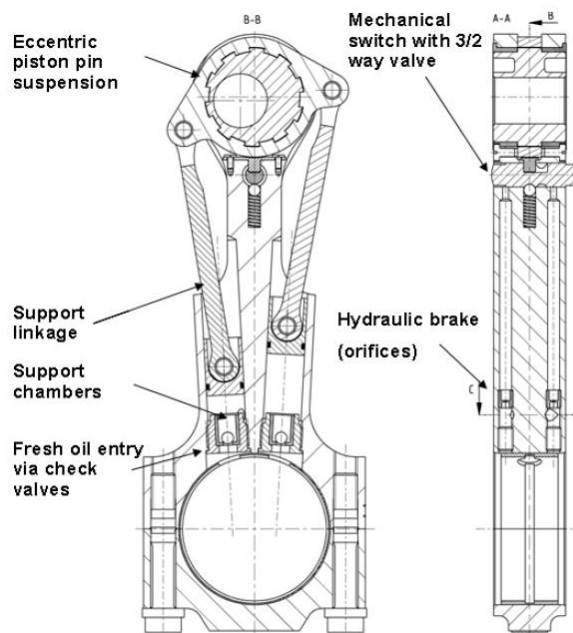


Figure 4 – Scheme of a variable length connecting rod [4]

1.4 Objective of the dissertation

The objective of the following work is the development of a *Matlab* model for the evaluation of fuel consumption and the possible advantages in fuel economy coming from the usage of a VCR system. The idea behind this dissertation is the need of the automotive industry to find a feasible solution to reduce emissions and fuel consumption of vehicles, without substantially increasing the cost to consumers, or reducing engine performance. At first, attention was focused on evaluating the impact of the compression ratio switch time, both on consumption and on the capability of achieving complete length adjustments. Then, the dependency of the results on vehicle characteristics and drive cycles was analyzed. Finally, the effects of the introduction of a 3-stage VCR was evaluated.

Chapter 2

Code inputs and assumptions

Before proceeding to explain the methodology followed by the code to determine the engine operating points and the outcomes of a switch in compression ratio, the following section discussed the necessary inputs and assumptions made in order to simplify the study.

In particular, in order to evaluate the fuel consumed during a given drive cycle, a Brake Specific Fuel Consumption (BSFC) map is a necessary input in order to determine the fuel consumption for every engine operating condition. The latter is a function of the power requested for motion, which, in turn, is related to vehicle data, such as the mass and the coast down coefficients, and to the speed profile of the chosen drive cycle.

2.1 Engine maps

In order to have realistic results, experimental engine maps obtained from Oak Ridge National Laboratory [17] were used to study the benefits of a VCR system. While these engine maps were not obtained using a VCR system, two different compression ratios were studied with the same engine and at the same operating conditions, and these two independent maps were then blended in the analysis, simulating a VCR system. The engine used to generate the experimental maps was a Ford EcoBoost 1.6 L 4-cylinder engine. The engine is a turbocharged gasoline DI engine equipped with variable cam phasing for both the intake and exhaust camshafts. The production model is equipped with pistons that result in a compression ratio of 10.1. Additional pistons were fabricated to produce higher CRs by reducing the piston bowl volume, which in turn reduces the total clearance volume of the cylinders. The modified pistons provided a compression ratio of 11.4.

The limited difference between the two compression ratios constituted the first obstacle to this study. Indeed, as reported in a study from Smith and Heywood. [1], the engine efficiency, and correspondingly the BSFC, continues to improve to 14:1 CR and beyond, though at a diminishing rate. Therefore, in practice it would be desirable for a VCR system to represent a much larger difference in compression ratio between the low and high extremes in order to maximize the potential fuel economy benefit. In particular, the cumulative efficiency increase from a CR increase can be evaluated through the following equation [1]:

Code inputs and assumptions

$$\Delta\eta_{CR} = -0.207\% \times (CR_{new}^2 - CR_{base}^2) + 6.44\% \times (CR_{new} - CR_{base}) \quad (2)$$

where $\Delta\eta_{CR}$ is the cumulative relative efficiency increase as a function of CR, whereas CR_{base} and CR_{new} are the compression ratios of the baseline engine and the new engine configuration. Regarding the engine mapping, the collection of data started at 1 *bar bmep* going up to the maximum *bmep* in increments of 1 *bar*. Data were collected at engine speed of 1000 *rpm*, 1500 *rpm*, 2000 *rpm*, 2500 *rpm* and 5000 *rpm* with additional points on the maximum torque curve between 3000 *rpm* and 5000 *rpm*. **Figure 5** shows the points at which data were collected for the production piston, whereas **Figure 6** shows the points at which data were collected for the CR=11.4 pistons.

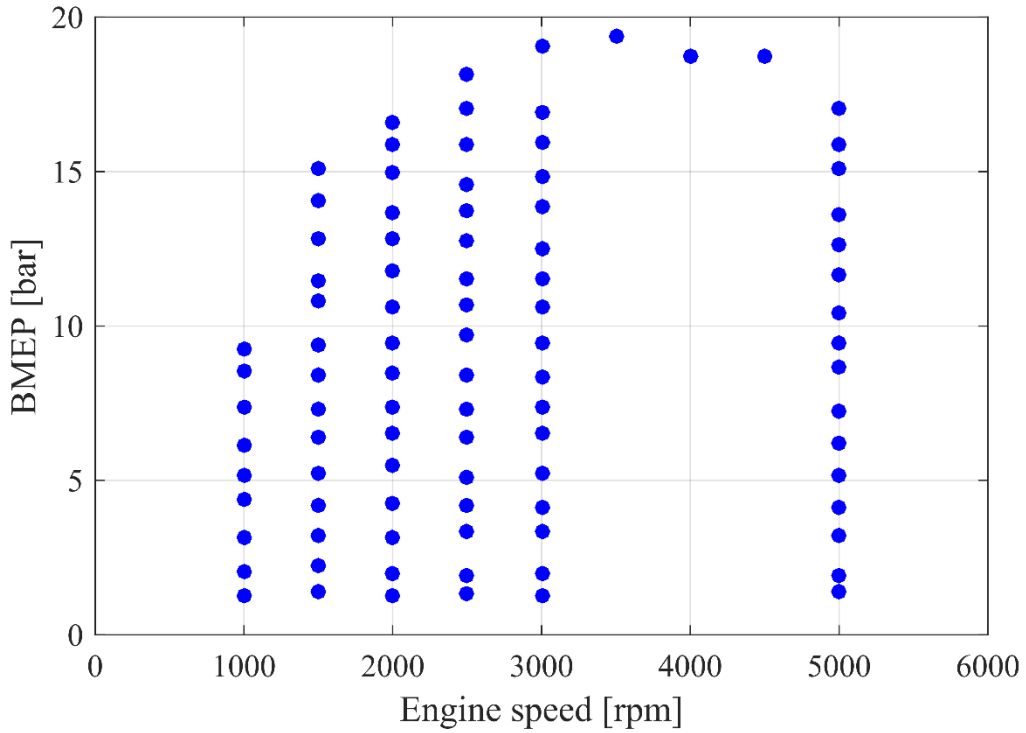


Figure 5 - Points at which data were collected for CR=10 pistons.

Code inputs and assumptions

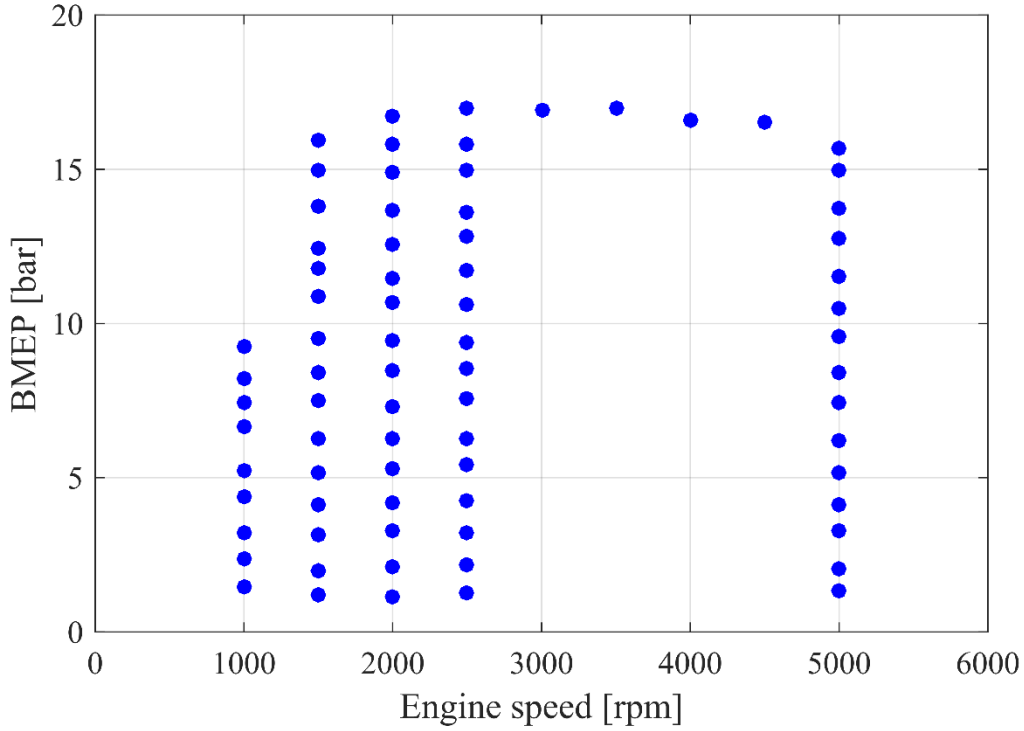


Figure 6 - Points at which data were collected for the CR=11.4 pistons.

For each engine operating condition, the BSFC was calculated based on experimental measurements of brake power output and fuel flowrate, thus allowing for the generation of a separate BSFC map for both of the compression ratios. **Figure 7** and **Figure 8** report the BSFC maps for the CR=10 and the CR=11.4 respectively.

2.1.1 Identification of the switch line

The engine maps for the two different compression ratio have to be merged in order to form a map for the engine operating with a representative variable compression ratio system. The new map has to blend the best characteristic of each compression ratio, to minimize the fuel consumed over a given drive cycle. In order to accomplish this, the following procedure is followed.

First, the difference, in terms of BSFC, between the two maps is computed:

$$\Delta BSFC = BSFC_{HCR} - BSFC_{LCR@WOT_{HCR}} \left[\frac{g}{kWh} \right] \quad (3)$$

Code inputs and assumptions

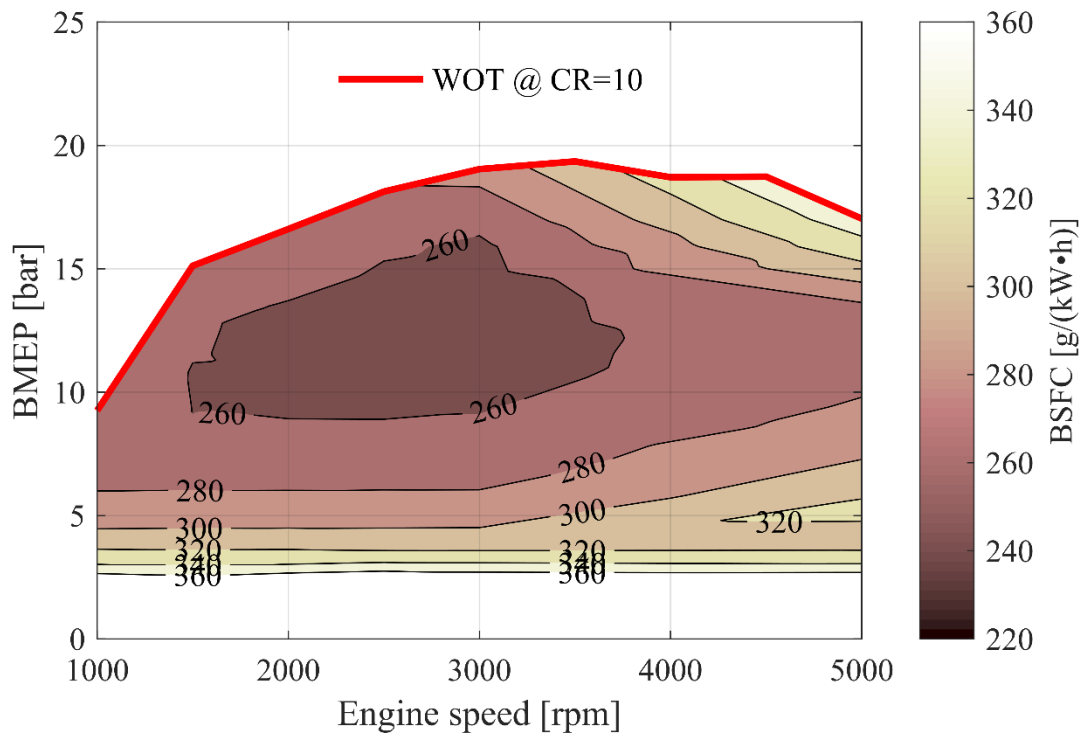


Figure 7 - BSFC map for the 10 : 1 CR

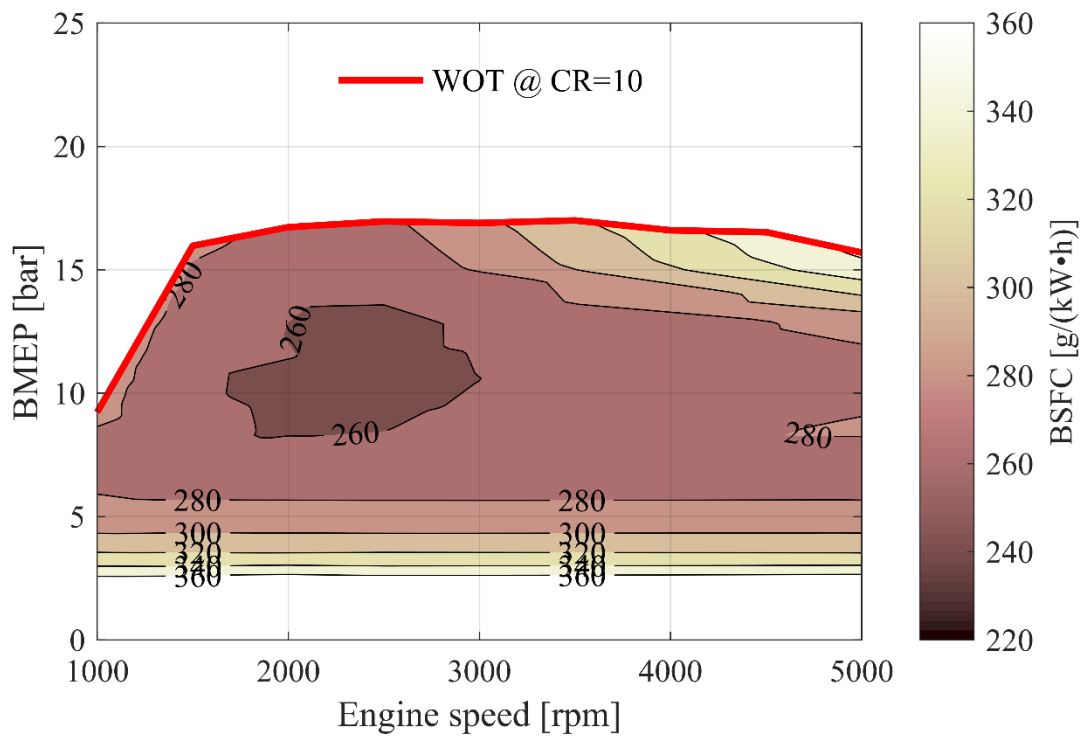


Figure 8 - BSFC map for the 11.4 : 1 CR

Code inputs and assumptions

where $\Delta BSFC$ is the differential map, $BSFC_{HCR}$ is the BSFC map for the high compression ratio and $BSFC_{LCR@WOT\ HCR}$ is the BSFC map for the low compression ratio but limited to the WOT curve of the HCR, since, obviously, the high compression ratio cannot be used above its knock limit.

$\Delta BSFC$ may assume positive or negative values, where positive values indicate that, in the considered point, $BSFC_{HCR}$ is higher than $BSFC_{LCR@WOT\ HCR}$ and so the low compression ratio configuration is better. If it is negative, the opposite is true, and so the HCR is better. Normally, a high compression ratio is characterized by increased efficiency, and thus better BSFC. This is true at low loads where the engine is not knock-limited. At high loads however, because of the aforementioned knock limitations, the low compression offers better BSFC values, and thus is preferred. Hence, two different operating areas for the two compression ratios can be identified. The line separating the two areas will be referred to as *Switching line* and it corresponds to the locus of the points where $\Delta BSFC$ is null (i.e. the transition in speed-load space above which the low-compression ratio is preferable):

$$\forall (bmep, n): \Delta BSFC(bmep, n) = 0 \quad (4)$$

Once the switching line has been obtained, it is possible to merge the two maps. Below the switching line, the map for the engine with a variable compression ratio will be identical to the one of the HCR, whereas above the switching line, it will be identical to the LCR one. A detail of the differential map and of the obtained switching line is reported in **Figure 9**, whereas the result of the merging of the two maps is reported in **Figure 10**.

Two important remarks have to be made at this point. First of all, in case of an incomplete switch (i.e. a switch in compression ratio which is longer than the time between simulated operating points), the length of the connecting rod is neither the one corresponding to the low compression ratio nor the one corresponding to the high compression ratio, thus the actual compression ratio of the engine would be some intermediate value between the two limits. Thus, under these conditions, the switching line would be different than that shown. In reality, the switching line is not fixed and it changes depending on the compression ratios involved in the switching procedure. In other words, the switching line reported in **Figure 9** is valid for an instantaneous compression ratio switch case. However, as will be discussed in the next chapter, in the case of an incomplete switch, measures will be taken to overcome this problem.

Code inputs and assumptions

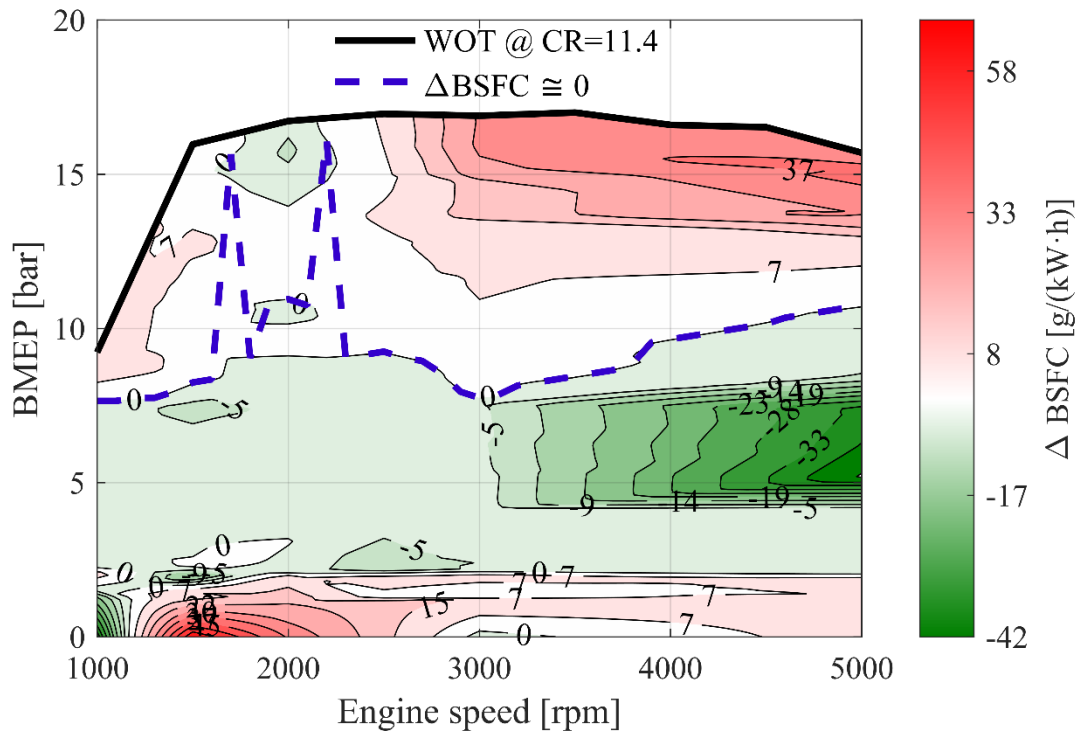


Figure 9 – Plot of the differential map $\Delta BSFC$ and detail of the switching line

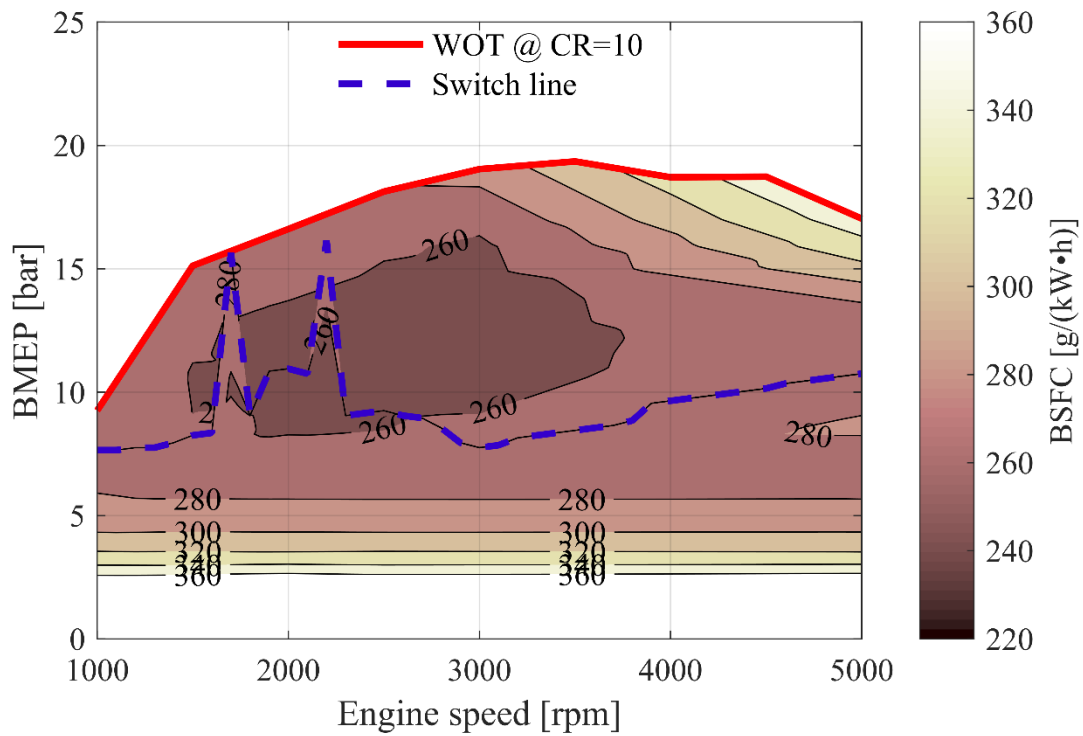


Figure 10 – Plot of blended fuel map

Code inputs and assumptions

As a second remark, as can be noticed by **Figure 9**, it is difficult to find just two distinct operating areas for the two compression ratios. In particular, for almost all the range of speed of the engine and for loads under 1 *bar*, the LCR is the compression ratio characterized by the best BSFC even if under the switching line the HCR should always be the better. In the same way, for an engine speed of 2000 *rpm* and a load ranging from 9 *bar* up to the WOT curve, the HCR is better than the LCR, even if the latter should be the optimal one in this area. These irregularities are due to the fact that the experimental data from which the maps for the two compression ratios have been obtained are not perfectly uniform and this led to the generation of spikes in the switching line. Additionally, the method by which the compression ratio was altered in the experimental campaign (i.e. changing this piston bowl shape) is not directly analogous to a VCR system, which would accomplish a change in compression ratio solely with an effective change in connecting rod length. Changes in the piston bowl shape may have resulted in significant differences in charge motion which could lead to unanticipated results in terms of BSFC.

However, since the procedure used to obtain the switching line is correct, no changes have been made on the switching line and, since the previously mentioned irregularities are located in points where normally the engine does not operate, an approximation has been made; beneath the switching line only the HCR can be used whereas above it only the LCR can be used.

2.2 Vehicle data



Figure 11 – Picture of the Ford Escape

Since the engine maps were obtained from a Ford EcoBoost 1.6 L 4-cylinder production engine, it was decided to, not only use a Ford vehicle, but to use a vehicle that is equipped with this particular engine. For this reason, the Ford Escape was chosen as a representative vehicle. This particular model was equipped with the previously mentioned engine from model

Code inputs and assumptions

years 2013 through 2016, thus the data for the 2014 model has been considered. All the necessary characteristics of the vehicle were found in the EPA Database [18], and are reported in **Table 1**:

Test mass [<i>lbs</i>]	4000
Target coefficient A [<i>lbf</i>]	28.01
Target coefficient B [$\frac{lbf}{mph}$]	0.5607
Target coefficient C [$\frac{lbf}{mph^2}$]	0.02308
Wheel radius [<i>in</i>]	13.6
Final drive ratio τ_f [–]	3.51
Model year	2014

Table 1 – EPA vehicle characteristics

1 st gear [–]	4.58
2 nd gear [–]	2.96
3 rd gear [–]	1.91
4 th gear [–]	1.45
5 th gear [–]	1.00
6 th gear [–]	0.75

Table 2 – Gear ratios for the manual transmission equipped on the selected vehicle

It is important to notice that the production vehicle was equipped either with a manual transmission or an automatic transmission, however, as it will be explained in the next chapter, a continuously variable transmission (CVT) will be considered in addition to the manual transmission.

Code inputs and assumptions

2.3 Drive cycle

The final input necessary to the code is the speed profile of the drive cycle that the vehicle is following. As will be explained later on, the code has no predictive capability, but the drive cycle speed profile is the only characteristic completely known a priori. In this study five different drive cycles will be considered. T.J. Barlow et al. [19] have collected during their work all the characteristics about the major drive cycles used worldwide, and their work will be used as reference for the characterization of the drive cycles used in this study. The main characteristics of each drive cycle are listed below:

	FTP-75	HWFET	US06	NEDC	WLTP
Distance [<i>mi</i>]	7.5	10.26	8.01	6.85	14.41
Duration [s]	1369	765	596	1180	1800
Average speed [<i>mph</i>]	21.2	48.3	48.4	20.88	28.89
Average acceleration [$\frac{ft}{s^2}$]	1.38	0.52	1.77	1.06	5
Maximum speed [<i>mph</i>]	62.32	60.02	80.3	74.56	81.59
Maximum acceleration [$\frac{ft}{s^2}$]	5.83	4.65	12.47	3.42	5.18
Idling time [s]	371	5	44	267	242

Table 3 – Drive cycle characteristics

Code inputs and assumptions

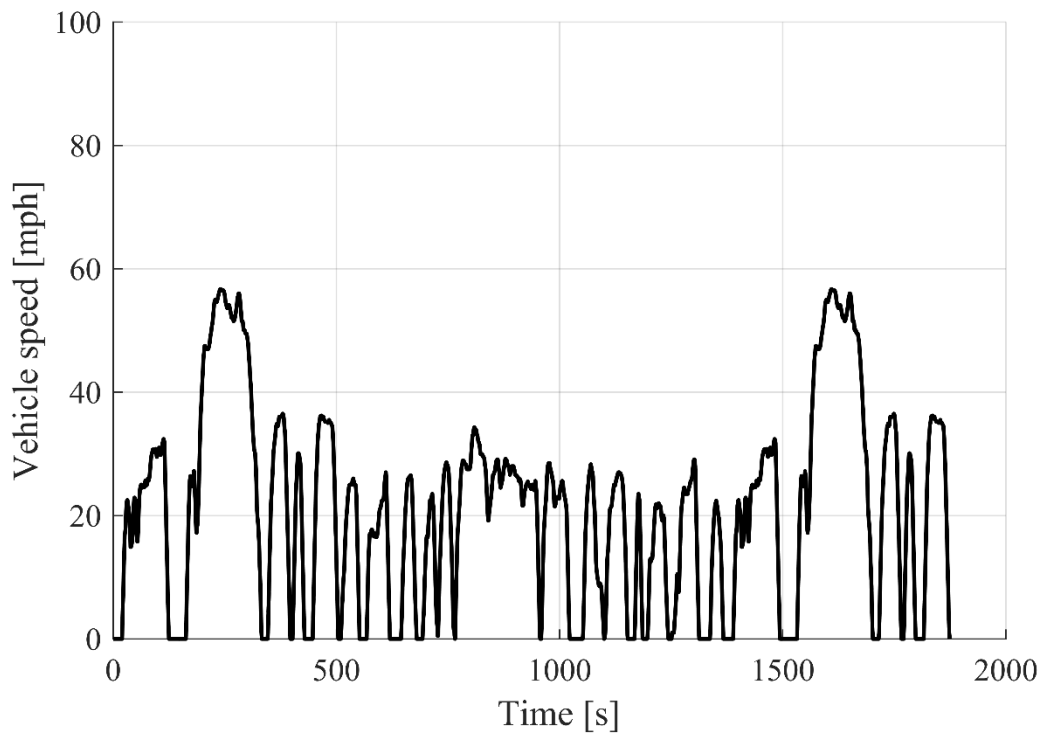


Figure 12 – FTP speed profile

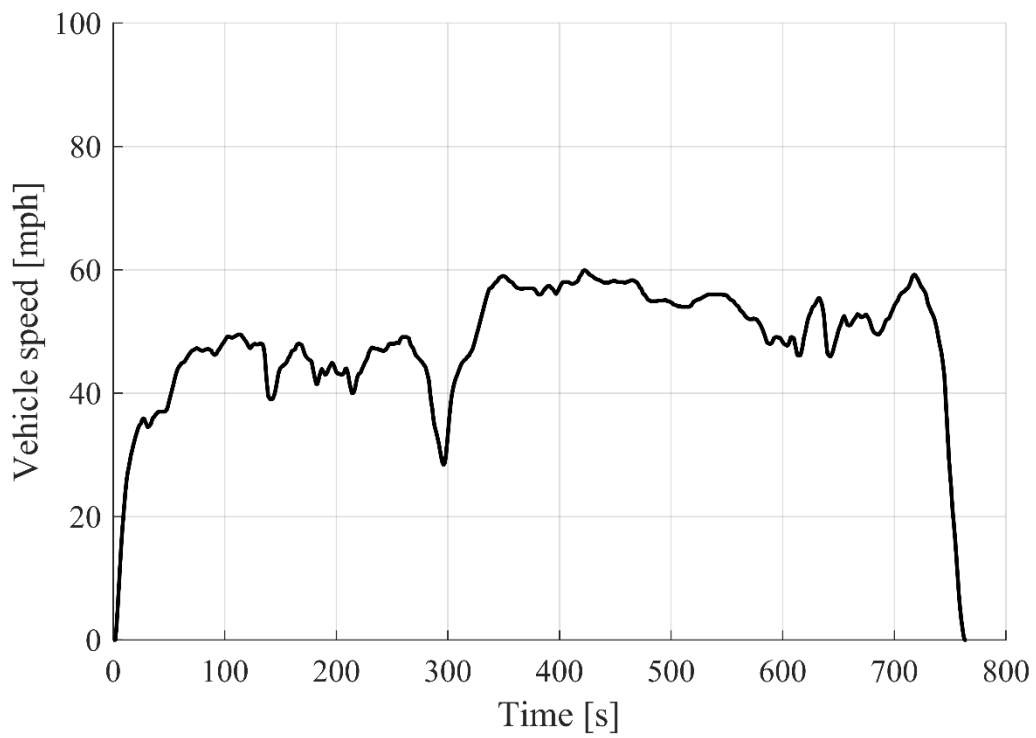


Figure 13 – HWFET speed profile

Code inputs and assumptions

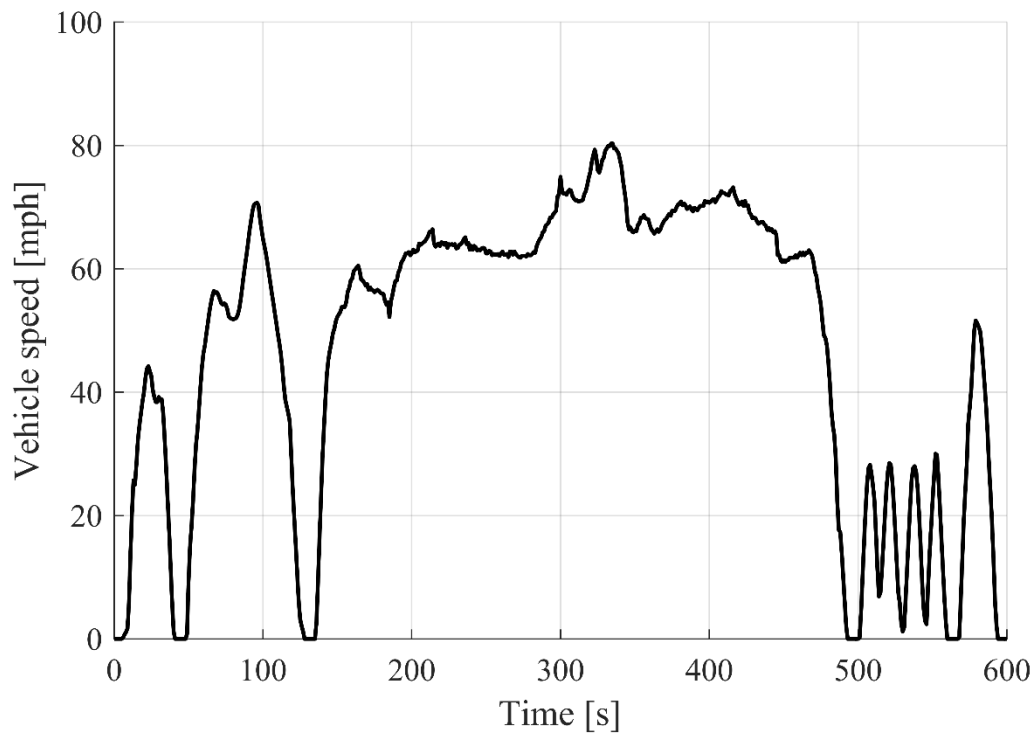


Figure 14 – US06 speed profile

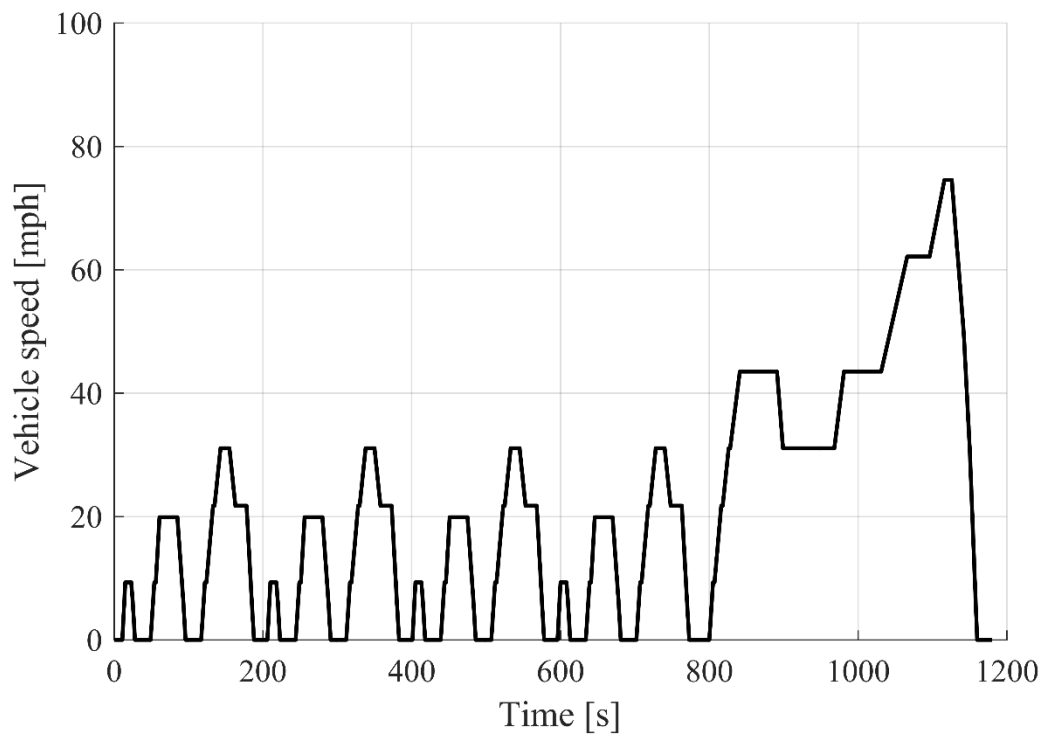


Figure 15 – NEDC speed profile

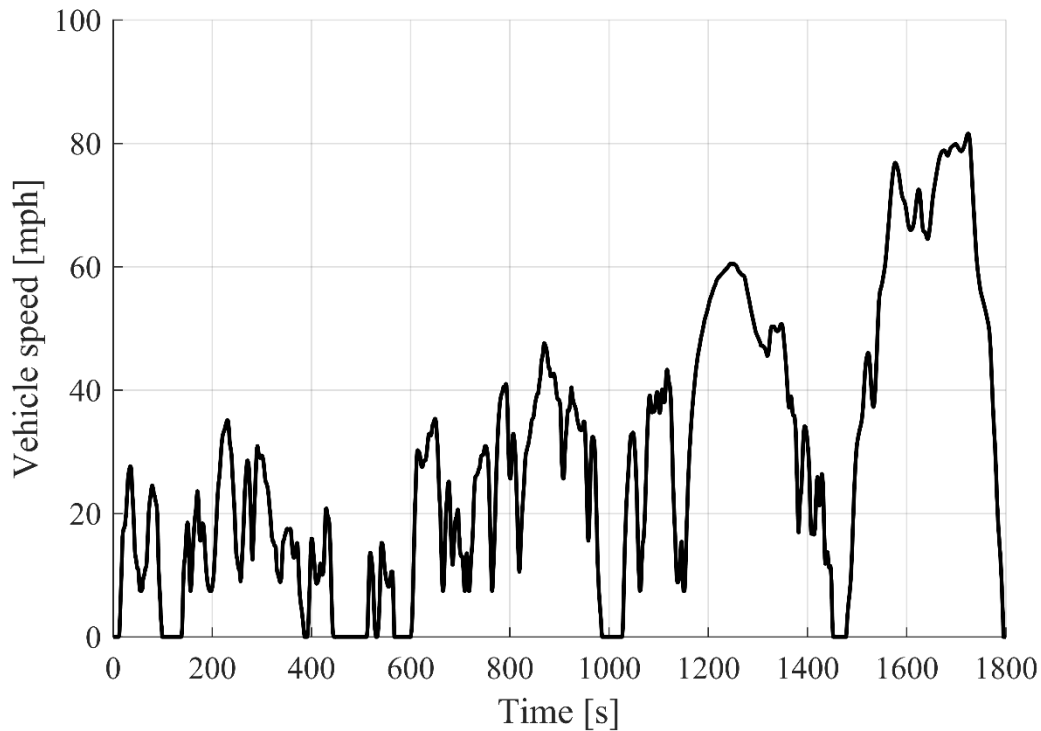


Figure 16 – WLTP speed profile

In order to give to the reader a better understanding of how the different drive cycles are shaped, from **Figure 12** to **Figure 16** the speed profile of the different drive cycles are reported. Moreover, a rough cycle characterization has been performed. For every drive cycle an average operating point has been computed. This point has been obtained simply doing the average of the engine speed and the engine load along the drive cycle, both for the CVT and the manual transmission. **Figure 17** and **Figure 18** show the results of this analysis for the CVT and manual transmission respectively. It can be noticed that the US06 is the drive cycle characterized by the highest power demand for both the transmissions. This result was predictable also looking at table **Table 3**, where the US06 is the drive cycle characterized by the highest average acceleration, the highest maximum acceleration and the maximum speed. These are all parameters that highly weigh on the power demand. Moreover, it can be seen that the average operating points for the manual transmission are slightly moved toward higher engine speeds with respect to the CVT. This is a direct consequence of the working principle of the manual transmission.

Code inputs and assumptions

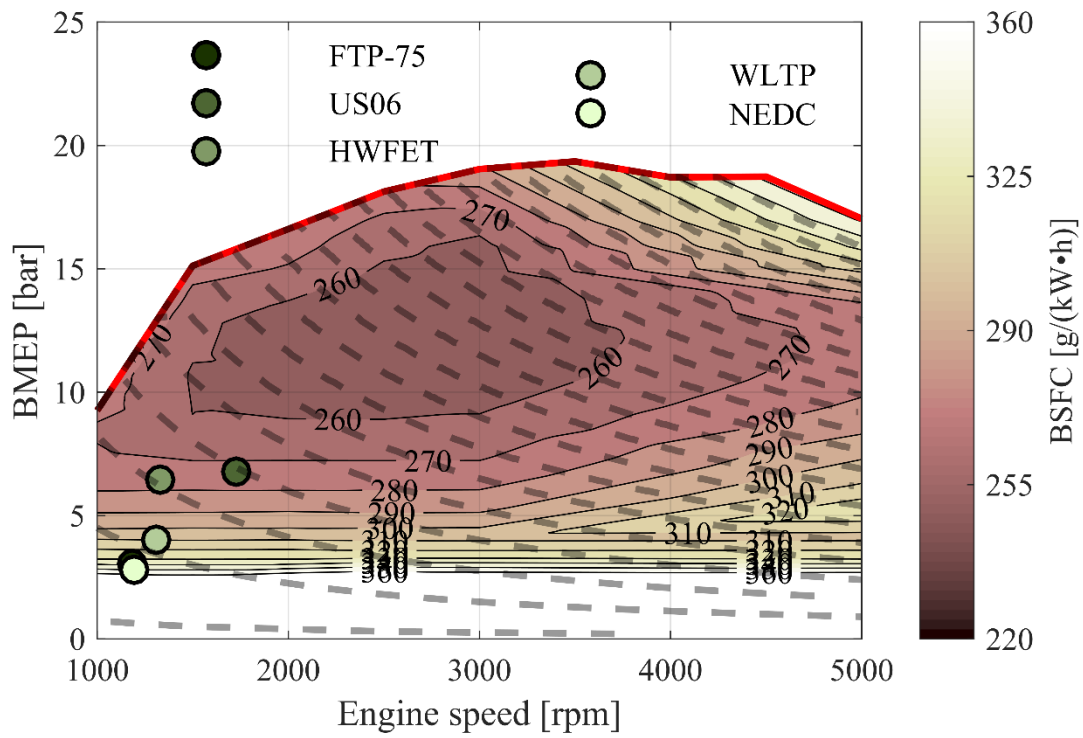


Figure 17 – Cycle characterization for the CVT

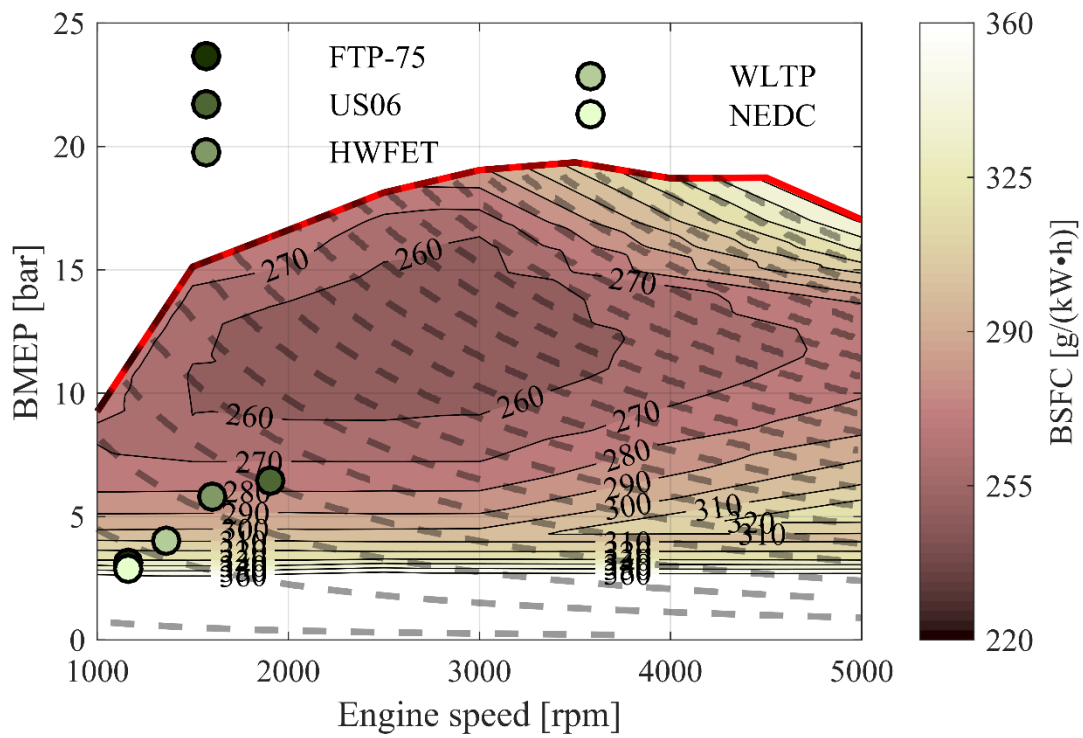


Figure 18 – Cycle characterization for the MT

2.4 Assumptions

Finally, it is necessary to list the assumptions that will be applied during the evaluation of the vehicle fuel consumption. It is important to notice that here the assumptions made for the modelling of the two different transmissions are not reported, they will be listed later.

The assumptions made are the following:

- The engine maps are obtained, as shown before, through testing performed at steady-state operating points, hence every type of transient is neglected.
- The change in compression ratio is assumed to have no impact on the engine dynamics, in other words, every transient related to a change in compression ratio is neglected.
- When the vehicle is idling, the fuel consumption is assumed to be null. This implies the vehicle is equipped with a sort of stop-start system.
- When the power demand is null or negative, e.g. when the vehicle is decelerating, the fuel injected is assumed to be null, implying a sort of fuel cut-off during deceleration.
- Changes in engine operating condition (i.e. engine speed/load) can occur instantaneously.

Chapter 3

Evaluation of the engine operating points

In order to evaluate the fuel consumption, and consequently the possible advantages coming from the usage of a VCR system, it is necessary to determine the engine operating points at every point along the selected drive cycle. The engine speed and load are obviously related to the transmission ratio used, and so the type of transmission equipped on the vehicle also influences the engine operating conditions. For this reason, in this study two different types of transmissions have been considered, a Continuously Variable Transmission (CVT), and a Discrete Transmission (DT) which could represent either a manual or automatic transmission.

2.1 Vehicle with continuously variable transmission

As a first approach, the vehicle is considered to be equipped with a Continuously Variable transmission. This choice has been made since the modelling of this transmission is less complex, thus allowing for the proper development of the logic behind the changes in compression ratio.

3.1.1 Assumptions

Since the aim of this study was to evaluate the potential improvements in fuel consumption of a VCR system compared to a fixed compression ratio engine, steps were taken to limit the influence of the transmission. While this simplification will lead to over-prediction in the modelled vehicle fuel economy, the relative change in fuel economy between a fixed CR engine and a VCR engine will still be captured. To this end, the CVT considered in the modelling work presented would be considered an ideal CVT, where the assumptions made about the transmission are as follows:

- The efficiency of the transmission is assumed to be constant and equal to 1.
- The number of transmission ratios that can be used is infinite.
- All gear shifts are instantaneous.
- All the engine transients consequent to a gearshift are neglected.
- No fuel penalties due to gearshifts have been considered.

Evaluation of the engine operating points

3.1.2 Procedure

The code presented in this work does not have any predictive capability, so the engine operating conditions are evaluated instant by instant. The inputs necessary to the calculation of engine operating conditions are simply the velocity profile of the drive cycle, completely known a priori, and all the vehicle data. At first, the vehicle acceleration is determined starting from the speed profile:

$$a_v = \frac{v_{t_{i+1}} - v_{t_i}}{t_{i+1} - t_i} \left[\frac{ft}{s^2} \right] \quad (5)$$

where a_v is the vehicle acceleration, $v_{t_{i+1}}$ is the vehicle velocity at time t_{i+1} and v_{t_i} is the vehicle velocity at time t_i . Once the acceleration is known, the resistant force can be evaluated through the target coefficients of the vehicle:

$$F_{res} = A + B \cdot v_{t_{i+1}} + C \cdot v_{t_{i+1}}^2 [lbf] \quad (6)$$

where F_{res} is the resistant force and A,B,C are the target coefficient of the chosen vehicle which lump together the effects of aerodynamic drag, rolling resistance, an driveline losses. Given the vehicle acceleration and the resistant action, it is possible to determine the power that the engine has to deliver to ensure that the vehicle follows the velocity profile:

$$P_{eng} = \frac{(F_{res} + a_v \cdot M_{app}) \cdot v_{t_{i+1}}}{1000 \cdot \eta} [kW] \quad (7)$$

where P_{eng} is the power that the engine has to deliver, M_{app} is the apparent mass of the vehicle, equal to $1.03 \cdot M_{eq}$ where M_{eq} is the equivalent test mass of the vehicle and η is the transmission efficiency. Given that the transmission efficiency η is assumed equal to unity, the following equality is true:

$$P_{eng} = P_{wheel} \quad (8)$$

where P_{wheel} is the power that must be present at the drive wheels to ensure that the vehicle exactly follows the drive cycle.

Evaluation of the engine operating points

Normally, knowing the transmission ratios and the speed profile followed by the vehicle, the engine speed is determined according to:

$$n = \frac{v_{t_{i+1}} \cdot 60}{2\pi \cdot R_0} \cdot \tau_{final} \cdot \tau_{gear} [rpm] \quad (9)$$

where n is the engine speed, R_0 is the wheel radius, τ_{final} is the final drive transmission ratio and τ_{gear} is the engaged gear transmission ratio. However, since the considered CVT is ideal, the number of transmission ratios usable is infinite and so, for a given vehicle velocity, the engine speed can assume any value, obviously remaining between some practical limits. In particular, the engine speed cannot drop below 1100 *rpm* and cannot go above 5000 *rpm*. The first limit is related to the working principle of a CVT, whereas the second one is imposed to avoid mechanical damage to the engine. For this reason, given the power demand, for every possible engine speed the load is determined according to:

$$bmep = 1200 \cdot \frac{P_{eng}}{n \cdot V_{tot}} [bar] \quad (10)$$

where $bmep$ is the brake mean effective pressure and V_{tot} is the engine displacement. Hence, for every requested power, a set of operating points able to deliver that power is evaluated. These points all together create the so-called constant power lines, characterized by a hyperbolic trend, as shown in **Figure 19**. At each of the operating points defining the iso-power line, a BSFC value is determined by interpolation of the BSFC map. Among these points, one will be characterized by a minimum BSFC, and this will constitute the optimal operating point for the engine, i.e. the operating point which minimizes the fuel consumption for the current power demand. In some cases it is possible that the operating point identified as optimal is not able to satisfy the power demand while staying beneath the Wide Open Throttle curve (WOT). For the CVT there is no other possibility than accepting to not meet the power demand, indeed the selected point is limited to the previously mentioned curve. Although, in order to reduce the gap between the power demand and the power actually produced by the engine, the latter is maximized by moving the point to the engine speed where the maximum power is developed. Moreover, since the BSFC map used is obtained by blending the maps relative to the two compression ratios, each possible operating point is associated with a BSFC value as well as a corresponding compression ratio. In other words, the optimal operating point is the combination of engine speed/load and compression ratio that yields the minimum BSFC for a given power demand while staying within the bounds of the engine map. At this point, the optimal operating point for the engine and the corresponding compression ratio will have been

Evaluation of the engine operating points

identified, and it is then necessary to understand whether a switch in compression ratio is necessary or not.

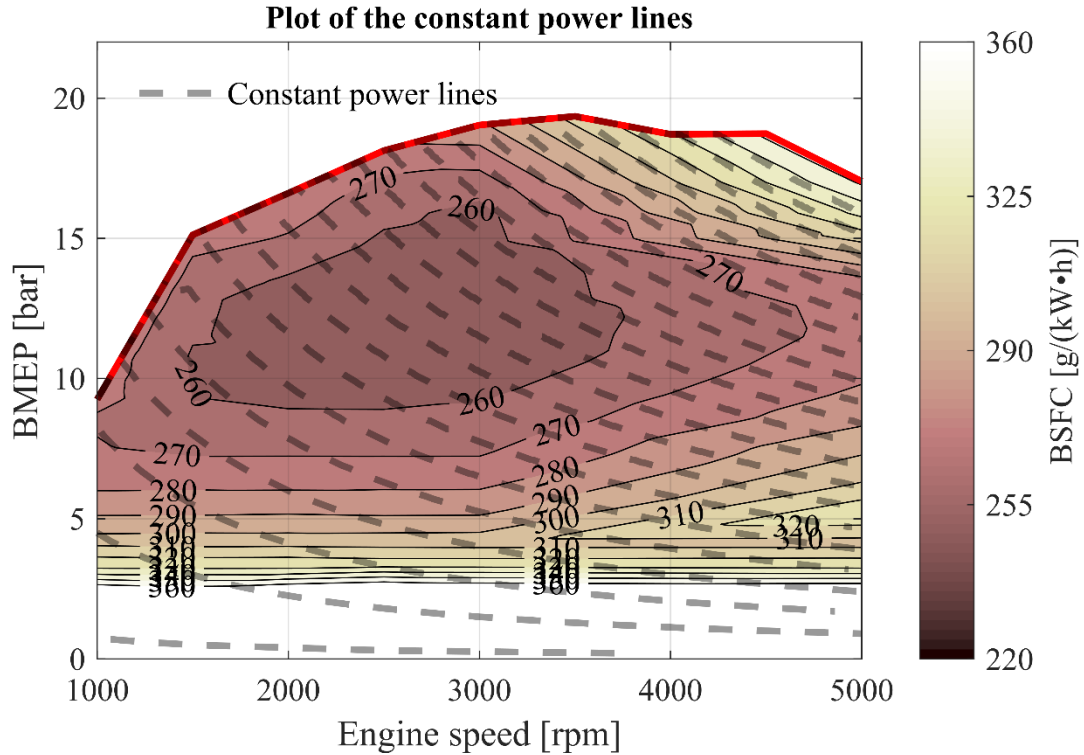


Figure 19 – Plot of the constant power lines over the BSFC map

3.2 Vehicle with discrete transmission

In order to have a case closer to reality, a second type of transmission has been considered. The transmission in question is a Discrete Transmission (DT). Derived from a manual transmission, it is not considered as such for multiple reasons. In particular, since no model for a human driver has been developed, the gearshift logic is based on the minimization of the fuel consumption. Every gearshift is performed in order to bring the engine to operate at the minimum BSFC possible for a certain power demand. While this obviously is not something that a human driver would explicitly be capable of, it is feasible that an automatic transmission or a computer controlled transmission could accomplish this given extensive calibration effort. As such, the discrete transmission presented in this work simply represents an idealized transmission with a set of discrete fixed gear ratios, contrasting the continuously variable transmission discussed in the previous section.

Evaluation of the engine operating points

3.2.1 Assumptions

As was the case for the CVT analysis, some assumptions have been made to minimize the impact of the transmission on the fuel consumption. The assumptions made are the following:

- The efficiency of each gear and of the final drive is assumed to be constant and equal to 0.94.
- All the gearshifts are instantaneous.
- All the engine transients consequent to a gearshift are neglected.
- No fuel penalties due to gearshifts have been considered.

3.2.2 Procedure

Also for the DT, the engine operating points are determined instant by instant, and the inputs necessary are the speed profile of the chosen drive cycle and the vehicle data. As for the CVT, the vehicle acceleration a_v and the resistance to motion F_{res} are evaluated according to Equations (1) and (2) respectively. Then, the power that the engine has to deliver is evaluated according to (3) but with a slight difference. In this case, the transmission efficiency is no longer equal to unity, and moreover, it is split in two components, the efficiency of the engaged gear and the efficiency of the final drive. Given this, equation (3) becomes:

$$P_{eng} = \frac{(F_{res} + a_v \cdot M_{app}) \cdot v_{t_{i+1}}}{1000 \cdot \eta_g \cdot \eta_{fd}} [kW] \quad (11)$$

where η_g is the gear efficiency and η_{fd} is the final drive efficiency. It is then possible to evaluate the engine speed n exploiting equation (5). However, the gear that will be engaged at the instant t_{i+1} is still not known, thus the engine speed corresponding to each gear is evaluated. Also in this case, some constraints on the speed that the engine can assume have to be imposed. First of all, the engine speed cannot drop under the engine idling speed, equal to 800 *rpm*, since this would potentially cause the engine to stall. Also, the speed must remain under the maximum allowable speed, equal to 5000 *rpm*, to again avoid mechanical damages to the engine. All the operating points characterized by an engine speed that does not lie in this interval are neglected. Then, knowing the power that the engine has to deliver P_{eng} , the *bmep* for each gear is evaluated through equation (6). Hence, as in the CVT case, a set of possible operating points for the engine at the time instant t_{i+1} is evaluated. However, differently from the continuously variable transmission, the possible points are different for each gear ratio. The BSFC value at each possible engine operating point is then determined by interpolating the BSFC map as is the case for the CVT. From this point onward there are no longer analogies

Evaluation of the engine operating points

between the CVT and the DT. Indeed, a gearshift logic specific to the DT case must be introduced.

As mentioned before, the gear to be engaged is selected because is the one that minimizes the fuel consumption for a certain power demand. However, since the transmission is derived from one of the manual type, some constraints have to be imposed in order for the gear selection process to be similar to the process that a real driver or automatic transmission would employ. The constraints imposed on potential gearshifts are the following:

A gearshift can be performed only if, when starting from a gear other than neutral, the engine speed before and after the gearshift are above a certain threshold. This threshold, equal to 1100 *rpm*, is imposed mainly for safety and NVH reasons. In particular, the engine speed after the gearshift has to be above the idling speed to keep the engine from stalling but, at the same time, less than the maximum engine speed to avoid mechanical damage. In practice, upshifts and downshifts may have different limits, but for the sake of simplicity, in this study the same limit was imposed on both up and down shifts.

- If the vehicle is decelerating, only downshifts can be performed. Downshifts do not have to be of only one gear; any gear lower than the current one can be engaged, including neutral.
- If the vehicle is at stand-still, the neutral gear must be engaged.
- If the vehicle is accelerating from stand still, it is mandatory to engage the first gear, no other gear is considered.
- If the vehicle is in neutral, accelerating but not from stand still, any gear may be engaged.
- During accelerations, upshifts of only one gear at a time can be performed.

Imposing these constraints, the set of possible operating points for the next time instant is further limited and it is possible to choose the optimal one by comparing the BSFC values associated to each one of those points, and selecting the minimum BSFC value, which then corresponds to a specific engine operating condition and gear ratio.

As in the CVT case, it is possible that the identified point is not capable of delivering the required power while staying under the WOT curve. However, in the DT case, it is possible that another point that has been previously neglected due to not adhering to the gearshift logic, is capable of delivering the requested power while staying in the engine map boundaries. In

Evaluation of the engine operating points

particular, gears lower than the optimal one are associated with higher engine speeds and so, at given the same requested power, lower loads. Thus, if the maximum engine speed is not exceeded and the engine *bme_p* is under the WOT limit, the first gear down from the one previously identified as optimal is chosen as new optimal gear and the operating point associated to it is selected as next operating point. If this is not sufficient, the operating point is simply limited to the WOT curve following the same procedure explained for the CVT. Finally, as in the CVT, the corresponding compression ratio is evaluated, making it possible to understand if a switch in compression ratio is necessary.

3.3 Compression Ratio Switching logic

At first, it is necessary to mention that there is no difference in the logic behind a change in compression ratio between the CVT and the DT. Moreover, it is necessary to differentiate between:

- Actual compression ratio, which is the compression ratio actually used by the engine at a given instant in time, it can vary in a range from 10 to 11.4.
- Optimal compression ratio, it is the compression ratio that the engine should ideally use to minimize fuel consumption, it can be either 10 or 11.4. It may differ from the actual one since there is the possibility of incomplete switches.

As mentioned for both the CVT and the DT, the optimal operating point for the next time instant t_{i+1} is identified along with its corresponding compression ratio. This compression ratio constitutes the optimal compression ratio for the time instant t_{i+1} . By comparing the actual compression ratio at time instant t_i to the optimal compression ratio at time instant t_{i+1} , it is possible to understand if a switch in compression ratio is necessary. If the actual and optimal compression ratios are identical, then there is no need to change compression ratio, and the engine will actually operate at the optimal operating point without requiring a switch. However, if the two compression ratios are not identical, this implies that a change in compression ratio is necessary.

In order to determine the outcome of the switching procedure, the operating conditions of the engine over the duration of the switch are considered constant and equal to the optimal ones. In other words, the engine operating condition (speed/load) is defined as that which minimizes BSFC at the target compression ratio, and does not necessarily correspond to the optimal BSFC

Evaluation of the engine operating points

condition for a given power demand at the current compression ratio. This implies that the engine operating condition changes instantaneously at the start of a switch, and does not necessarily follow a minimum BSFC path as it traverses the range of compression ratio.

The first step in the switch procedure is to evaluate the compression ratio at the end of the switch, indeed, as mentioned before, depending on the amount of time required to switch compression ratio, the switch may not be completed within a single simulation time step. To have a complete switch, a certain number of engine cycles is required and, depending on its rotational speed, the engine may or may not be able to achieve this number in a single time step. Thus, different scenarios can take place:

- The previous switch in compression ratio has been completed and the engine is capable of completing more cycles than necessary to have a complete switch; the compression ratio at the end of the switching procedure is equal to the optimal one.

$$CR_{@t_{i+1}} = CR_{opt@t_{i+1}} \quad (12)$$

where $CR_{@t_{i+1}}$ is the actual compression ratio at the time instant t_{i+1} and CR_{opt} is the optimal compression ratio for the same time instant.

- The previous switch in compression ratio has been completed and the number of cycles executed by the engine is lower than the one necessary to have a complete switch; the procedure will not be completed and the compression ratio at its end will be determined through:

$$CR_{@t_{i+1}} = CR_{@t_i} + \left(CR_{opt@t_{i+1}} - CR_{opt@t_i} \right) \cdot \left(\frac{cyc_{interval}}{cyc_{complete}} \right) \quad (13)$$

where $CR_{opt@t_i}$ is the optimal compression ratio at the time instant t_i , $cyc_{interval}$ is the number of engine cycles in a single time step and $cyc_{complete}$ is the number of engine cycles necessary to have a complete switch.

- The previous switch in compression ratio was not completed, and $CR_{opt@t_i} = CR_{opt@t_{i+1}}$ thus, the switch has to continue in the same direction. If the engine is capable of completing the number cycles required to accomplish a complete switch in a single time step, the compression ratio at the end of the switching procedure is evaluated through equation (8). If instead, it is not able to achieve such number of

Evaluation of the engine operating points

cycles, the compression ratio at the end of the switching procedure is evaluated through (9).

- The previous switch in compression ratio was not completed and $CR_{opt@t_i} \neq CR_{opt@t_{i+1}}$. This means that the switching procedure has to be reversed. Also in this case there are two possibilities. If the engine is capable of completing the requisite number of cycles in a single time step, the switching procedure will be completely reversed and so the compression ratio at the end of the procedure will be evaluated through equation (8). If not, the compression ratio will be stuck to an intermediate level evaluated through equation (9).

Once the compression ratio at the end of the switching procedure $CR_{@t_{i+1}}$ is known, it is possible to evaluate the BSFC at the end of the switching procedure through a linear interpolation of the two BSFC maps at the given engine operating condition:

$$BSFC_{@t_{i+1}} = \left| \left(\frac{CR_{@t_{i+1}} - LCR}{HCR - LCR} \right) \cdot (BSFC_{HCR} - BSFC_{LCR}) + BSFC_{LCR} \right| \quad (14)$$

where $BSFC_{@t_{i+1}}$ is the BSFC at the end of the switching procedure, LCR and HCR are the high and low compression ratio respectively, $BSFC_{HCR}$ is the BSFC value associated to the chosen operating point obtained entering in the HCR map and $BSFC_{LCR}$ is the BSFC value associated to the chosen operating point obtained entering in the LCR map. At this point, it is necessary to evaluate how the BSFC changes throughout the switching procedure. In order to do that, it is at first necessary to determine the BSFC at the start the switching procedure. Indeed, the switching procedure will not start from $BSFC_{@t_i}$, that is the BSFC at which the engine is operating at the time instant t_i , since the operating conditions have changed. For this reason, the starting BSFC is evaluated according to:

$$BSFC_{start} = \left| \left(\frac{CR_{@t_i} - LCR}{HCR - LCR} \right) \cdot (BSFC_{HCR} - BSFC_{LCR}) + BSFC_{LCR} \right| \quad (15)$$

This equation is almost identical to equation (10), the only difference is that $CR_{@t_i}$ is the actual compression ratio at the time instant t_i , hence at the start of the switching procedure. Now, two cases can be identified:

1. $cyc_{complete} = 0$, which constitutes the best case possible, implying an instantaneous switch in compression ratio. Under this condition, the BSFC, starting

Evaluation of the engine operating points

from $BSFC_{start}$, will not change for a time equal to the control delay, that is the time physically needed for the system to start to elongate the connecting rod, to instantaneously pass to the final value $BSFC_{@t_{i+1}}$, that will be equal to the optimal one, since no incomplete switches are possible under these conditions. **Figure 20** shows the typical trend of the BSFC over time during this type of switch.

2. $cyc_{complete} \neq 0$. In this case the BSFC is assumed to linearly change from $BSFC_{start}$ to $BSFC_{@t_{i+1}}$. To determine the BSFC at every instant of the switching procedure, it is divided in smaller time steps of 0.01 s. Furthermore, under these conditions, a switch can be completed or not, so it is possible that the optimal BSFC is never reached. The trend followed by the BSFC during these two cases is reported

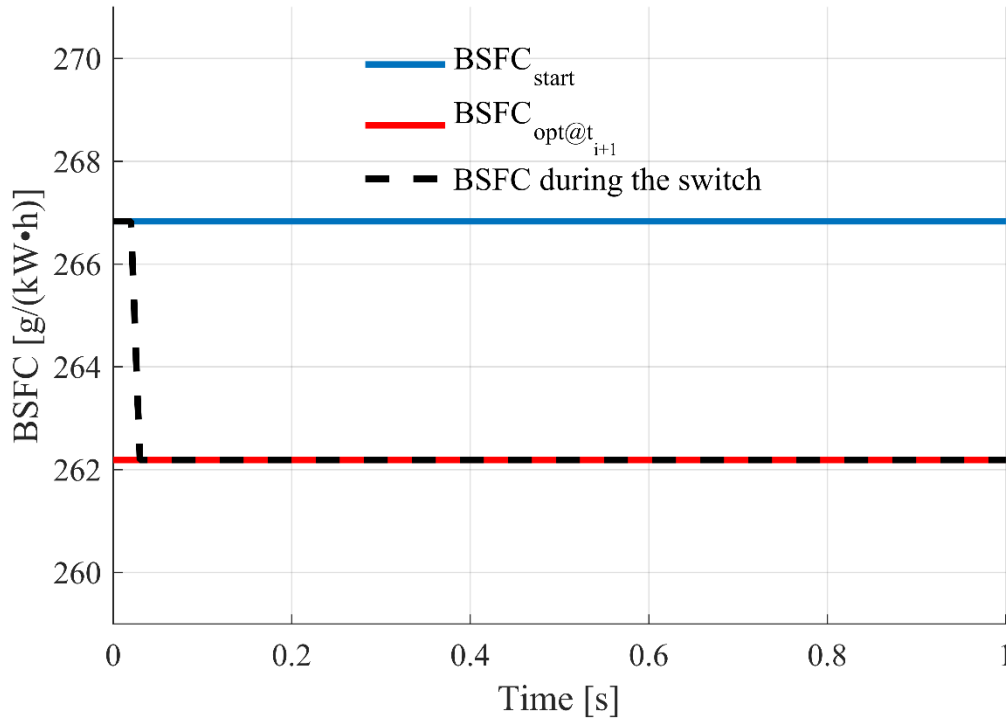


Figure 20 – Detail of the changing BSFC during an instantaneous switch
in **Figure 21** and **Figure 22** which show a completed but not instantaneous switch
and an incomplete switch respectively.

Evaluation of the engine operating points

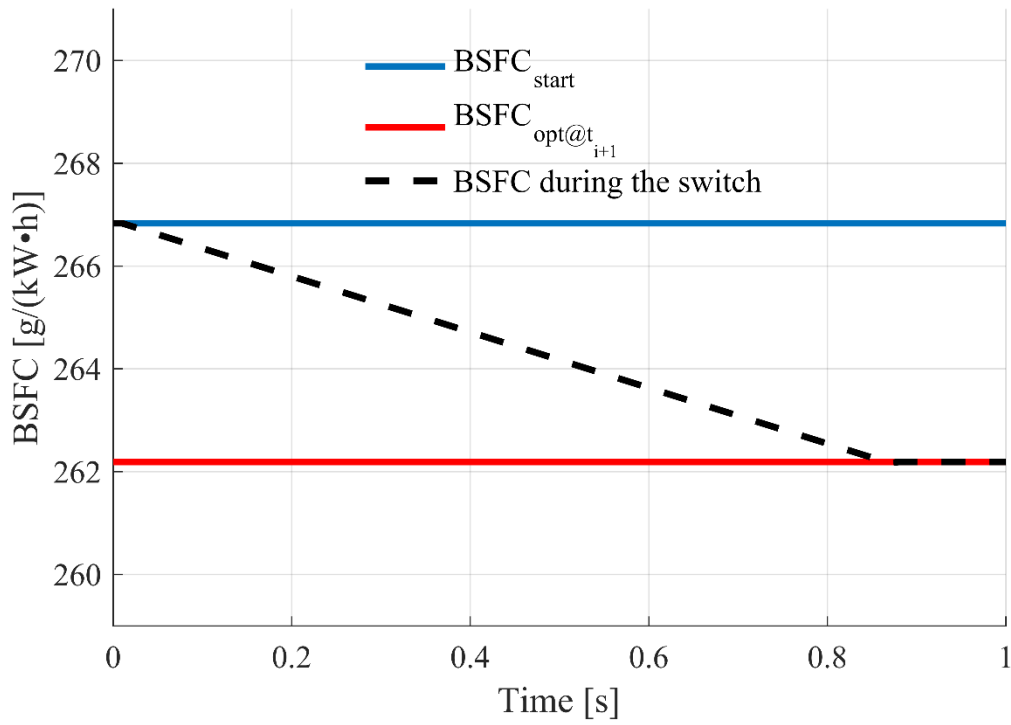


Figure 21 – Detail of the BSFC changing during a non-instantaneous completed switch

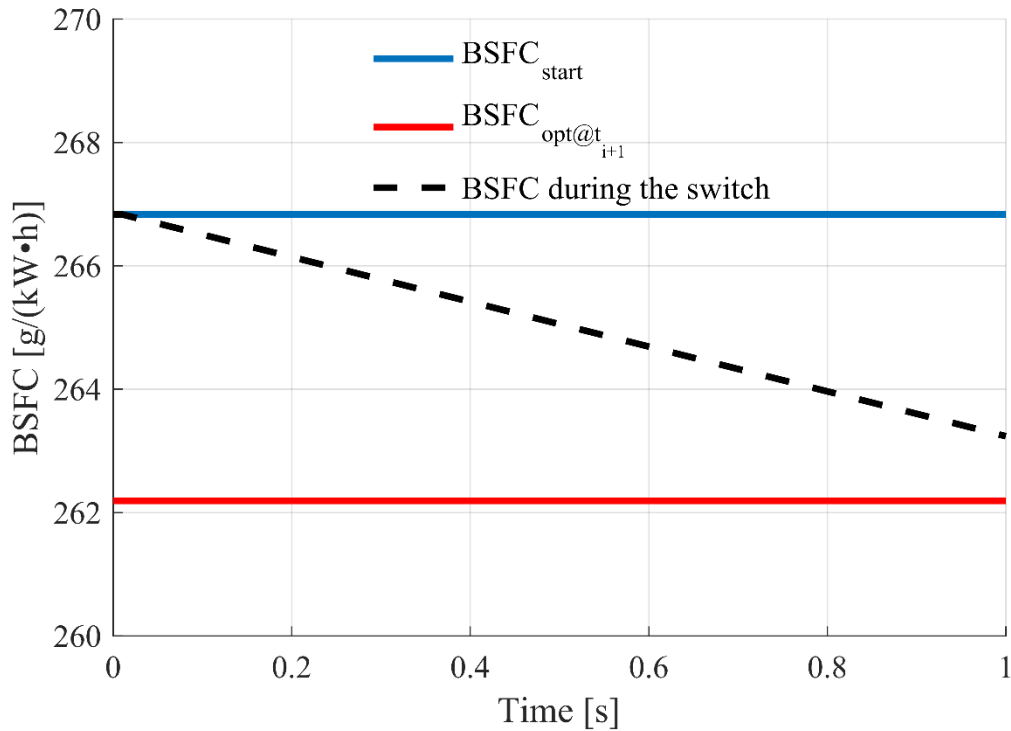


Figure 22 - Detail of the BSFC changing during a non-instantaneous not completed switch

It is important to notice that, in the case of an incomplete switch moving from high to low compression ratio, the possibility of knock insurgence is increased, indeed, since the compression ratio at the end of the switching procedure $CR_{@t_{i+1}}$ is evaluated through equation

Evaluation of the engine operating points

(9), that is a linear interpolation between HCR and LCR, it will be higher than the latter. In particular, if the target compression ratio is the low one, during the switching procedure the engine is operating at the point identified to be optimal for that compression ratio. This means that this operating point is positioned in the area where the LCR is the best, thus above the switching line and, possibly above the knock limit of the HCR. Obviously, for an intermediate CR, it would be expected that the knock limit would be between the bounds defined by the HCR and LCR, but for the sake of simplicity, and to be conservative, the knock limit for each intermediate CR has been considered equal to the one of the HCR. Thus, under these conditions, the operating point chosen for the engine is changed to a point under the knock limit for the HCR, and the outcomes of the switching procedure are re-evaluated. Once all these passages have been completed, the mass of fuel injected during the switch is simply computed through:

$$m_{fuel} = \sum_{i=t_i}^{t_{i+1}} BSFC(i) \cdot P_{eng} \cdot \frac{t_{step}}{3600} [g] \quad (16)$$

where $BSFC(i)$ is the BSFC at the step i of the switching procedure and t_{step} is the time duration of each step of the switching procedure.

Chapter 4

Impact of the switching time

The effectiveness of a VCR system is highly dependent on the time length of a switching procedure. The aim of this chapter is to identify a limit time under which the implementation of a VCR system is advantageous, and to analyze the impact of the switching time on the fuel consumption and on the number of completed switches in compression ratio. All the results presented in this chapter were obtained considering the FTP-75 drive cycle only, however, the role of the vehicle drive cycle on the effectiveness of a VCR system will be discussed in Chapter 7.

4.1 Impact of switching time on fuel consumption

To evaluate the role of switching time of the modeled VCR system, the improvement in fuel economy obtainable through a VCR system under ideal conditions was first evaluated. The ideal case corresponds to an instantaneous switch procedure, indeed, under these conditions, every switch in compression ratio is completed instantly, and the engine always operates at the optimal operating conditions which minimizes fuel consumption along the chosen drive cycle. **Figure 23** and **Figure 24** present the results for a vehicle equipped with a CVT and with a DT respectively. In the first case, an improvement of 0.33% in fuel economy was obtained through the usage of a VCR with null switch time with respect to the case with a static CR equal to 10. While for the DT case, the improvement achievable increased to 0.46%. The primary reason for the merely modest improvements in fuel economy for these cases is the very small difference between the two compression ratios utilized by the VCR system modeled. As shown in Chapter 1, the greater is the gap between the two CRs employed, the larger the increase in engine efficiency.

In the same figures, the results related to an increasing switch time, measured in terms of number of engine cycles, are presented. The outcomes of the switching procedure depend on the time available to switch, as explained in Chapter 3. The longer the length adjustment of the connecting rod takes, the larger the quantity of fuel injected during the switching procedure. This will correspondingly lead to an increase in fuel consumption. Looking at **Figure 23** and **Figure 24** it is possible to notice that the fuel economy decreases for an increasing number of switching cycles. In particular, the results converge toward the case of the static CR equal to 11.4, due to the fact that at the initial time instant the engine is assumed to work with a high compression ratio and, for long switching times, the compression ratio will never change significantly from this value.

Impact of the switching time

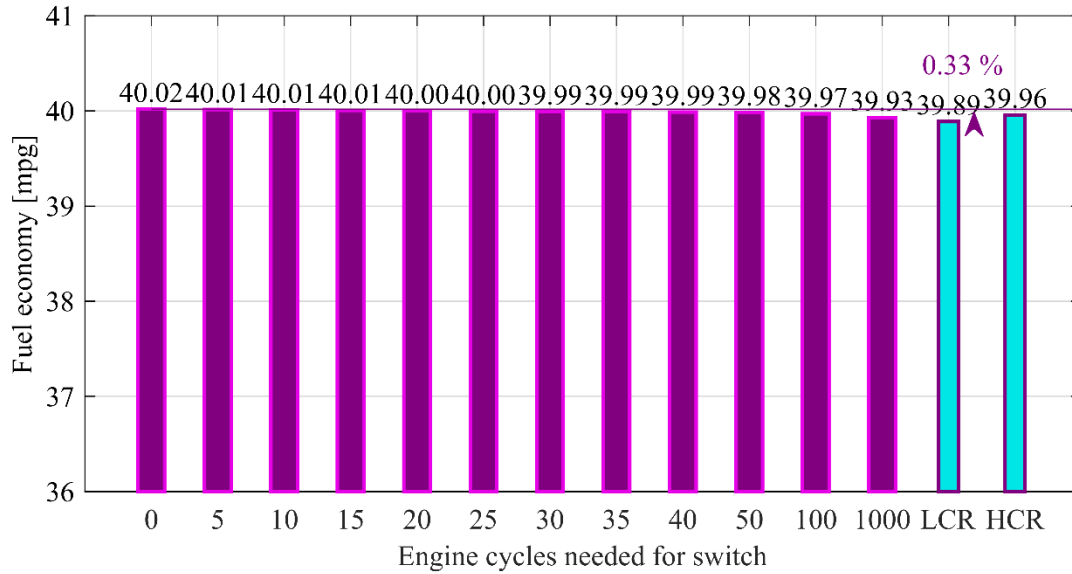


Figure 23 – Bar plot of the fuel economy for a vehicle equipped with a CVT for various VCR switching times (magenta), and two fixed CR cases (cyan)

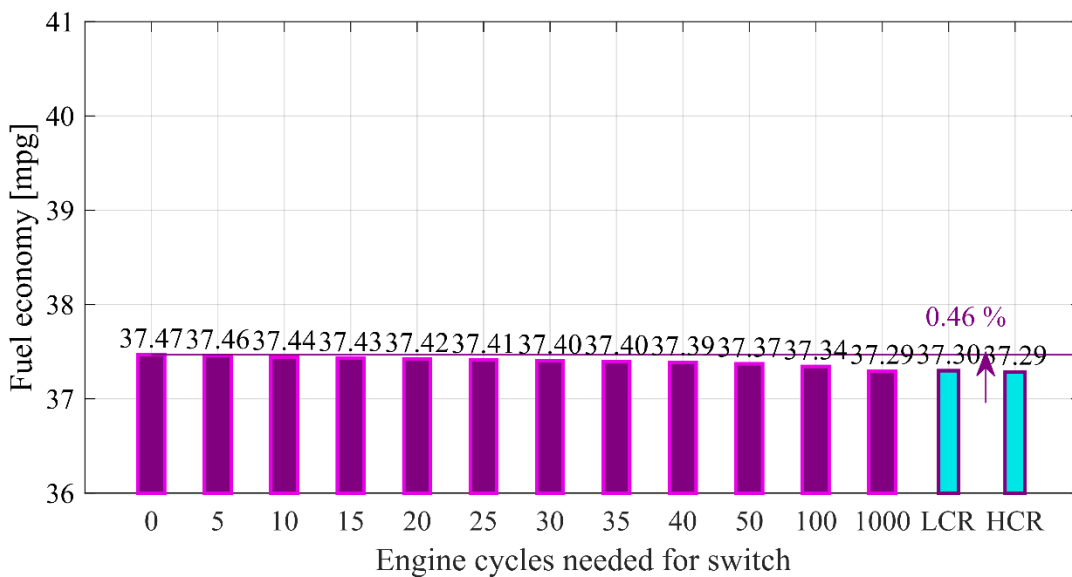


Figure 24 – Bar plot of the fuel economy for a vehicle equipped with a DT for various VCR switching times (magenta), and two fixed CR cases (cyan)

Focusing on the results for the CVT, it is possible to notice that the fuel economy for a VCR system, for every number of switch cycles, is always better than the baseline. This is, once again, due to the very small difference in BSFC between the two compression ratios. However, for very long switch times (i.e. greater than 100), the fuel economy of the VCR system is worse than the value for the static HCR case. Despite this, it seems that very high number of switching cycles are still capable of providing modest fuel economy improvements with respect to the baseline LCR case for both transmissions. However, this analysis neglects the potential negative effects of incomplete switching procedures.

Impact of the switching time

4.2 Impact of the switch time on the number of incomplete switches

Incomplete switches can be extremely detrimental for two reasons in particular. First of all, in the case of incomplete switch, the engine will not operate with the ideal compression ratio, and this will lead to an increase in fuel consumption. Moreover, incomplete switches increase the risk of knock insurgence, as explained in Chapter 3. For these reasons, it is necessary to limit the switch time to avoid incomplete switches. **Figure 25** and **Figure 26** present the results for the CVT for compression ratio switches from high-to-low and low-to-high respectively, while **Figure 27** and **Figure 28** present the same results for the DT cases.

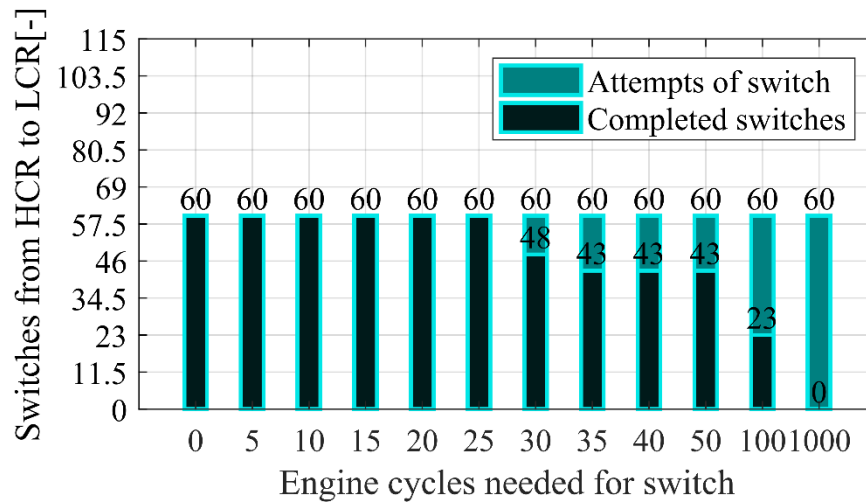


Figure 25 – Bar plot for the number of switches from HCR to LCR for the CVT for various switching times

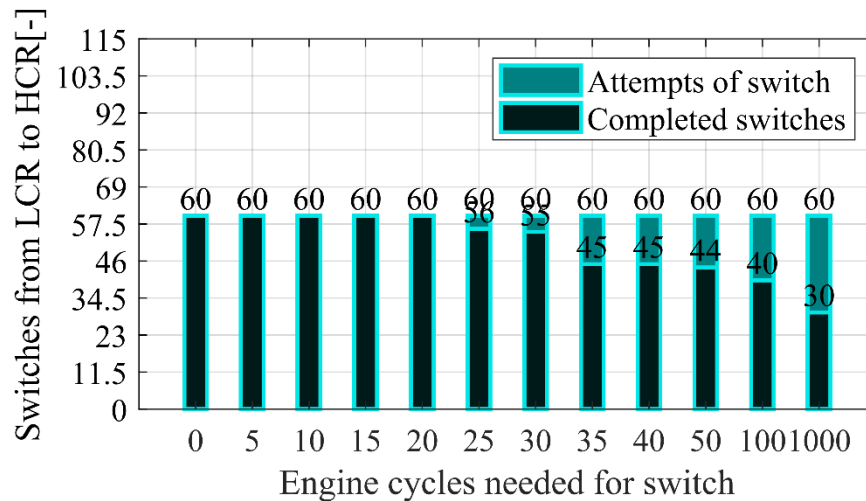


Figure 26 – Bar plot for the number of switches from LCR to HCR for the CVT for various switching times

Impact of the switching time

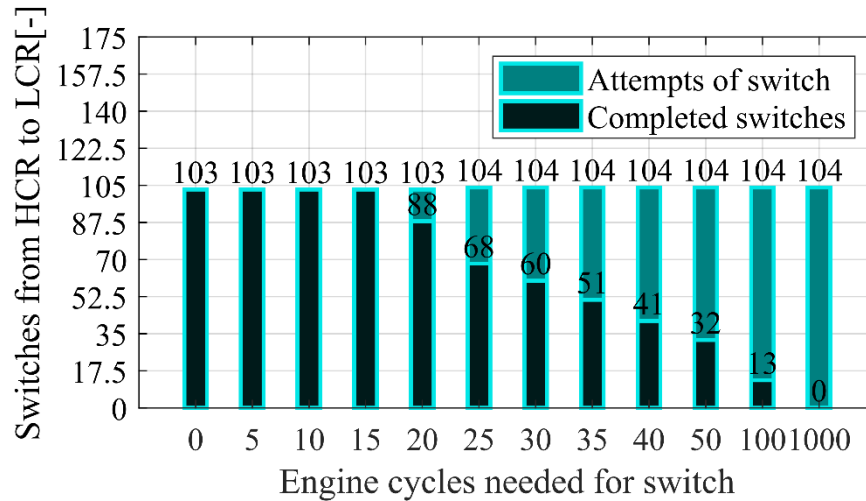


Figure 27 – Bar plot for the number of switches from HCR to LCR for the DT

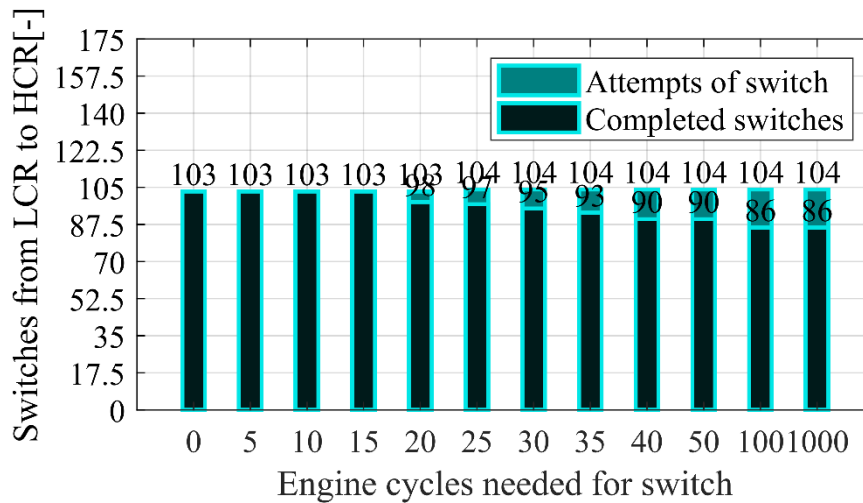


Figure 28 – Bar plot for the number of switches from LCR to HCR for the DT

Looking at the results for both the CVT and the DT, it is possible to notice that the number of attempts of switch for a CVT are much less than those for the DT. Using a Discrete Transmission, the operating points of the engine are much more spread over the engine performance map because of the limited number of transmission ratios. This condition forces the engine to try to change its compression ratio several times in order to optimize fuel consumption. For the CVT case, incomplete switches start to appear in transitions from the low to the high compression ratio at a switching time of 25 engine cycles, while for the DT, incomplete switches start to appear, in both directions, at 20 engine cycles. These two numbers therefore constitute the limit under which the switch time must remain such that incomplete switches can be avoided for this particular drive cycle. While it is likely that the switching time for a realistic VCR system will not remain constant independent of the engine operating conditions, any viable VCR system should be able to accomplish compression ratio switches within 20-25 engine cycles at every relevant engine speed/load condition in order to avoid the negative effects of incomplete switches.

Chapter 5

Speed-Load Dependent Switch time

Until now, a constant number of engine cycles necessary to switch was considered. However, given that the conrod is subjected to drastically different magnitudes of forces during engine operation, it is reasonable to think that, depending on the engine operating conditions, the time necessary to adjust its length may vary. In this chapter, the logic followed for the implementation of a Speed-Load Dependent Switch (SLDS) time based on a practical VCR system is explained, and the results in term of fuel consumption and number of completed switches will be presented.

5.1 Implementation of a Speed-Load Dependent Switch time

As explained in Chapter 1, one method for achieving a 2-stage VCR system exploits oil pressure to adjust the length of the connecting rod. However, Huettner and Millward [20] showed that to achieve length changes in both directions, the Gas Force (FG) and the Inertia Force (FI) are used. These forces, both acting on the small end of the conrod, generate a Resultant Force (FR). This force, depending on the crankshaft angular position, can exert a compressive or tensile action on the conrod. In the case where FR is a compressive force, the connecting rod will shorten, otherwise it will extend. This translational movement is limited in both directions by mechanical stops.

Since the magnitude of these forces depends on the engine operating conditions, the amount of time required to switch from length to another will also vary with them. Generally, with increasing load, FG will increase and, since this force always exerts a compressive action on the conrod, extending the connecting rod (i.e. increasing compression ratio) will be more difficult. Instead, with increasing engine speeds, the time when FI is acting during each engine cycle becomes shorter, and also the increase in FG outweigh the increase of FI, and as a result the connecting rod needs more engine cycles to extend. Considering the time necessary to collapse the conrod, FG helps this transition independently from the engine operating conditions. Huettner and Millward [210] showed that the number of engine cycles necessary to expand varied between 5 and 16 engine cycles, depending on the engine speed and load, while the conrod collapsed in 2-3 engine cycles independently from the operating conditions. This is very useful for immediate knock mitigation during driver maneuvers like tip-in, since the compression ratio of the engine can be decreased rapidly, thereby avoiding the use of the high compression ratio configuration at knock-prone operating conditions. More in detail, two series of data were provided, one for the engine operating under boosted conditions and the other for a natural aspirated engine. Not having informations about the engine loads, the boosted data from [20] were mapped to the Wide Open Throttle curve of the Oak Ridge engine map, while the NA data

Speed-Load Depending Switch time

from [20] were mapped to half the WOT loads. A third set of data was created for the engine operating at idle. Under these conditions, the number of switching cycles was considered constant for the whole range of operating speeds of the engine and equal to 3. Furthermore, the data coming from [20] were reported only for engine speeds up to 3500 *rpm*. For this reason, a polynomial fit was applied to series of data corresponding to the different loads so that to extrapolate results up to 5000 *rpm*. In particular, a second order polynomial was fit to the three different series of data. At this point it was possible to interpolate between the different series and obtain the map presented in **Figure 29**.

In particular, this map will be used only to evaluate the switch time necessary to expand the conrod, since, as highlighted before, the time necessary to collapse it is almost constant, and for the purposes of this analysis was assumed to always be equal to 3 engine cycles independent of speed and load. **Figure 29** shows a surface plot of the engine cycles required to extend the connecting rod (i.e. switch from low to high compression ratio) based on the data from [20].

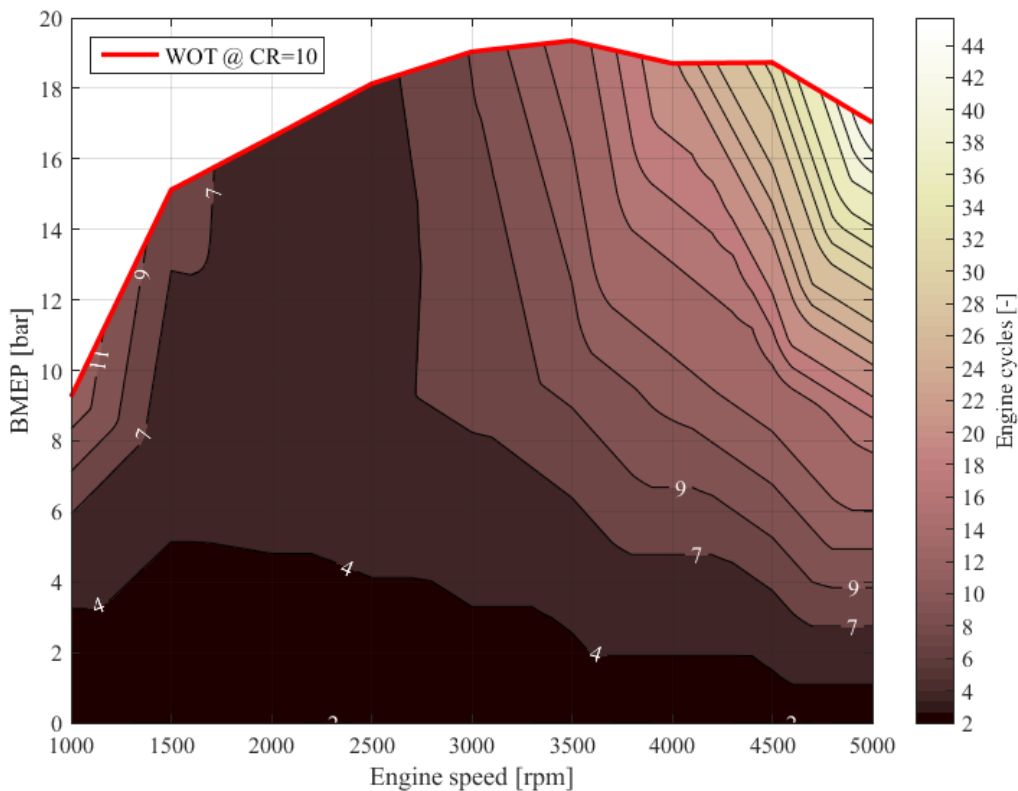


Figure 29 – Surface plot of the number of engine cycles required for a switch from low to high compression ratio as a function of engine speed and load, mapped to the baseline engine map discussed in Chapter 3

It is important to mention that all the data used to create these maps were obtained from motored tests. Under firing conditions, because of the different magnitudes of FI and FG in particular, the results could be different. For this reason, a constant called the “switch multiplier” was introduced in order to increase the switching time by simply multiplying the switch time map by some constant

Speed-Load Depending Switch time

factor that would represent the increased time required to switch under fired conditions. The impact of a SLDS time on fuel consumption and number of completed switches was analyzed. Furthermore, the effect of the switch multiplier was also studied.

5.2 Impact of a LDS time on fuel consumption

First of all, it is necessary to state that the “switch multiplier” is assumed equal to unity. Its impact will be analyzed later in this chapter. **Figure 30** and **Figure 31** report the results relative to a vehicle equipped with a CVT and a DT respectively operating on the FTP-75 drive cycle. In both bar plots, the fuel economy achieved using a fixed switching time is compared with the fuel economy obtained through a SLDS time.

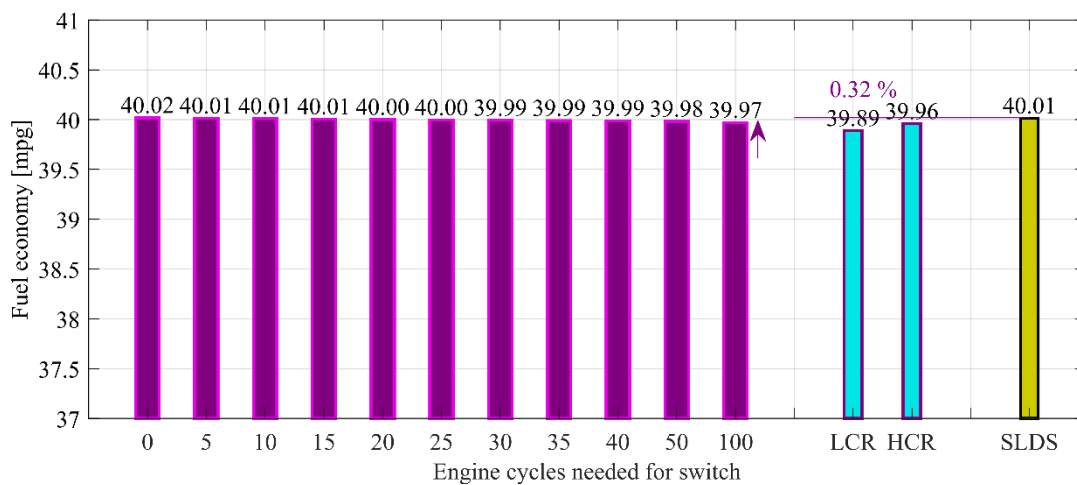


Figure 30 – Bar plot for the comparison of the consumptions for a vehicle equipped with a CVT using a SLDS time or a fixed time.

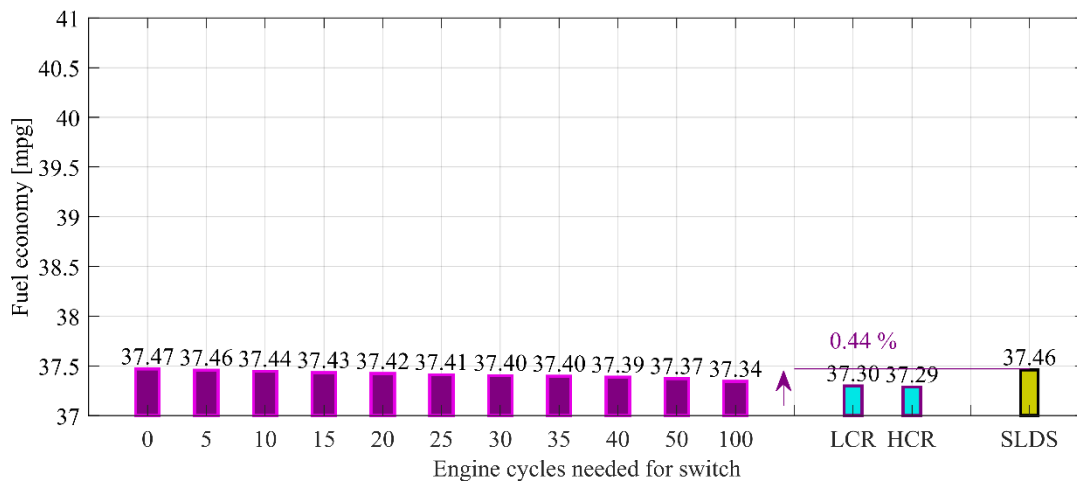


Figure 31 – Bar plot for the comparison of the consumptions for a vehicle equipped with a DT using a SLDS time or a fixed time.

As can be noticed, using a SLDS time, not only is the fuel economy improved with respect to the baseline LCR engine, but also the resulting miles per gallon are very near to those of an instantaneous

Speed-Load Depending Switch time

switch. These considerations are true for both types of transmission. This suggests that the average number of switching cycles will be between 0 and 5 engine cycles, with obvious results in terms of number of completed switches.

5.3 Impact of a SLDS time on the number of incomplete switches

Figure 32 - Figure 35 depict bar plots of the number of switch attempts, and number of completed switches for both transmission types and both switch directions (i.e. LCR to HCR, and HCR to LCR). As can be seen from the figures, no incomplete switches were present for either type of transmission, or for switches in either direction.

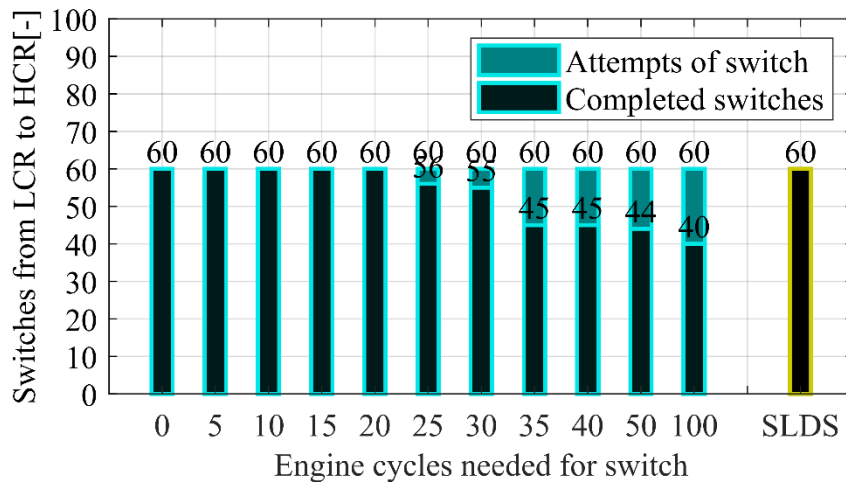


Figure 32 – Bar plot of the number of switches from LCR to HCR for a CVT

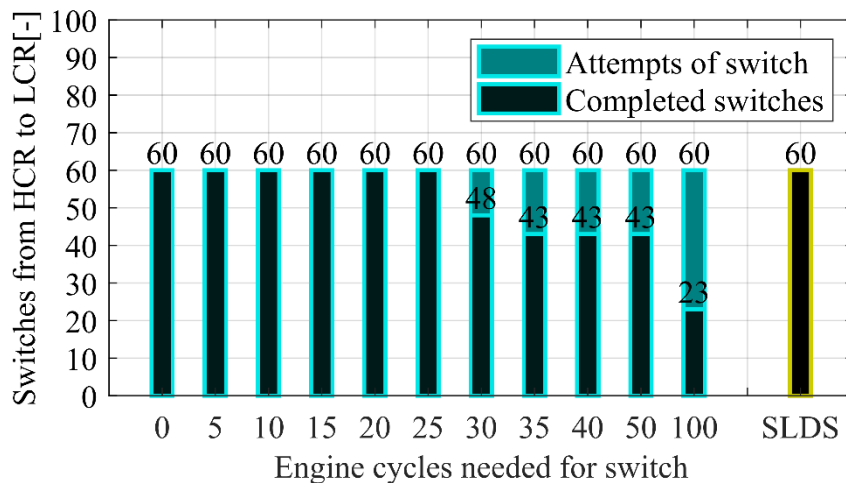


Figure 33 – Bar plot of the number of switches from HCR to LCR for a CVT

Speed-Load Depending Switch time

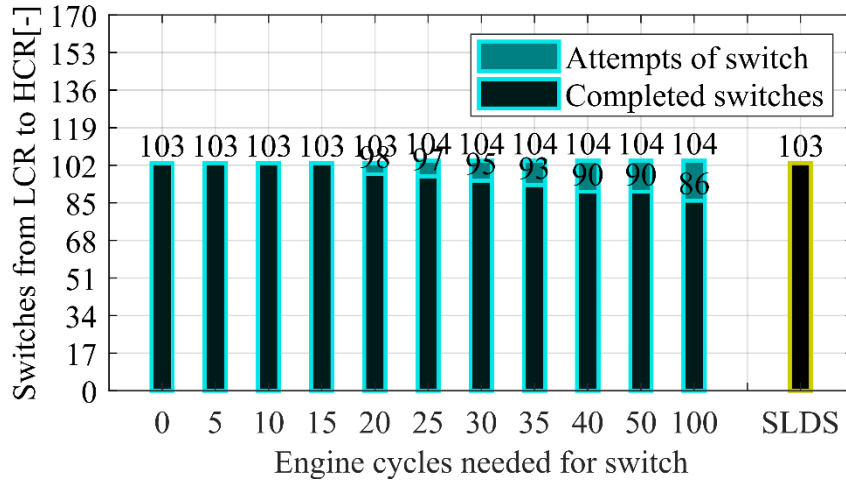


Figure 34 – Bar plot of the number of switches from LCR to HCR for a DT

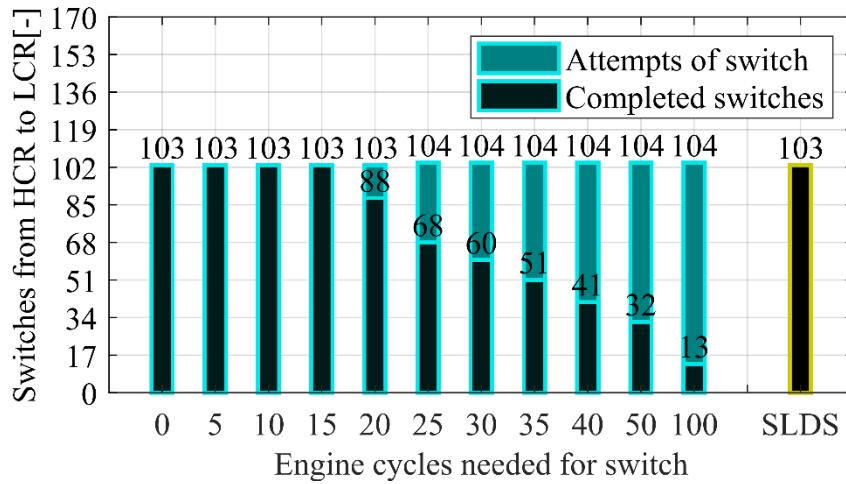


Figure 35 – Bar plot of the number of switches from HCR to LCR for a DT

For transitions from a high to a low compression ratio a constant number of cycles equal to 3 was used, as mentioned earlier in the chapter. This very short switching time allows the system to perform the length adjustment of the connecting rod in the available time at all conditions. Regarding the changes in compression ratio in the opposite direction, with a SLDS time, the number of switching cycles is variable and potentially high. However, as shown in Chapter 3, for both the transmissions, engine operating points are mostly concentrated at low speed and low to medium engine load. Looking at **Figure 29**, these regions correspond to switching cycles varying from 4 to 11 cycles. As shown in Chapter 4, on an average basis, the number of switching cycles must stay under 25 cycles for the CVT and 20 for the DT to avoid incomplete switches, thus a VCR system exploiting a SLDS time such as the one modeled here is capable of operating well below these limits.

5.4 Impact of the “switch multiplier”

As mentioned earlier in the chapter, the map in **Figure 29** was obtained from motored tests. Hence a “switch multiplier” was introduced in order to simulate the behavior of the system under firing

Speed-Load Depending Switch time

conditions. The “switch multiplier” was varied in a sweep from 0 to 5 in order to identify a threshold from which incomplete switches started to appear. The impact of the “switch multiplier” on fuel consumption was not studied since it is already clear that longer switching times imply higher consumptions, and shorter switching times will always be better from a fuel economy perspective. Moreover, the “switch multiplier” was applied only to switches from low to high compression ratio, since transitions from high to low compression ratios, aided by the gas forces acting to shorten the conrod, were independent of speed-load condition [20]. Thus, moving from motored to fired conditions, it is reasonable to assume that the switching time in this direction should not be affected by the “switch multiplier”. **Figure 36** and **Figure 37** show the number of attempted switches and completed switches from LCR to HCR for the CVT and DT cases respectively. It can be noticed that, in both cases, incomplete switches start to consistently appear with a switch multiplier equal to 3. Thus, if results obtained with a “switch multiplier” equal to one are considered not reliable for the reasons explained before, even doubling the switch times reported in [20], the modeled VCR system would still be capable of completing nearly all required switches in CR in the required time.

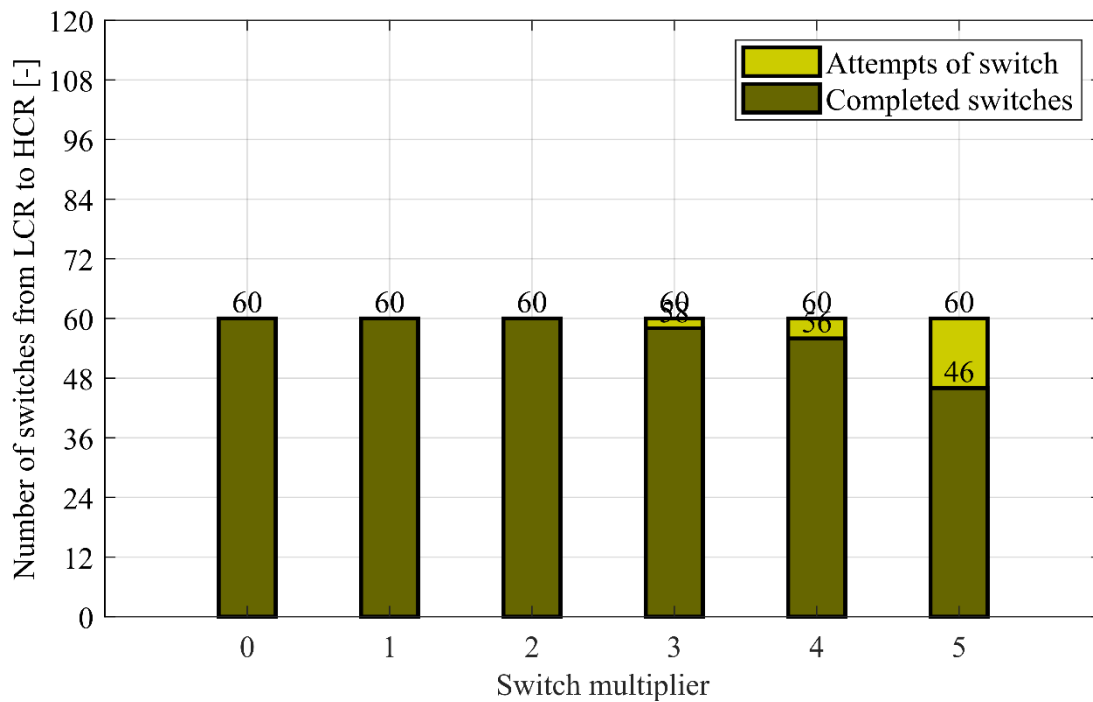


Figure 36 – Bar plot of the number of switches for a varying switch multiplier for a CVT.

Speed-Load Depending Switch time

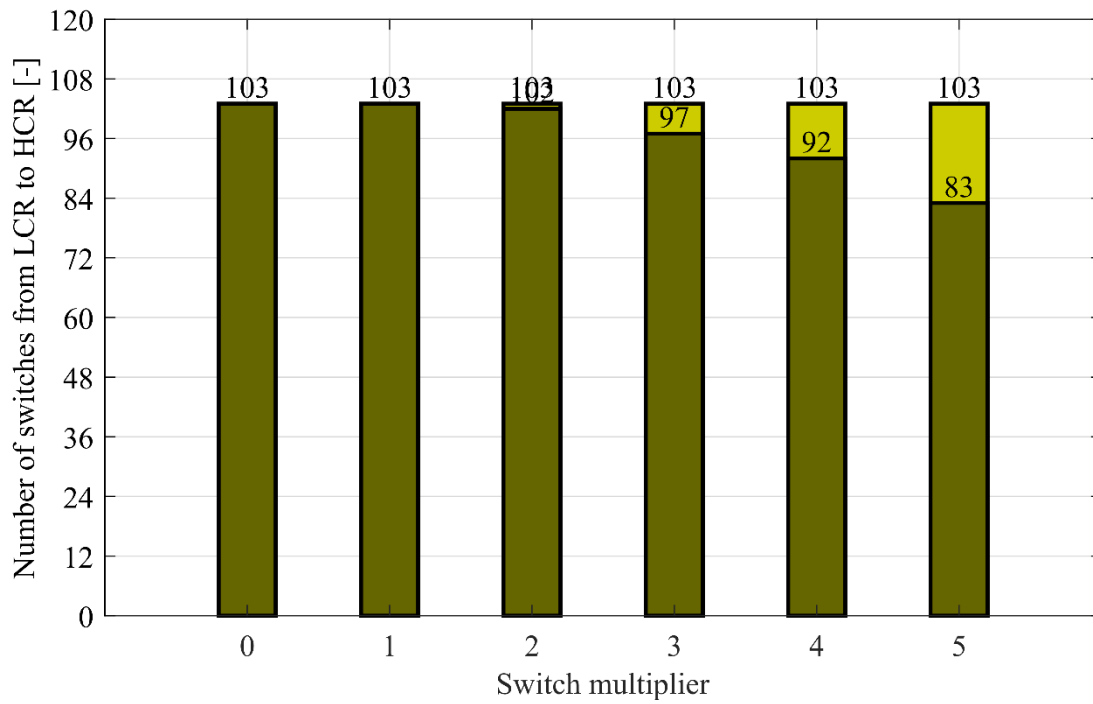


Figure 37 – Bar plot of the number of switches for a varying switch multiplier for a DT.

Chapter 6

Impact of the transients

Changes in compression ratio by means of extending or retracting the connecting rod have the capacity to generate transients that can lead to an increase in fuel consumption and easily counterbalance the advantages achievable through a VCR system. Additionally, during switching procedures, the engine may require adjustments to various parameters including spark timing, valve timing, and injection timing in order to optimize fuel economy. The transition through non-optimal operating points during switching procedures may further penalize the fuel economy of such a VCR system. In this chapter, the impact of transients on the effectiveness of a VCR system is thus studied.

6.1 Methodology for the study of transients

Modelling the transients generated by a change in compression ratios is not a simple task. Compression ratio influences the peak firing pressure, the engine efficiency, the cycle to cycle variation, the mass fraction burned and the Friction Mean Effective Pressure (FMEP), as shown in the work developed by AVL [2022]. For this multiplicity of reasons, it is difficult, if not impossible, to quantify how much transients contribute to increasing the quantity of fuel injected during a driving cycle. Hence, for the sake of simplicity, the impact of the transients was studied applying a fixed penalty to the quantity of fuel injected during the switching procedure. This penalty is applied in the form of a worsening percentage studied in a sweep from 0% to 5%. Moreover, differently from the “switch multiplier”, this worsening factor was applied to switches from low to high compression ratio, but also to switches in the opposite direction. Furthermore, an additional penalty factor was introduced. Indeed, as described by AVL [20], an increase of 0.6% in the FMEP is to be expected due to the high oil pressure required to actuate the connecting rod in the system modelled in this work. Different from the previous worsening percentage, this value is applied as constant penalty during any switch attempt.

6.2 Results

Figure 38 and **Figure 39** show the modelled vehicle fuel economy for various transient fuel penalties without and with the FMEP penalty respectively. From the two figures, it is possible to notice immediately that the FMEP penalty has only a small effect on modelled fuel economy. However, in both cases, it can be seen that an increase in fuel injected of 2% (i.e. a worsening factor of 1.02) is sufficient to counterbalance the fuel economy benefits from the modelled VCR system.

Impact of the transients

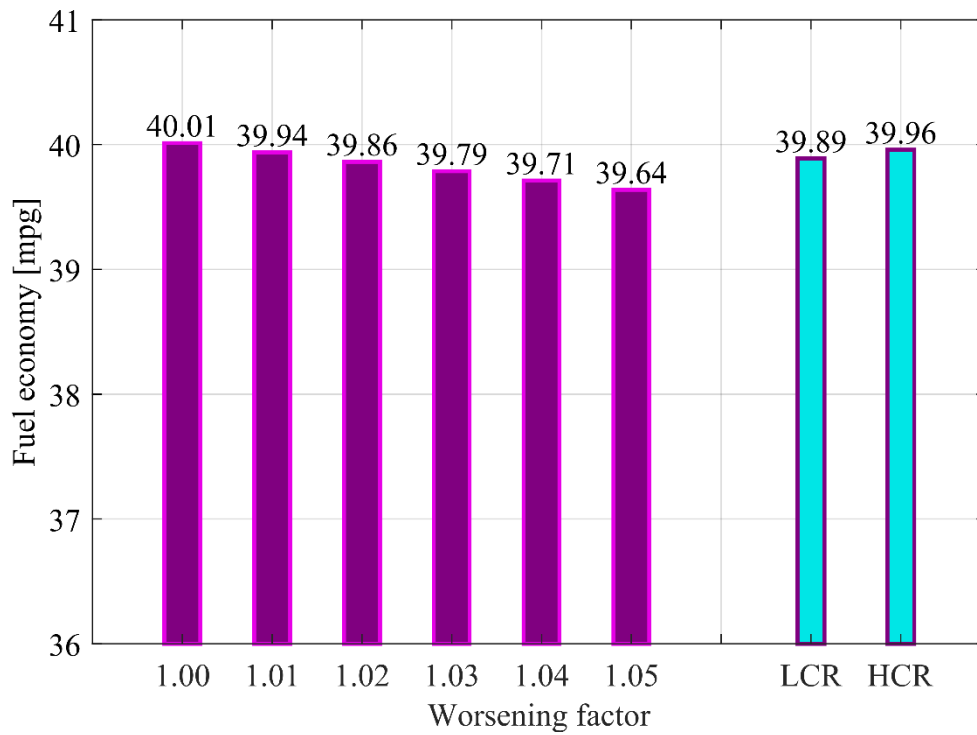


Figure 38 – Bar plot for the evaluation of the impact of the transients, neglecting the increased FMEP, for a vehicle equipped with a CVT.

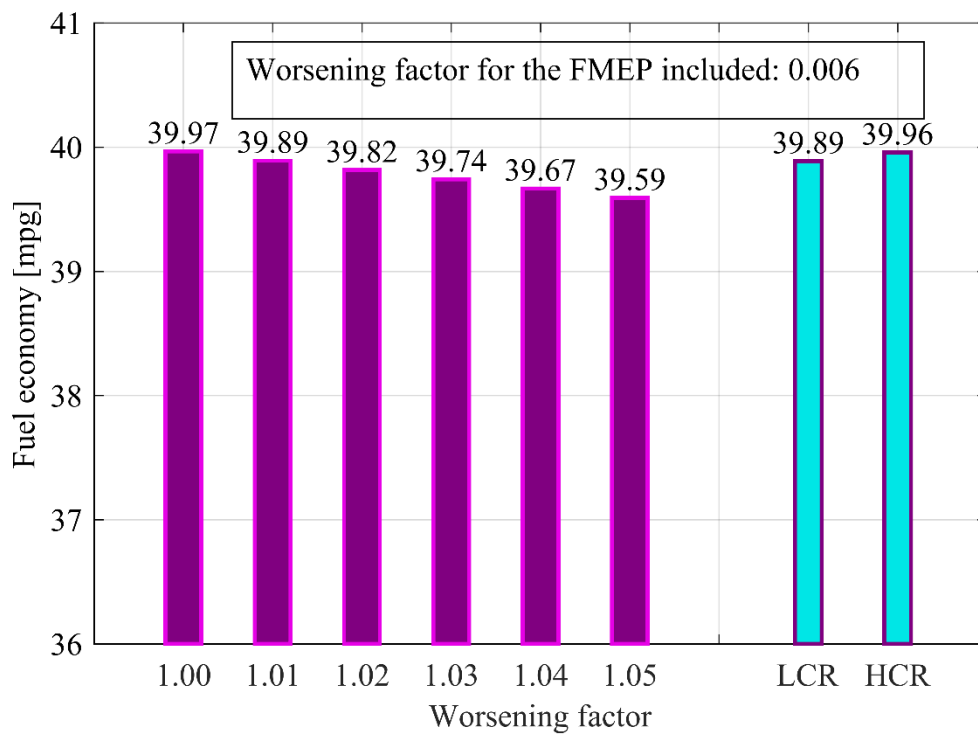


Figure 39 – Bar plot for the evaluation of the impact of the transients, including the increased FMEP, for vehicle equipped with a CVT.

Impact of the transients

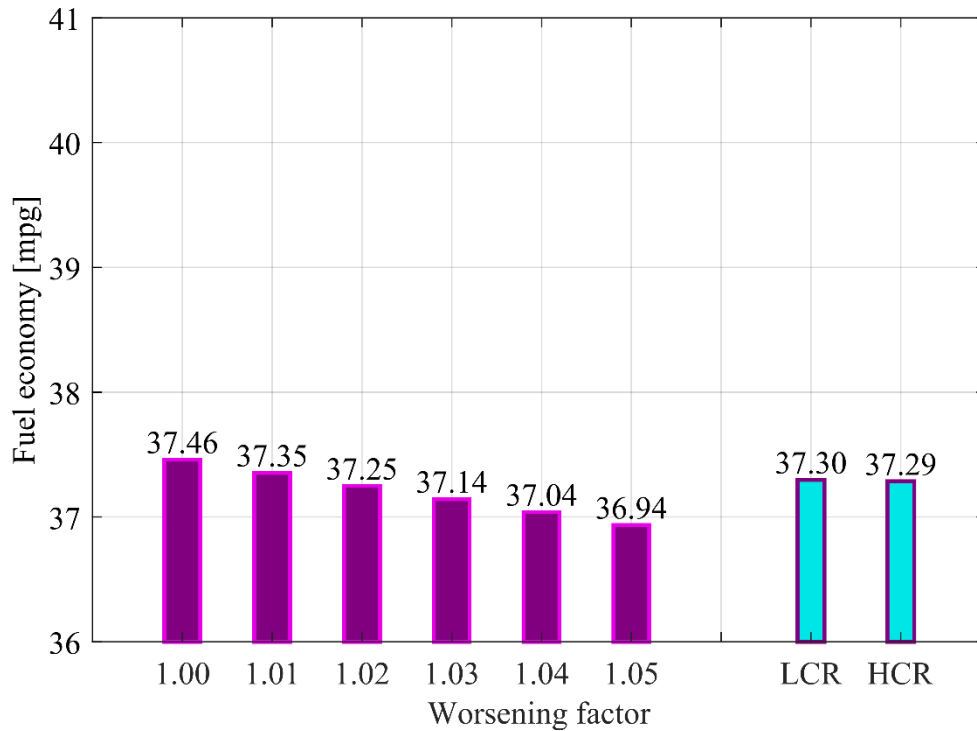


Figure 40 – Bar plot for the evaluation of the impact of the transients, neglecting the increased FMEP, for a vehicle equipped with a DT.

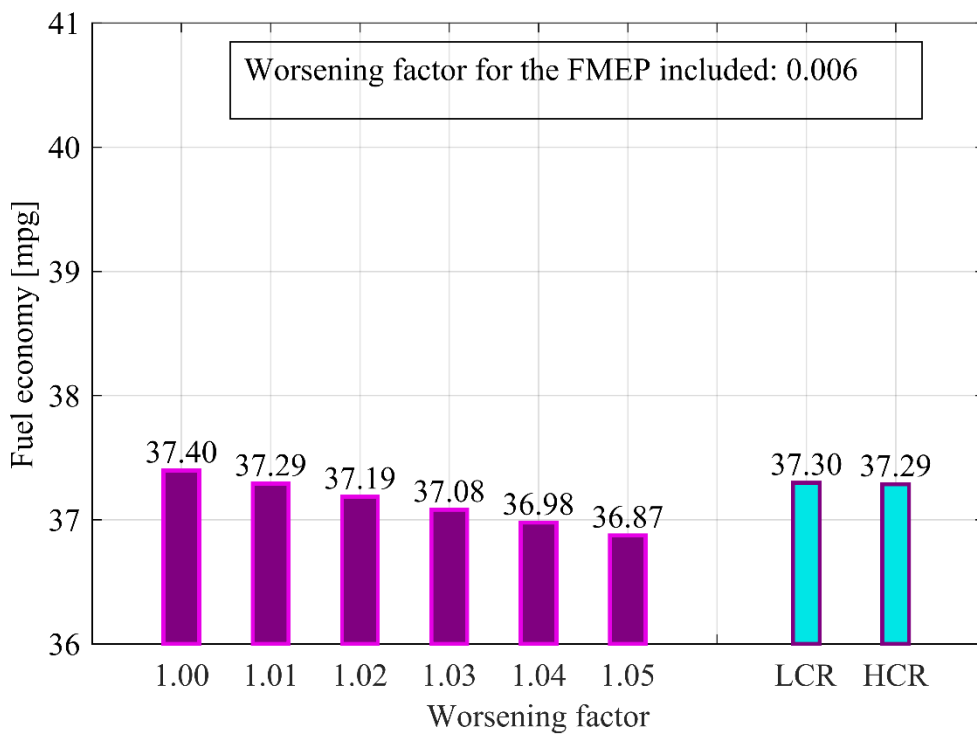


Figure 41 – Bar plot for the evaluation of the impact of the transients, including the increased FMEP, for vehicle equipped with a DT.

This behavior does not change for a vehicle equipped with a DT, as it can be seen from **Figure 40** and **Figure 41**. Also in this case the penalty factor related to the FMEP does not impact the results in

Impact of the transients

a significant way, but combined with a worsening percentage equal to 1%, is already sufficient to outweigh the benefit of the VCR system. In general, it is clear that transients are a huge obstacle for the implementation of a VCR system. However, it is worth noting that a higher transient fueling penalty could be tolerated if the overall fuel economy benefit of the VCR system were greater, but given the very small difference in CR of the modelled system, the improvement in fuel economy is minimal, and is therefore easily counterbalanced by transient effects.

Chapter 7

Impact of the vehicle characteristics and of the drive cycle

The power necessary for motion can highly impact the effectiveness of a VCR system. Increasing or decreasing the power that the engine has to deliver means that the position of its operating points will change, moving them to regions in which the BSFC can be higher or lower, which can have a significant impact on the relative effectiveness of a VCR system. The power required is determined mainly by the vehicle characteristics and by the speed profile followed, thus in this chapter, the impact of vehicle characteristics and of the drive cycle are studied.

7.1 Impact of the vehicle characteristics

Four different vehicles were considered in order to study the impact of the vehicle characteristics on the effectiveness of the VCR system. In particular, since the performance maps used are still the ones from Oak Ridge National Laboratories [17], using a Ford 1.6 L EcoBoost engine, the selected vehicles are all Ford vehicles that were actually equipped with that engine. Moreover, vehicles belonging to different segments were selected, and are as follows:

- Ford Escape, compact crossover.
- Ford Transit, light commercial vehicle.
- Ford Fusion, mid-size sedan.
- Ford Fiesta, supermini or B-segment vehicle.

The characteristics of the different vehicle are reported in **Table 4** and have been obtained from the EPA database [18]. Whereas in **Table 5**, the gear ratios of the transmissions equipped by the different vehicle are reported. The Ford Transit and the Ford Escape are the heaviest among the four vehicles, and they are also characterized by higher target coefficients, making them the two vehicles requiring the most power to follow the specified drive cycle. The Ford Fusion and Ford Fiesta are instead lighter and more aerodynamic, as can be noticed by their target coefficients. Thus, they will be characterized by a lower power demand. It can be also noticed from **Table 5** that the Ford Escape, Transit and Fusion are equipped with the same transmission ratios, despite different final drive ratios. These factors will influence the engine speed-load operating conditions encountered by the vehicles.

Impact of the vehicle characteristics and of the drive cycle

	Escape	Transit	Fusion	Fiesta
Test mass [lbs]	4000	4250	3750	3000
Target coefficient A [lbf]	28.01	27.93	25.45	24.66
Target coefficient B $\left[\frac{lbf}{mph}\right]$	0.5607	0.3687	0.3455	0.0732
Target coefficient C $\left[\frac{lbf}{mph^2}\right]$	0.02308	0.02411	0.019	0.01892
Wheel radius [in]	13.6	12.85	13.09	12,24
Final drive ratio τ_f [–]	3.51	3.07	3.07	3.89
Model year	2014	2014	2013	2014

Table 4 – EPA vehicles characteristics

	Escape	Transit	Fusion	Fiesta
1 st gear [–]	4.58	4.58	4.58	3.89
2 nd gear [–]	2.96	2.96	2.96	3.92
3 rd gear [–]	1.91	1.91	1.91	2.43
4 th gear [–]	1.45	1.45	1.45	1.44
5 th gear [–]	1.00	1.00	1.00	1.02
6 th gear [–]	0.75	0.75	0.75	0.87

Table 5 – Gear ratios for the manual transmission equipped on the selected vehicles

Impact of the vehicle characteristics and of the drive cycle

For all four vehicles, a run on the FTP-75 was simulated. The results in term of fuel economy are shown in **Figure 42** and **Figure 43** for CVT and DT cases.

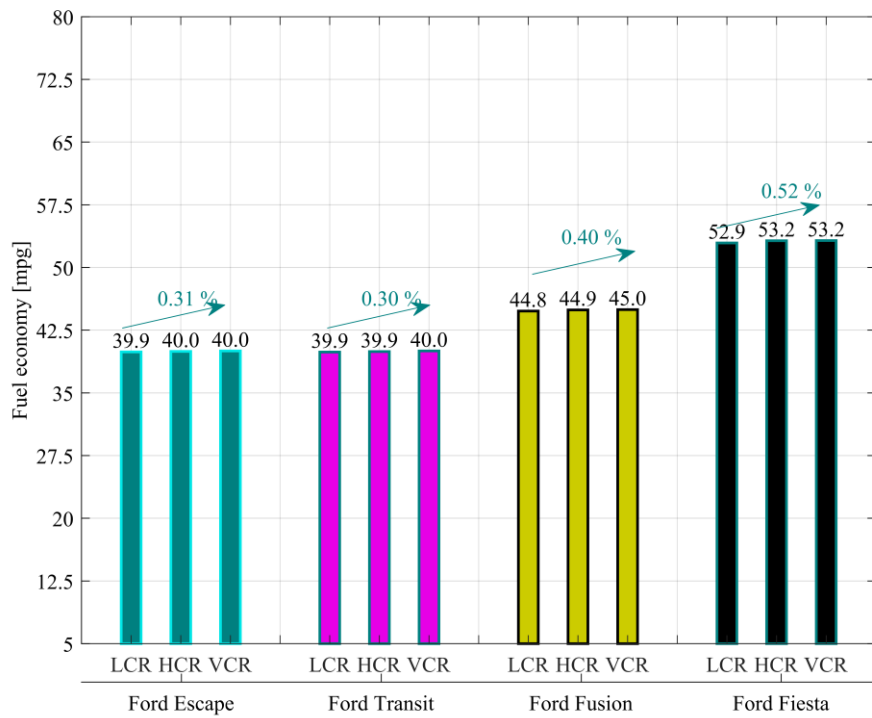


Figure 42 – Bar plot for the fuel economy of the different vehicles, considering a CVT.

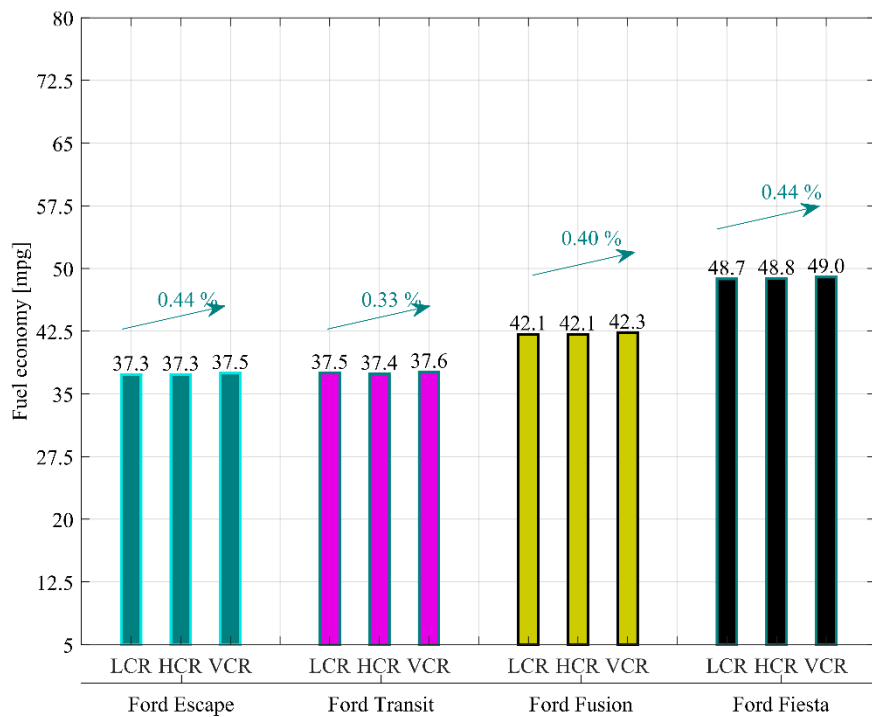


Figure 43 – Bar plot for the fuel economy of the different vehicles, considering a DT.

Impact of the vehicle characteristics and of the drive cycle

Considering the CVT case, obviously the different transmission ratios are not an impacting factor, hence the results are only due to the different masses and target coefficients. In particular, it can be noticed that with decreasing vehicle mass, the effectiveness of the VCR system increases. The Ford Fiesta, the lightest among all the vehicles considered, is the one that minimizes the fuel consumption with an improvement of 0.52% in fuel economy with respect to the baseline.

In the DT case, the results are more complicated given the differences in gear ratios and final drive ratios. Nevertheless in this case, decreasing the vehicle mass also leads to increased benefit from the VCR system, where once more, the Ford Fiesta is the vehicle characterized by the largest improvement, with an increase of 0.44% with respect to the baseline. However, it is possible to notice that the Ford Escape is also characterized by the same improvement despite its relatively high mass. In order to better understand the reasons behind this behavior, the relative fuel consumption was considered. This is defined as the difference between the total fuel injected instant by instant over the drive cycle using just one CR and the one using a VCR system.

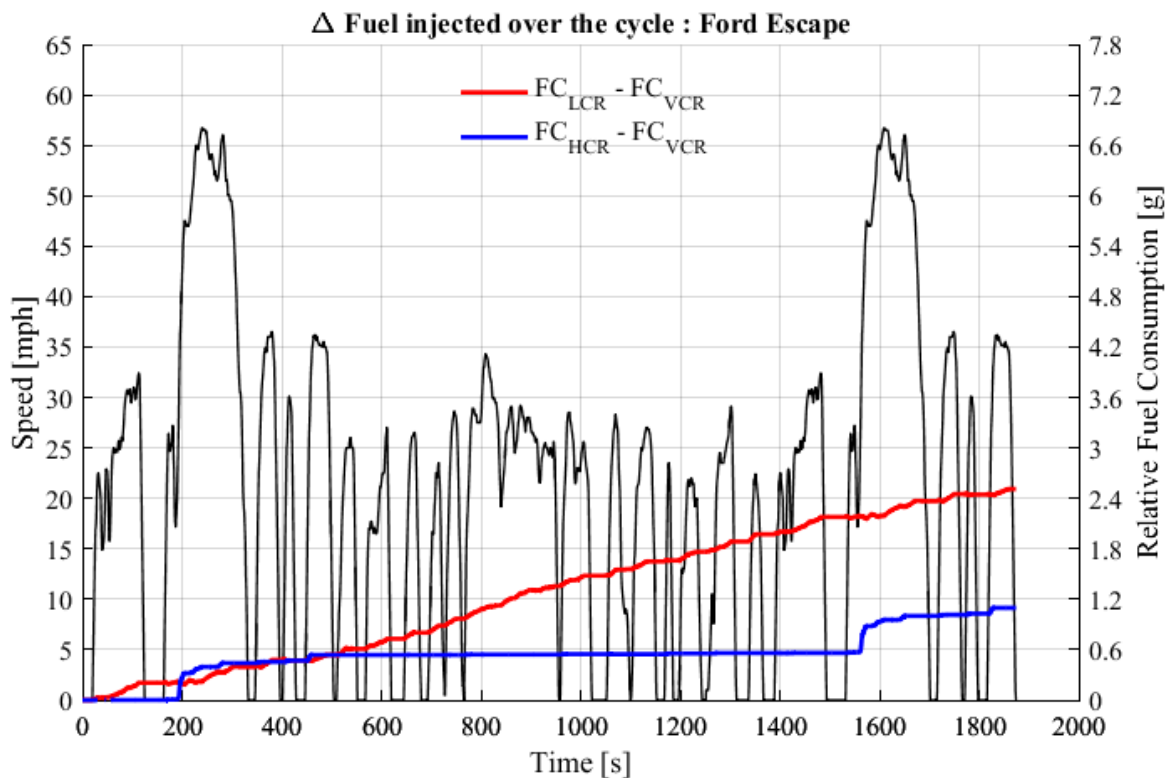


Figure 44 – Plot of the lines representing the relative fuel consumption of the LCR with respect to the VCR (red) and of the HCR with respect to the VCR (blue), considering a Ford Escape equipped with a CVT.

Impact of the vehicle characteristics and of the drive cycle

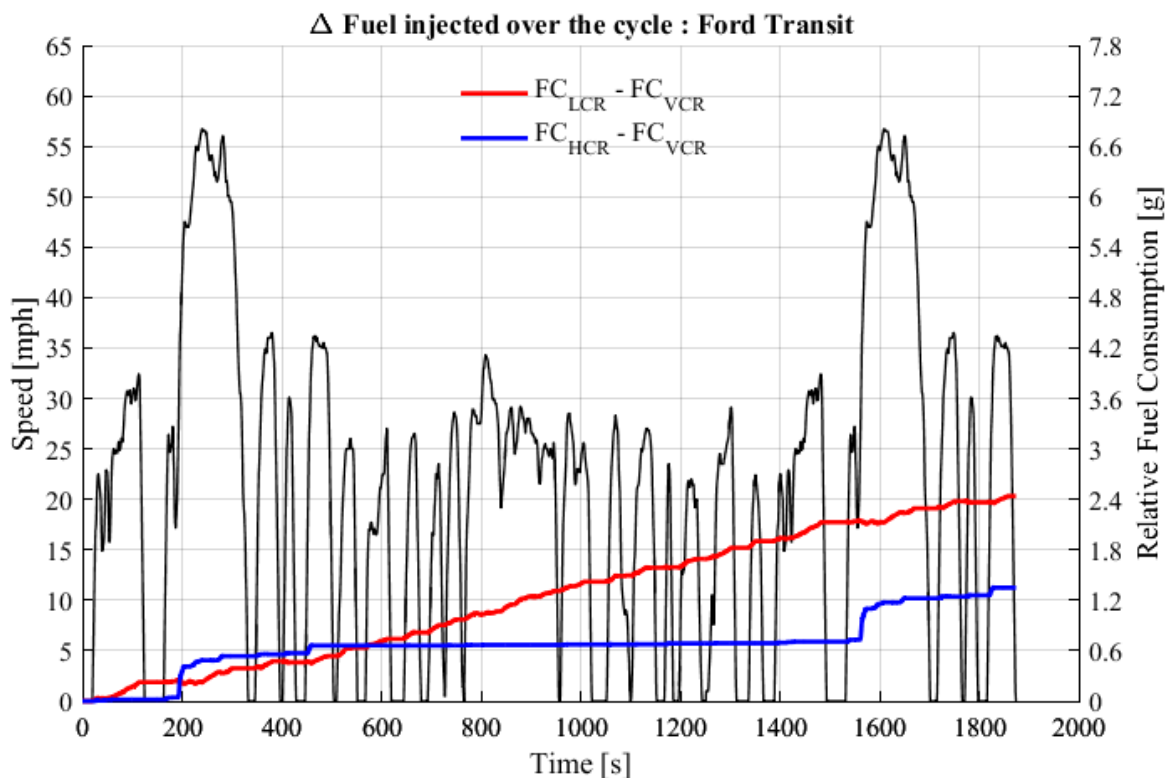


Figure 45 – Plot of the lines representing the relative fuel consumption of the LCR with respect to the VCR (red) and of the HCR with respect to the VCR (blue), considering a Ford Transit equipped with a CVT.

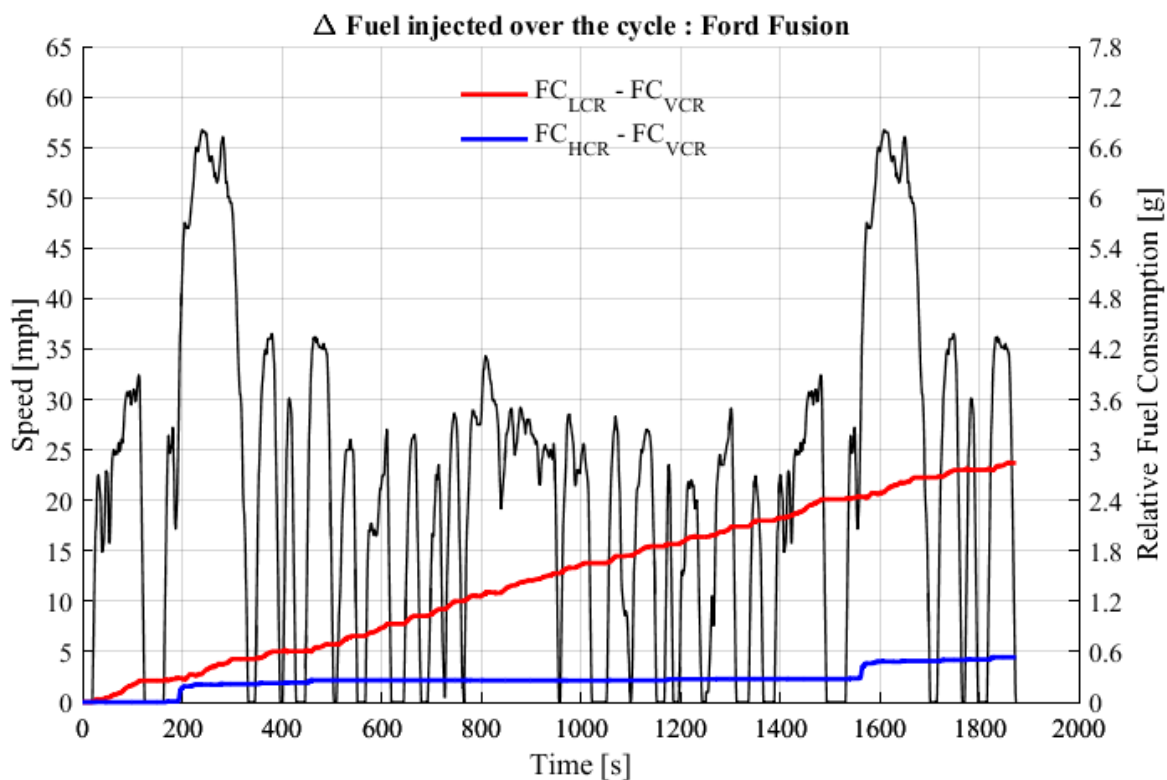


Figure 46 – Plot of the lines representing the relative fuel consumption of the LCR with respect to the VCR (red) and of the HCR with respect to the VCR (blue), considering a Ford Fusion equipped with a CVT.

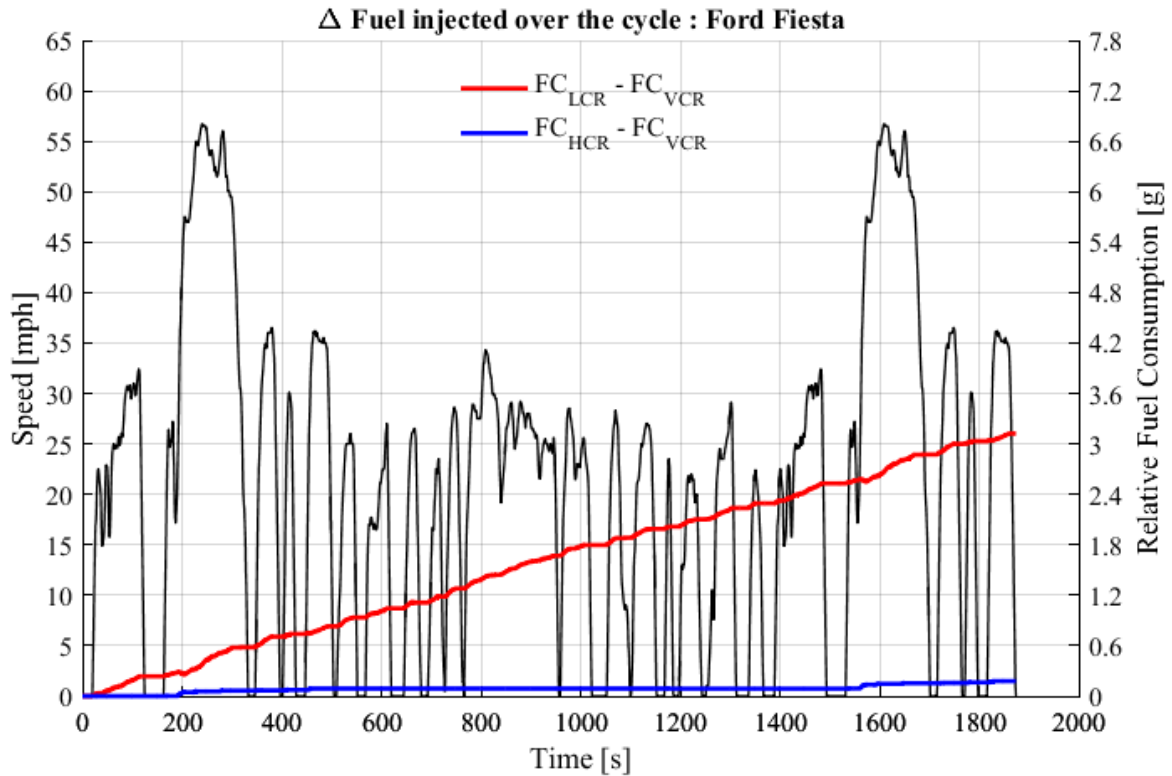


Figure 47 – Plot of the lines representing the relative fuel consumption of the LCR with respect to the VCR (red) and of the HCR with respect to the VCR (blue), considering a Ford Fiesta equipped with a CVT.

Figure 44 to **Figure 47** show the results in terms of relative fuel consumptions for the four vehicles equipped with a CVT. What can be noticed is that, the lower the power demand associated with a vehicle, the lower the relative consumption between the HCR and the VCR. This means that the HCR is used in almost every point of the drive cycle, increasing the overall efficiency of the VCR system. **Figure 48** to **Figure 51** show instead the results for the vehicle equipped with a DT. Looking at the plots, it is possible to notice immediately that there is not a clear relationship between vehicle characteristics and relative fuel consumption. Moreover looking at **Figure 50** and **Figure 51**, points in which the relative fuel consumption is decreasing can be identified. This means that the VCR system is not exploiting the optimal CR at that point of the drive cycle.

Figure 52 shows this behavior in more detail. As mentioned in Chapter 2, irregularities are present in the performances map, hence there are points, in particular at very low loads (about 1 *bar*), where the LCR is the optimal CR. However, being under the switch-line, the HCR is used due to the logic present in the modelling code. This explains the origin of these oscillations in the relative fuel consumption. As a further proof, **Figure 53** reports the engine operating points corresponding to the oscillations in the relative fuel consumption. It is possible to notice that they all lay under the switch line but in regions in which the LCR corresponds to a lower BSFC than the HCR.

Impact of the vehicle characteristics and of the drive cycle

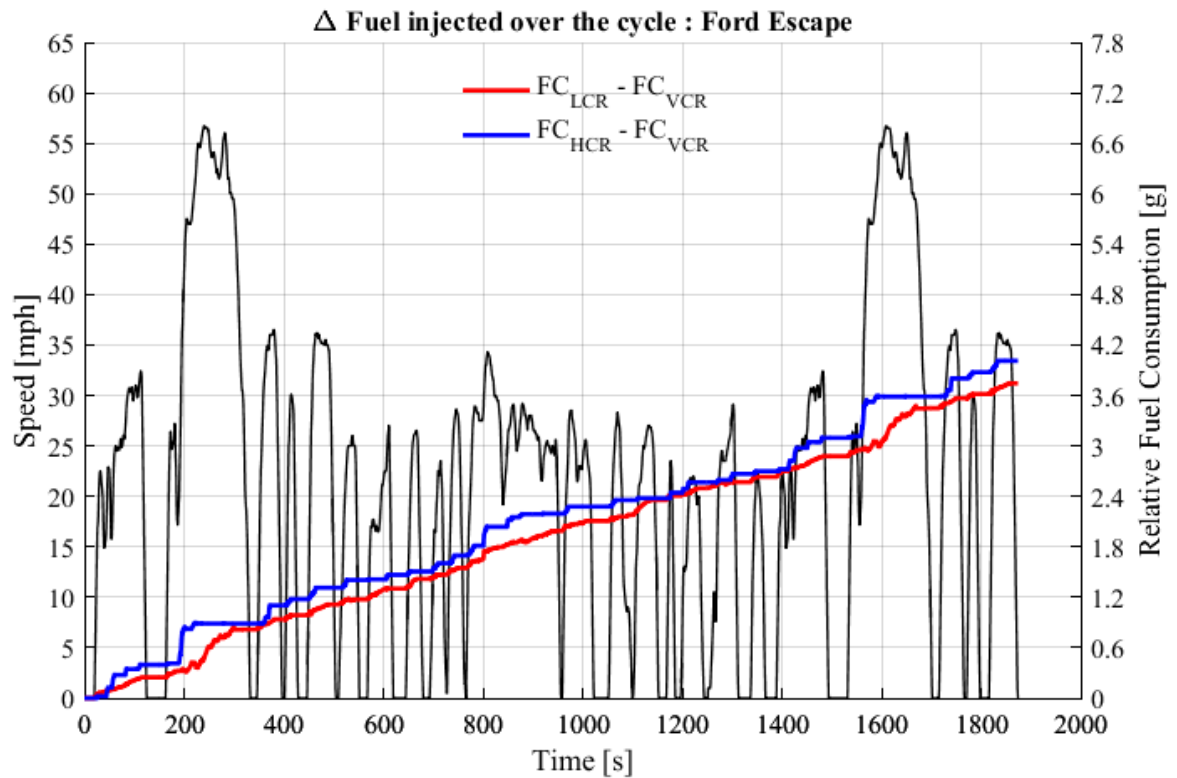


Figure 48 – Plot of the lines representing the relative fuel consumption of the LCR with respect to the VCR (red) and of the HCR with respect to the VCR (blue), considering a Ford Escape equipped with a DT.

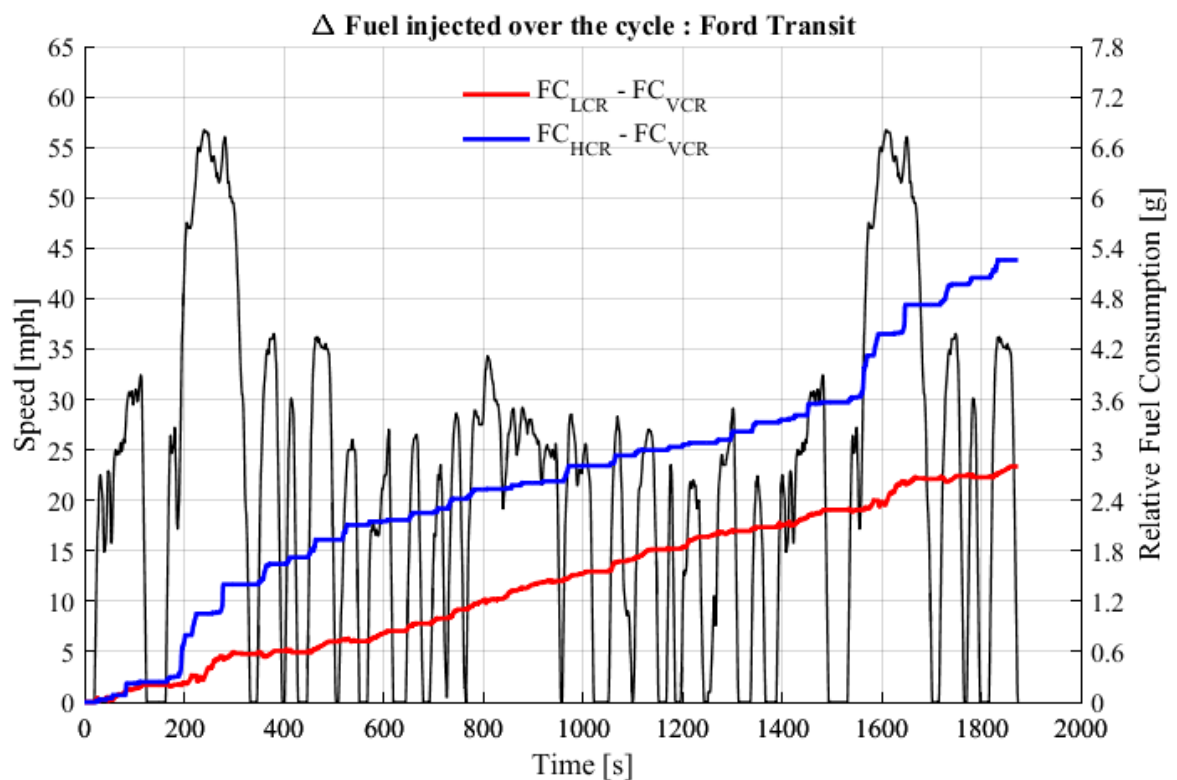


Figure 49 – Plot of the lines representing the relative fuel consumption of the LCR with respect to the VCR (red) and of the HCR with respect to the VCR (blue), considering a Ford Transit equipped with a DT.

Impact of the vehicle characteristics and of the drive cycle

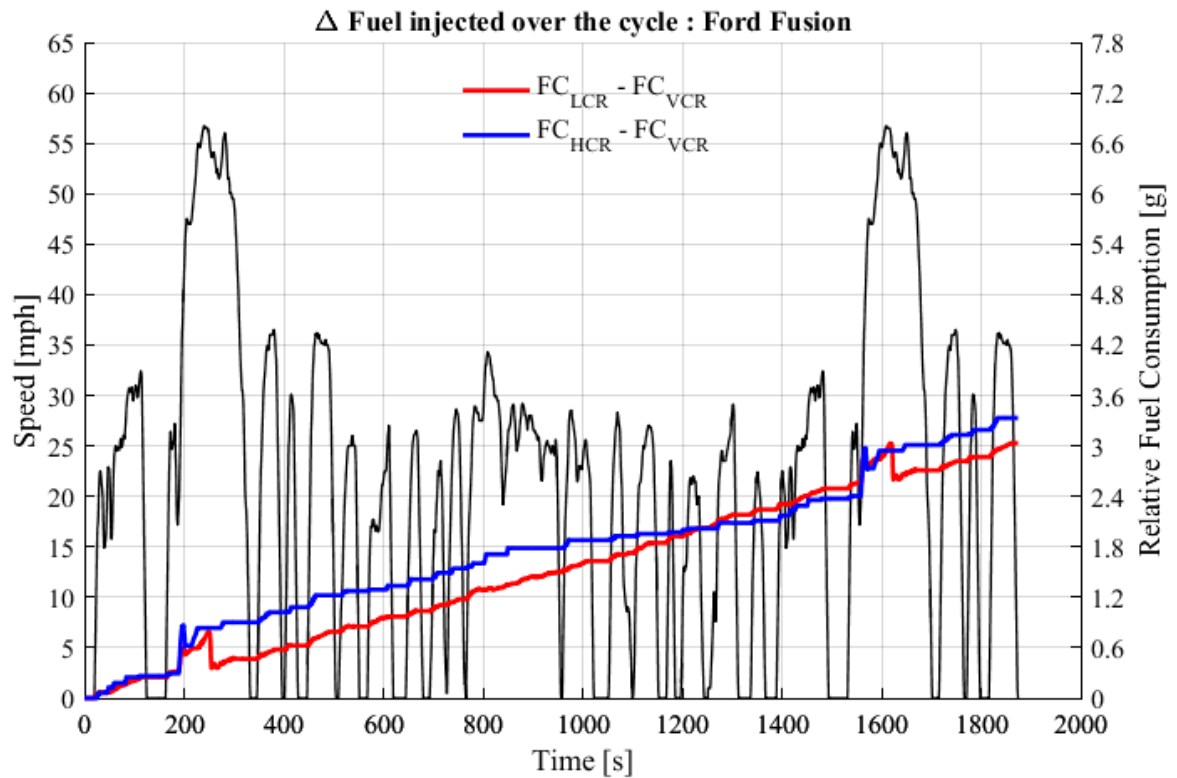


Figure 50 – Plot of the lines representing the relative fuel consumption of the LCR with respect to the VCR (red) and of the HCR with respect to the VCR (blue), considering a Ford Fusion equipped with a DT.

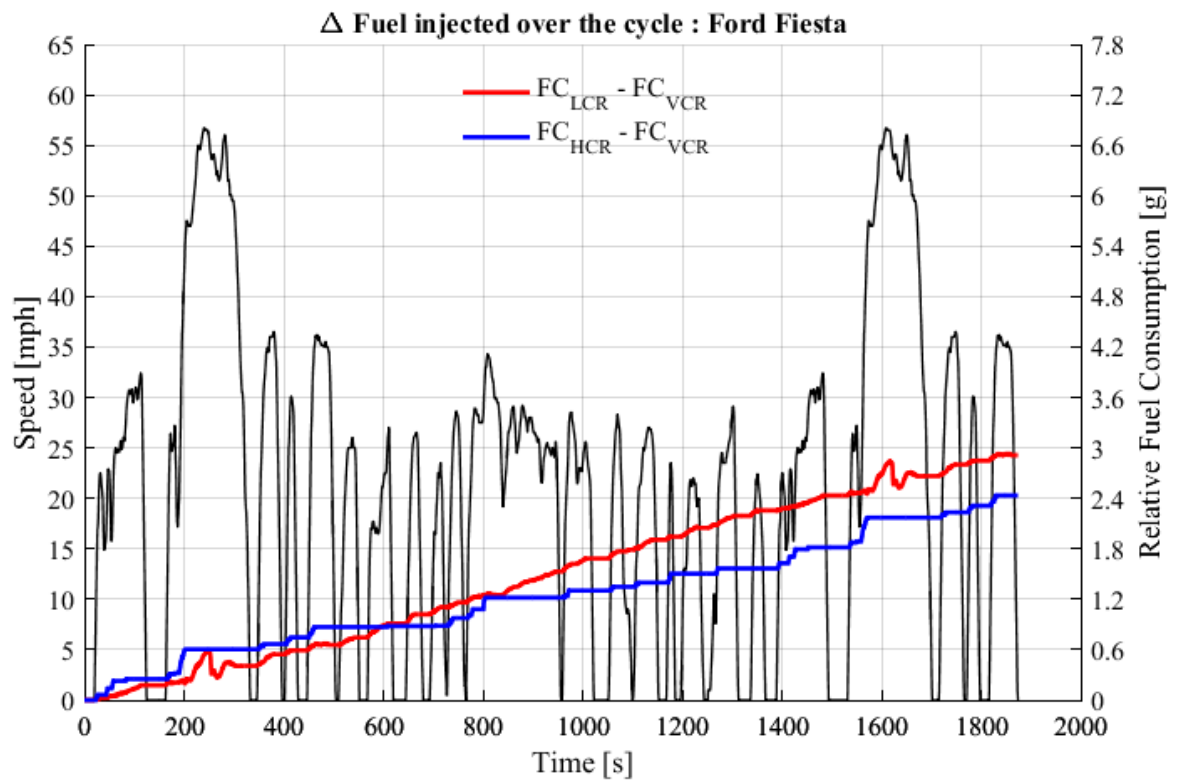


Figure 51 – Plot of the lines representing the relative fuel consumption of the LCR with respect to the VCR (red) and of the HCR with respect to the VCR (blue), considering a Ford Fiesta equipped with a DT.

Impact of the vehicle characteristics and of the drive cycle

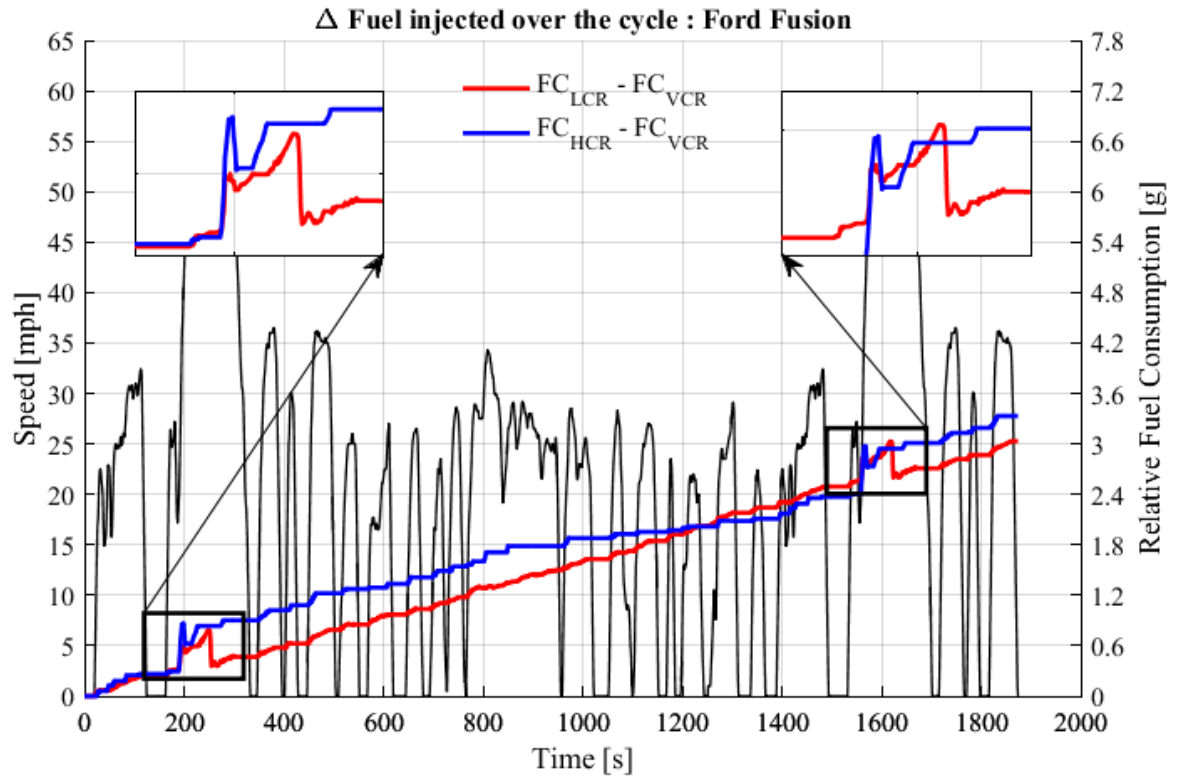


Figure 52 – Detail of the oscillations in the relative fuel consumption for the Ford Fusion

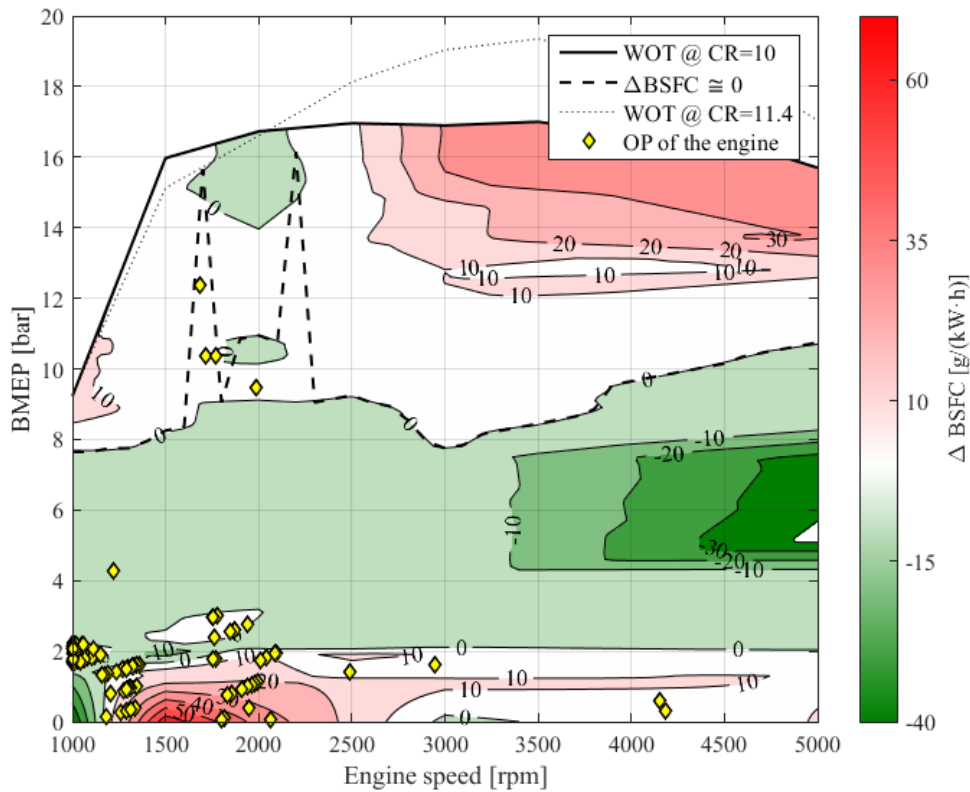


Figure 53 – Differential map $\Delta BSFC$ with operating points corresponding to the peaks highlighted in **Figure 52**

Impact of the vehicle characteristics and of the drive cycle

In conclusion, it is difficult to identify a clear relationship between the effectiveness of a VCR system and vehicles characteristics, indeed changing the modelled vehicle results in several parameters changing simultaneously, including weight, aerodynamic behavior, and transmission ratios. For this reason, an additional study in which mass and final drive ratio were changed independently was performed in order to isolate the role of these parameters on the effectiveness of a VCR system.

7.2 Impact of the mass and of the final drive ratio

For this study, only the Ford Escape was considered. In particular, three different masses and three different final drive ratios were considered: 3000, 4000 and 5000 *lbs* and 3, 3.51 and 4 as final drive ratios. As mentioned before, these two parameters were changed one at the time, keeping all the other vehicle characteristics unchanged. The drive cycle considered was the FTP-75.

At first the impact of the mass was considered. Two different runs were performed, one for the CVT and one for the DT. For each type of transmission, the fuel economy for the two static CR and for the VCR was determined for every different mass, so that to determine how the vehicle mass effects the effectiveness of a VCR system. **Figure 54** shows the results for the CVT, while **Figure 55** is relative to the vehicle equipped with a DT.

Figure 54 confirms that a VCR system is more effective with decreasing vehicle mass due to the lower power demand, and its tendency to thus operate with a high compression ratio over a larger portion of the drive cycle. **Figure 55** shows that similar to the CVT case, for a vehicle equipped with a DT, a VCR system is also more effective with reducing vehicle mass.

Impact of the vehicle characteristics and of the drive cycle

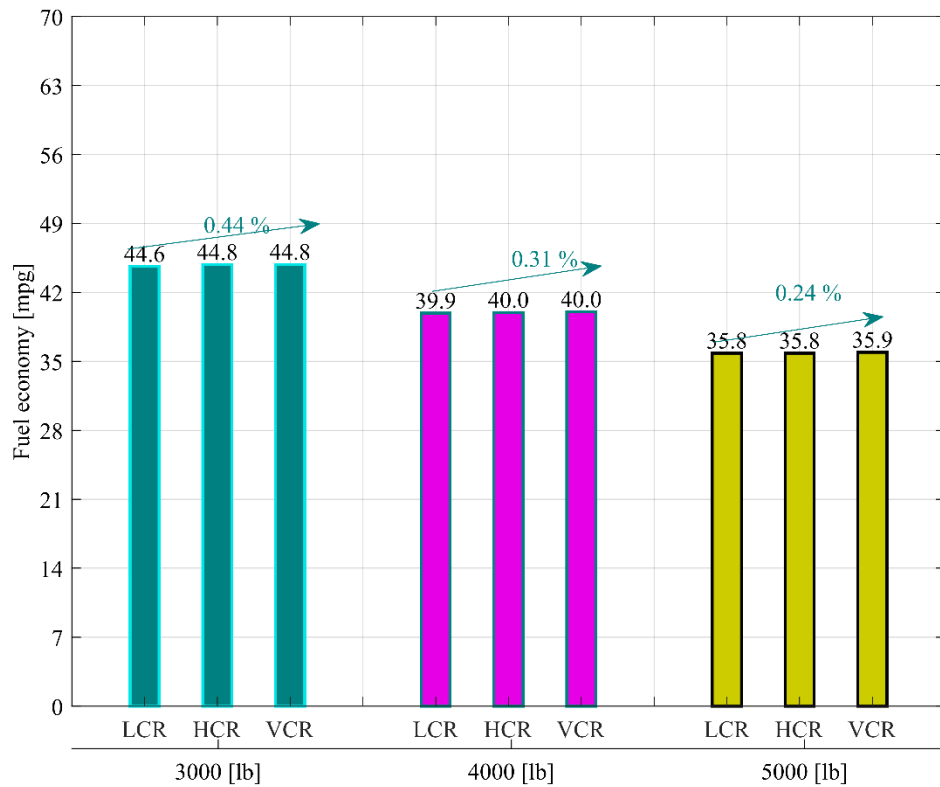


Figure 54 – Bar plot for the fuel economy considering different test masses, considering a CVT and the FTP-75 as drive cycle.

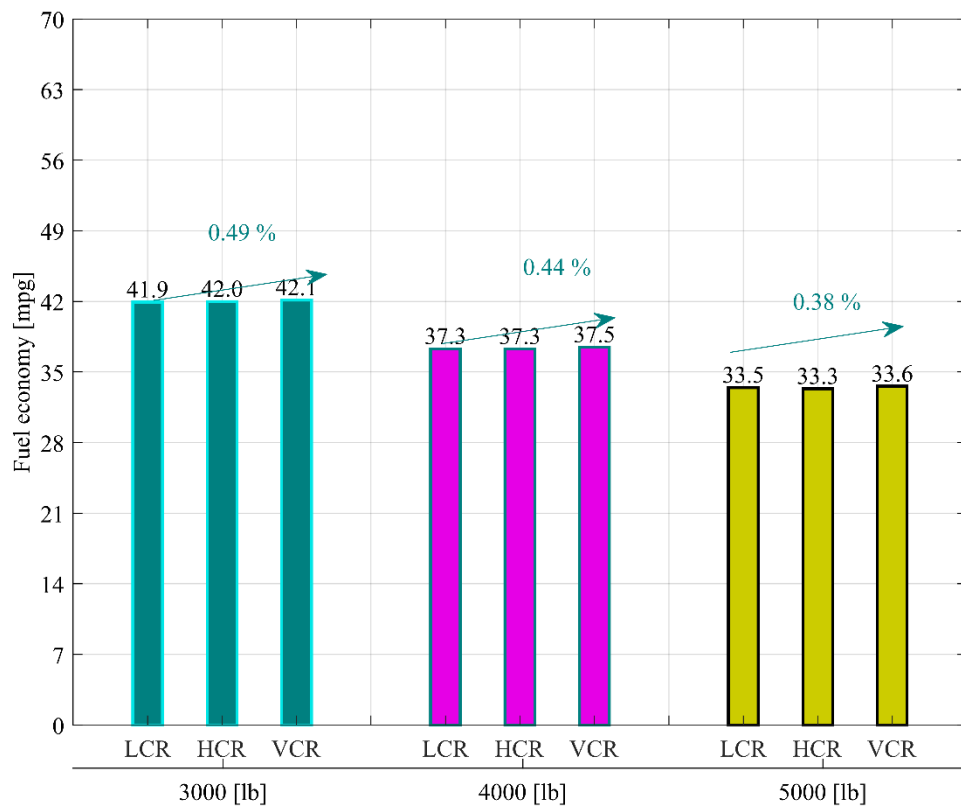


Figure 55 – Bar plot for the fuel economy considering different test masses, considering a DT and the FTP75 as drive cycle.

Impact of the vehicle characteristics and of the drive cycle

Considering the impact of the final drive ratio, **Figure 56** shows that the final drive ratio, in the case of a vehicle equipped with a CVT, does not have any influence on the behavior of a VCR system. Since an ideal CVT is considered, an infinite number of transmission ratios is available and so the engine will operate always at the point that minimizes the fuel consumption, independently from the final drive ratio.

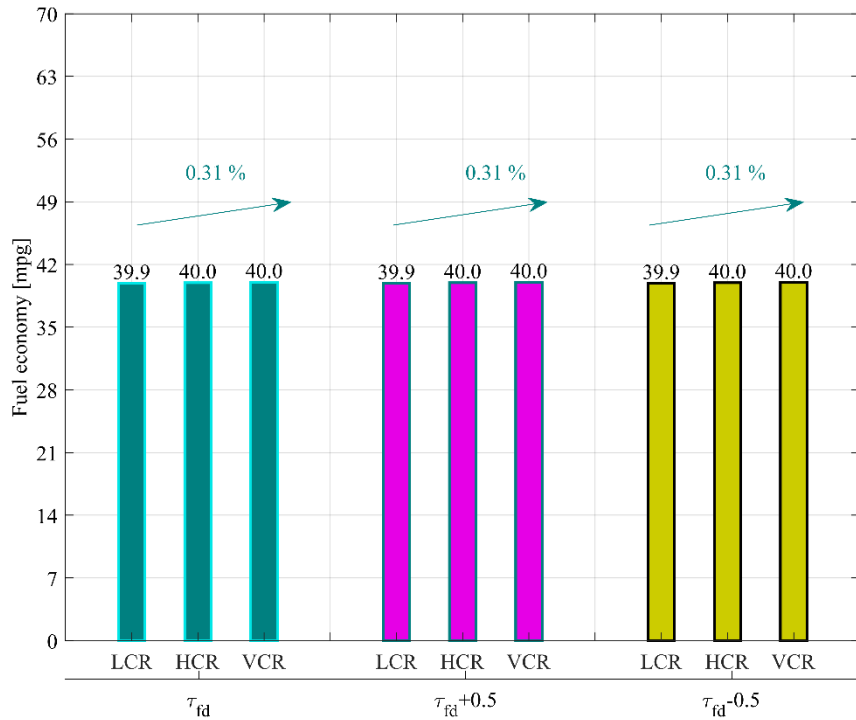


Figure 56 – Bar plot for the fuel economy considering different final drive ratios, considering a CVT and the FTP-75 as drive cycle.

In the case of a vehicle equipped with a DT, the final drive ratio does have an impact on the VCR system, as shown in **Figure 57**. In particular, with a reduced final drive ratio, the fuel economy benefits of a VCR system are increased.

Impact of the vehicle characteristics and of the drive cycle

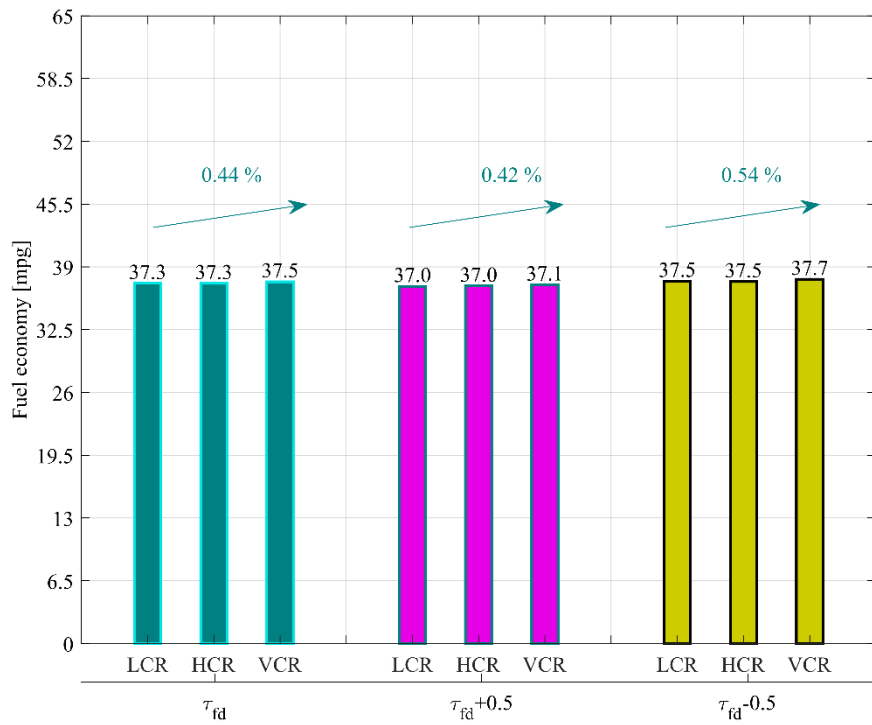


Figure 57 – Bar plot for the fuel economy considering different final drive ratios, considering a DT and the FTP-75 as drive cycle.

7.3 Impact of the drive cycle

At last, it is necessary to analyze the influence of the speed profile followed by the vehicle. All the considered drive cycles were already presented in Chapter 2, where a simple cycle characterization was also carried out. The FTP-75, WLTP and NEDC were determined to require overall lower power demands, while the HWFET was the one characterized by the lowest acceleration. Finally, the US06 required the highest average power demand over the drive cycle, but also represents the most “real-world” driving conditions. The comparison between the different drive cycles was performed considering the Ford Escape as the modelled vehicle.

Figure 58 and **Figure 59** show the results for the vehicle equipped with CVT and a DT respectively. In both cases it can be noticed that drive cycles characterized by low accelerations (i.e. FTP, HWFET, NEDC) are the ones over which a VCR is more effective. Whereas, for drive cycles characterized by high accelerations and high power demand (i.e. US06), the benefits from a VCR system are negligible due to the necessity of operating at low compression ratio over a larger portion of the drive cycle. In the case of the DT, the results relative to the US06 have to be neglected since the vehicle is not capable of meeting the power demand required over the drive cycle with the specified engine/transmission configuration.

Impact of the vehicle characteristics and of the drive cycle

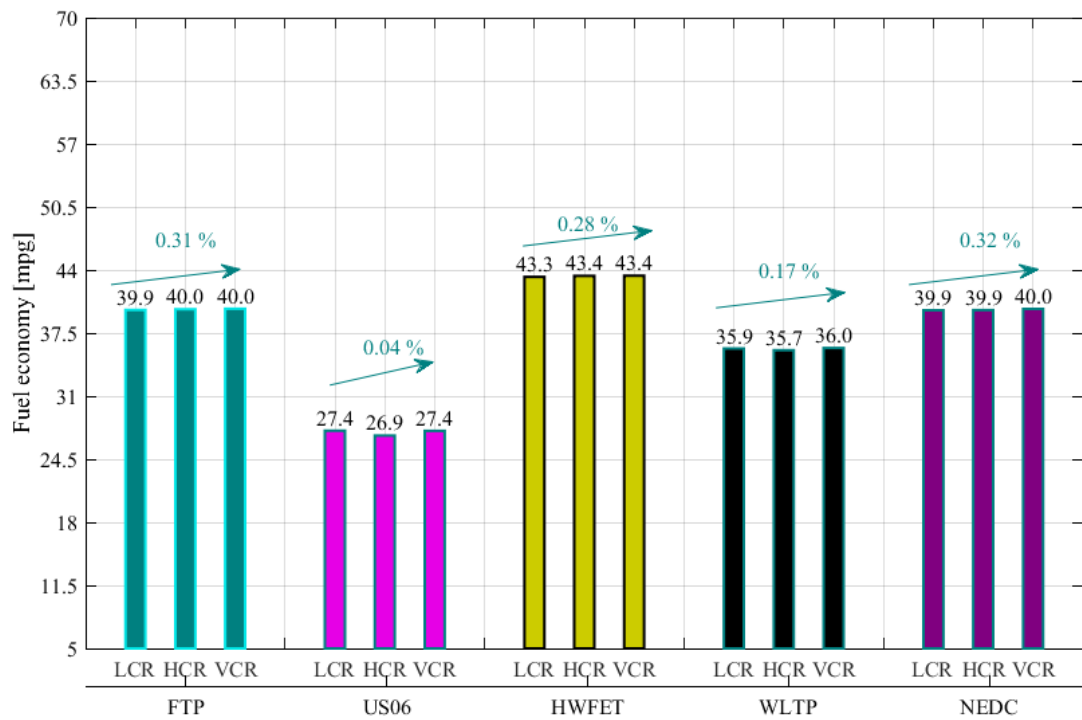


Figure 58 – Bar plot for the comparison between drive cycles, considering a vehicle equipped with a CVT.

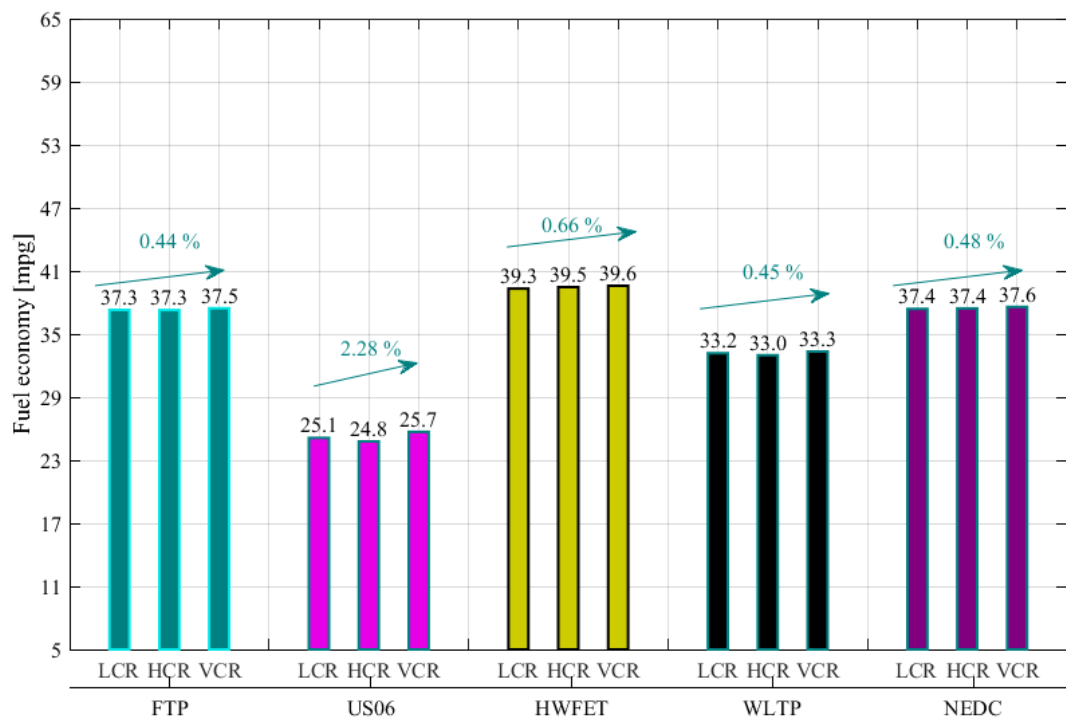


Figure 59 – Bar plot for the comparison between drive cycles, considering a vehicle equipped with a CVT

7.4 Conclusions

In **Table 7** and **Table 6**, the results of the analysis of the impact of the vehicle characteristics and of the drive cycles are summarized. Each percentage represents the improvement in fuel economy with respect to the baseline (i.e. the LCR). Once again, it is necessary to state that the results for the DT over the US06 should be neglected since the vehicle is not capable of following the drive cycle.

In conclusion, it is reasonable to say that VCR systems are better suited for lightweight vehicles and drive cycles characterized by low accelerations. Moreover, they perform at their best if applied to a vehicle equipped with a DT, indeed since CVTs already have the aim of minimizing fuel consumptions. Furthermore, the benefits observed in this study are strongly limited by the very small difference between the two compression ratios used to develop the engine maps, and greater fuel economy benefits could be expected with the usage of a wider range of compression ratio, or a 3-step VCR system.

Continuously variable transmission				
Drive cycle	Escape	Transit	Fusion	Fiesta
FTP	0.31%	0.30%	0.40%	0.52%
HWFET	0.28%	0.31%	0.48%	0.64%
US06	0.04%	0.03%	0.02%	0.02%
NEDC	0.32%	0.37%	0.53%	0.40%
WLTP	0.17%	0.17%	0.22%	0.30%
Combined	0.24%	0.23%	0.41%	0.62%

Table 6 – Results of the analysis of the impact of the vehicle characteristics and of the drive cycles for vehicle equipped with a CVT

Impact of the vehicle characteristics and of the drive cycle

Discrete transmission				
Drive cycle	Escape	Transit	Fusion	Fiesta
FTP	0.44%	0.33%	0.40%	0.44%
HWFET	0.66%	0.59%	0.68%	0.61%
US06	2.28%	3.91%	2.21%	3.18%
NEDC	0.48%	0.51%	0.69%	0.71%
WLTP	0.45%	0.32%	0.39%	0.52%
Combined	0.62%	0.48%	0.54%	0.60%

Table 7 – Results of the analysis of the impact of the vehicle characteristics and of the drive cycles for vehicle equipped with a DT

Chapter 8

3-stage VCR

In this chapter the effect of the addition of a third compression ratio to the VCR system is investigated. Increasing the number of CRs that can be exploited should, in principle, increase the effectiveness of the VCR system, due to the improved adaptability of the system to different working conditions. Moreover, the effect of an increased gap between the used CRs is analyzed as well. Since the performance maps used for this study are not yet publishable, no numeric results, in terms of BSFC and fuel economy, will be provided in this chapter.

8.1 Engine maps

In order to perform this study, new engine performance maps were necessary, since the data from Oak Ridge National Laboratories [17] presented in previous chapters utilized just two compression ratios. For this reason, new maps were provided by Argonne National Laboratory. Maps relative to three different compression ratios, 10.5:1, 12.5:1 and 14.5:1, ratios were provided. They will be referred to as LCR, MCR and HCR respectively. They were obtained from bench tests of a single cylinder, naturally aspirated engine run with E10. Being a single cylinder engine, the BMEP was estimated through an assumption on the friction. Moreover, this engine was not run at speeds higher than 2500 *rpm*, and no information about the engine geometry was provided.

Obviously, these maps were unusable as they were provided, as it was necessary, through some assumptions, to extrapolate them toward higher engine speeds. First of all, since the new maps were not from a production engine, no data about a vehicle equipped with this engine was available. Thus, in order to provide a better comparison to the previous work, the data for the Ford Escape were used. For the same reason, the displacement was assumed to be equal to 2.5 L, in order to develop approximately the same power as the 1.6 L Ford EcoBoost engine. Then, in order to extrapolate the maps, it was necessary to add points to the experimental data. In order to maintain the reliability of the engine maps, the number of additional points was limited to as few as possible. As shown in **Figure 60**, **Figure 61** and **Figure 62**, for each compression ratio, three approximately idle points were added to ensure the correct behavior of the maps at low loads, plus two to three points at the maximum engine speed, in order to ensure a correct extrapolation. The BSFC values associated with these additional points were determined by looking at performance maps of similar engines. In particular the study of Königstein and Grebe [21] shows a performance map for a 1.8 L naturally aspirated, multi-port fuel injection engine with a CR equal to 10:1. In particular this engine shows

3-stage VCR

that, moving from 2500 *rpm* to 5000 *rpm*, the BSFC increases by about the 15%, thus the same worsening factor was applied to the map of the 10.5:1 CR coming from Argonne National Laboratory to identify the BSFC values of the additional points at the maximum engine speed.

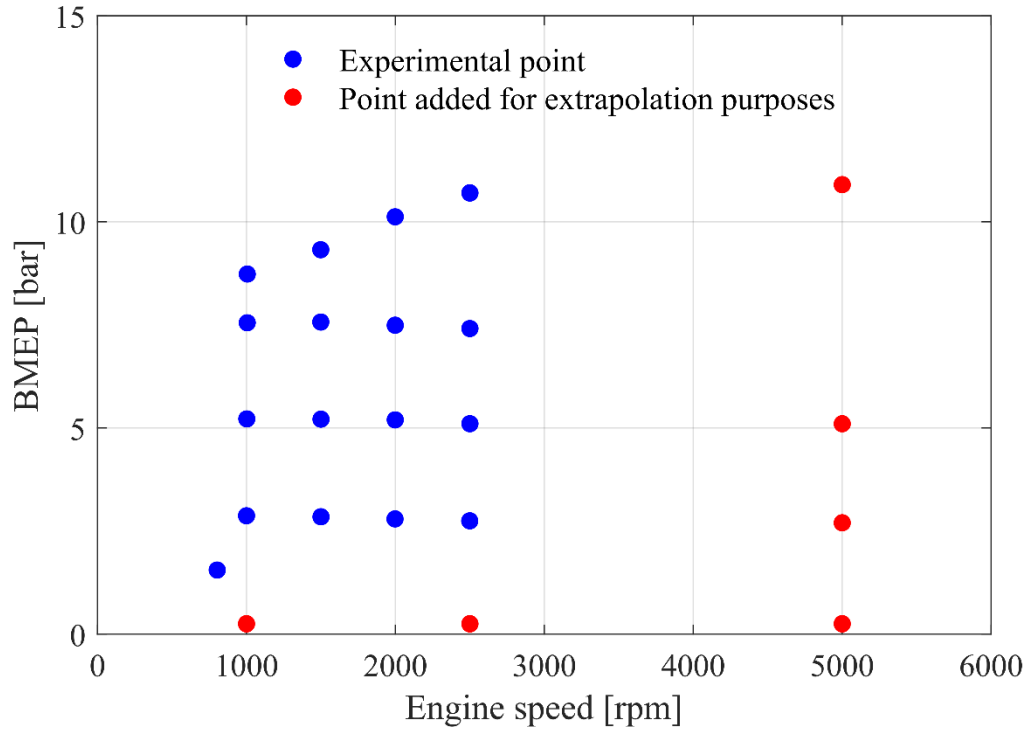


Figure 60 – Plot showing the location of the experimental points and of the additional points for the 10.5:1 CR

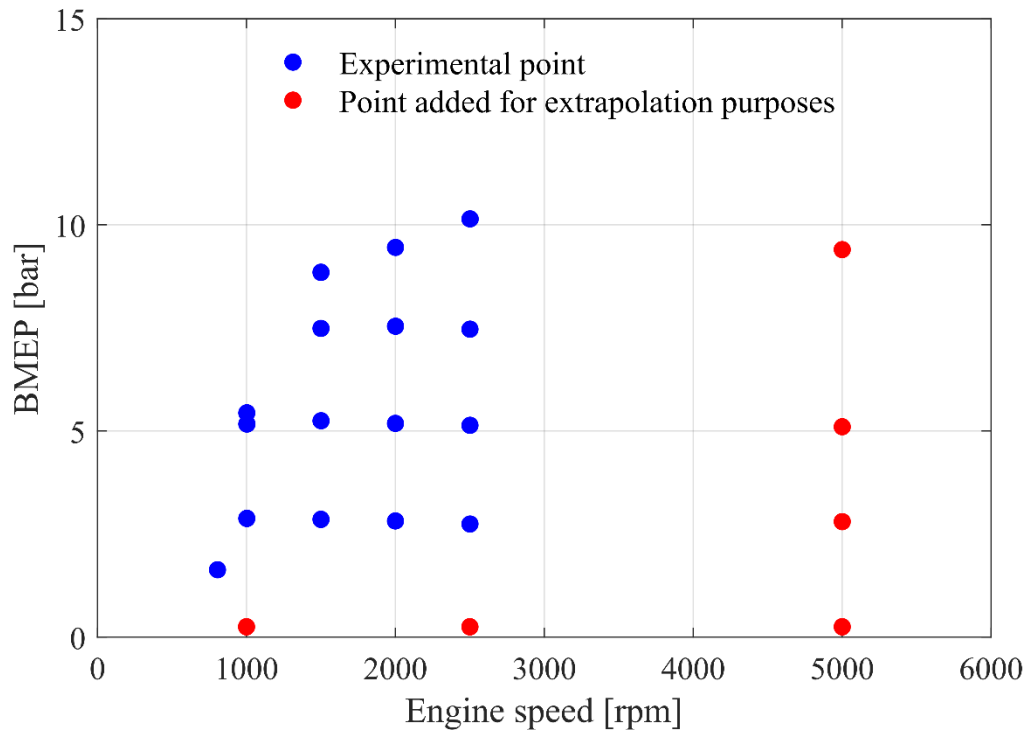


Figure 61 – Plot showing the location of the experimental points and of the additional points for the 12.5:1 CR

3-stage VCR

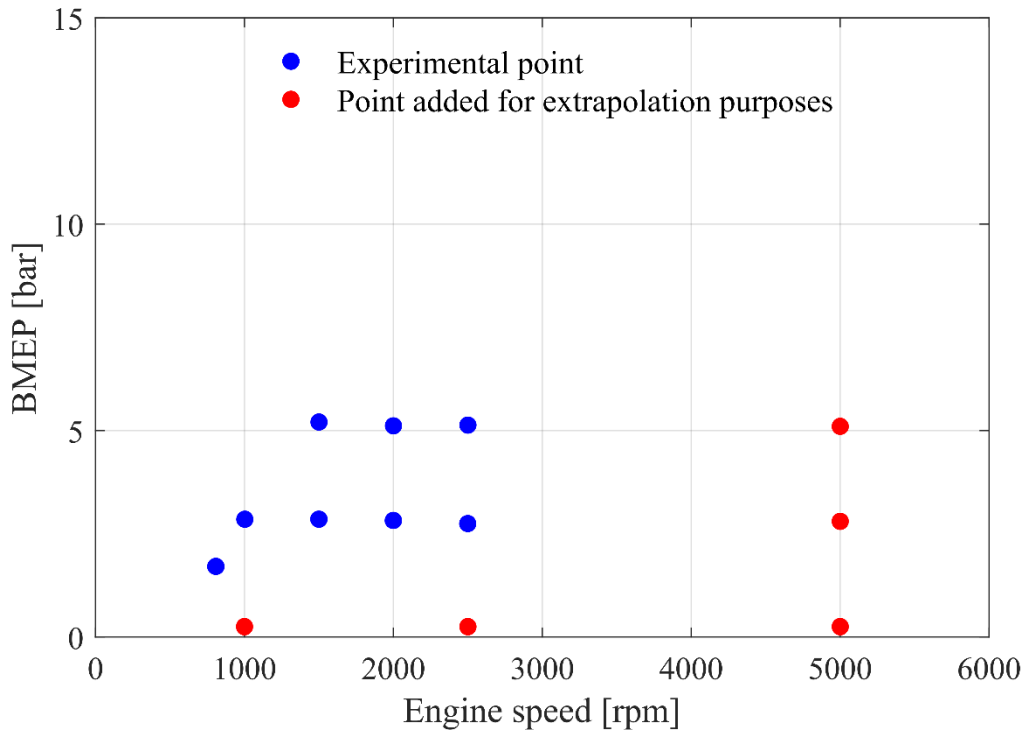


Figure 62 – Plot showing the location of the experimental points and of the additional points for the 14.5:1 CR

Next, the points at idle were added. At first a point at 2500 *rpm* was set, then, once again, the point at the same load but at 5000 *rpm* was associated to a BSFC value 15% worse than the one at 2500 *rpm*. Finally a point at 1000 *rpm* was set, imposing a BSFC value 5% worse than the 2500 *rpm* point. All these worsening percentages and the BSFC value of the point at 2500 *rpm* were selected making reference to the study of Königstein and Grebe [21].

In order to add points to the maps corresponding to the higher compression ratios, a scaling of the BSFC from the baseline 10.5:1 case was performed. The increase in engine efficiency due to the use of a higher compression ratio was evaluated according to Equation (2), presented in Chapter 2. The BSFC was assumed to improve by the same percentage. At this point it was necessary to make some assumptions also on the Wide Open Throttle curve (WOT) and on the Knock limit of the different CRs. Looking at the maps coming from the Oak Ridge National Laboratories [17], it was noticed that the WOT curve and the Knock limit can be well fitted by a polynomial function of third order. For this reason, a polynomial function of the previously mentioned order was fitted to the available point of the WOT curve of the 10.5:1 CR. In this way it was possible to extend the WOT curve up to 5000 *rpm*. For the 12.5:1 CR, the knock limit was obtained simply shifting down of 0.6 *bar* the WOT line of the lower compression ratio. A shift of this quantity was applied since the available point of the knock limit of the 12.5:1 CR are positioned at a load 0.6 *bar* lower than the available points of the

3-stage VCR

WOT curve of the 10.5:1 CR. Regarding the 14.5:1 CR, a knock limit at almost constant load was considered to be reasonable being the compression ratio very high.

Once the BSFC values of the additional points were specified and obtained the WOT curves and knock limits, it was possible to extrapolate the maps. **Figure 63**, **Figure 64** and **Figure 65** show the final result of this surface fitting. At this point, it was possible to identify the switch lines between the low and the intermediate compression ratio and between low and high compression ratio. The procedure followed to obtain them is the same presented in Chapter 2. **Figure 66** and **Figure 67** show a detail of the switch lines in the two possible cases.

It should be noted that due to the many approximations and assumptions made in the development of these maps, any results derived from them carry with them a high degree of uncertainty. Nevertheless, given the lack of available and complete maps, this approach was necessary, as the purpose of this work was to study the potential benefits of a 3-step versus a 2-step VCR system, and in particular, with a larger delta between the low and high compression ratios as would be represented in a production system.

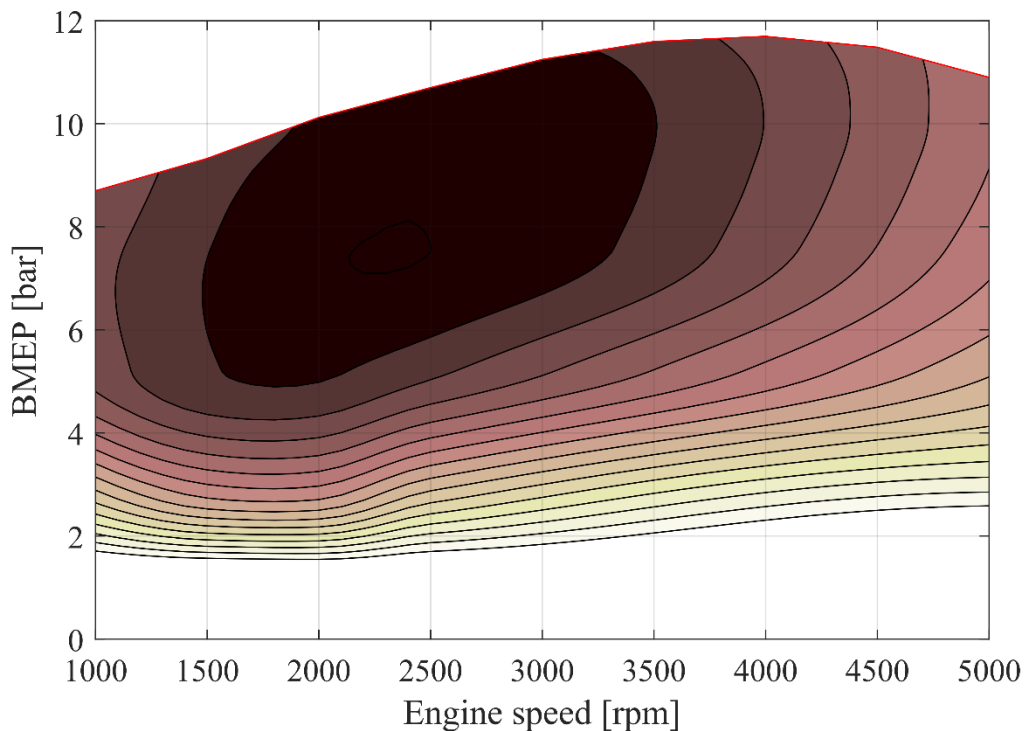


Figure 63 – BSFC map for the 10.5:1 CR

3-stage VCR

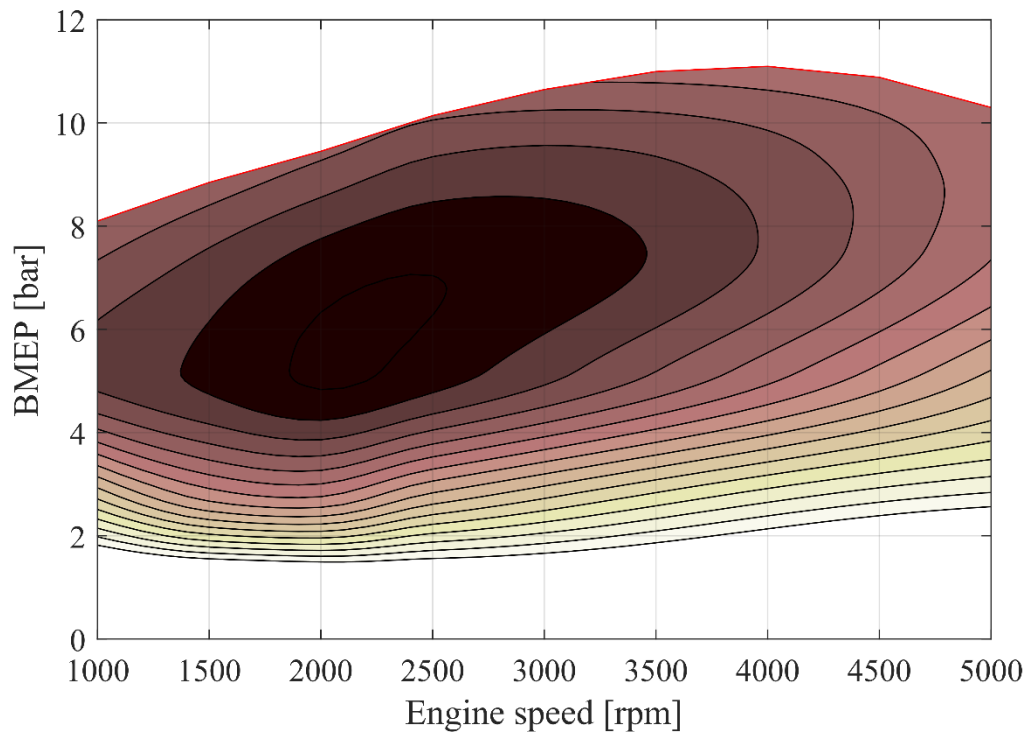


Figure 64 – BSFC map for the 12.5:1 CR

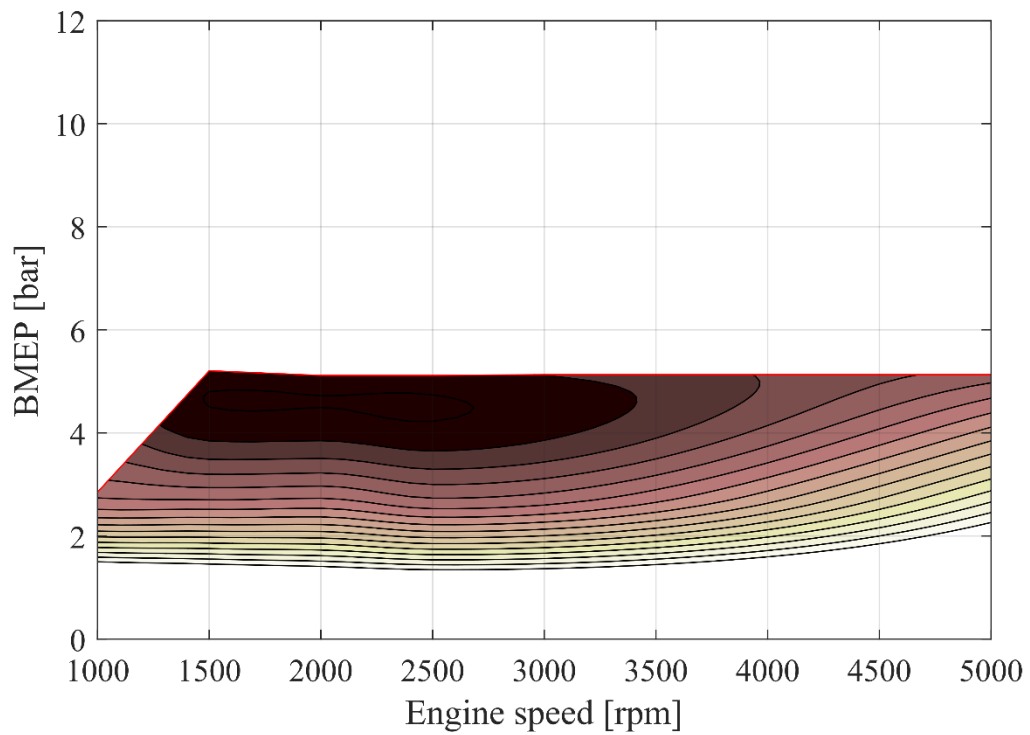


Figure 65 – BSFC map for the 14.5:1 CR

3-stage VCR

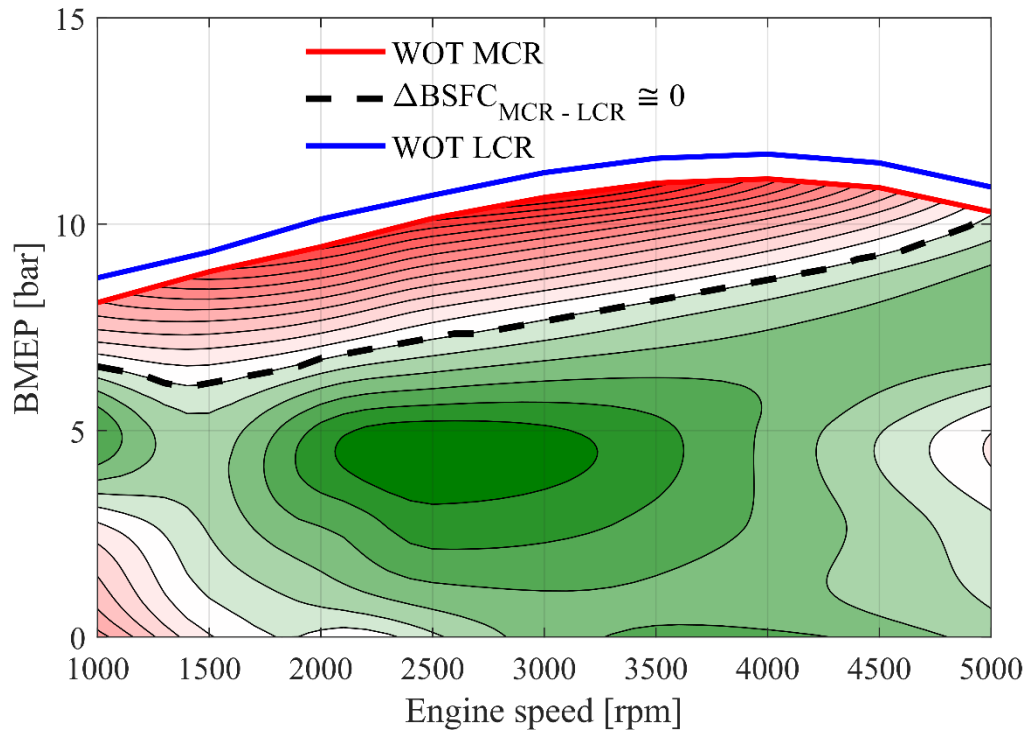


Figure 66 – Plot of the differential map $\Delta BSFC$ between LCR and MCR and detail of the switching line

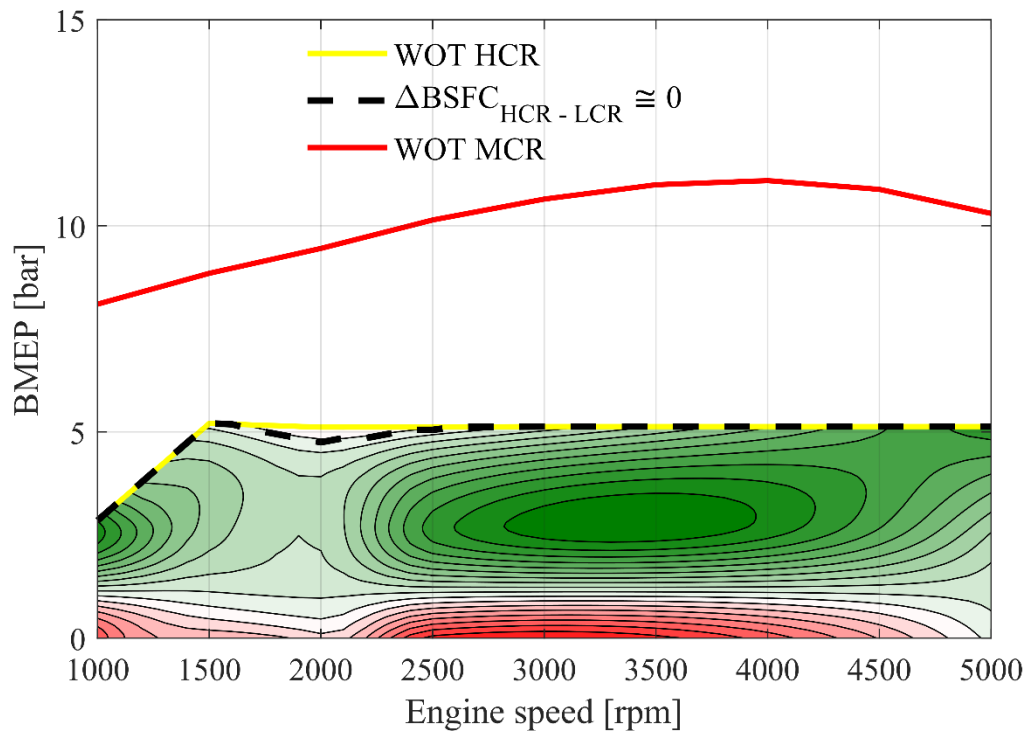


Figure 67 – Plot of the differential map $\Delta BSFC$ between LCR and HCR and detail of the switching line

3-stage VCR

Exactly as in the case of the maps from Oak Ridge National Laboratories, it is difficult to find distinct operating areas for the different compression ratios. In particular, considering **Figure 67**, for almost all the range of speed of the engine at loads under 1 *bar*, the LCR is the compression ratio characterized by the best BSFC, even if under the switching line the HCR should always be the better. In the same way, looking at **Figure 66**, for engine speeds lower than 1500 *rpm* and loads lower than 3 *bar*, the LCR is better than the MCR, even if the latter should be the optimal one in this area. These irregularities are both due to uniformities in the experimental data and to the method used to extrapolate and fit the maps. However, as mentioned before, this behavior is not different from that reported in the experimental performance maps for the Ford 1.6 L EcoBoost.

8.2 Results validation

First of all, it is necessary to ensure that the obtained results using these maps are reliable. For this reason, the new performance maps were used for simulations for both vehicles equipped with a CVT and a DT on two different drive cycles, FTP-75 and US06. The target of these simulations was to show that most of the engine operating points were concentrated at engine speeds lower than 2500 *rpm*, thus where all the experimental data are concentrated. Considering at first a vehicle equipped with a CVT performing the FTP-75, **Figure 68** shows the engine operating points for a 3-stage VCR, **Figure 69** shows the engine operating points for a 2-stage VCR exploiting the 10.5 and 12.5 CRs and **Figure 70** shows the engine operating points for a 2-stage VCR exploiting the 10.5 and 14.5 CRs.

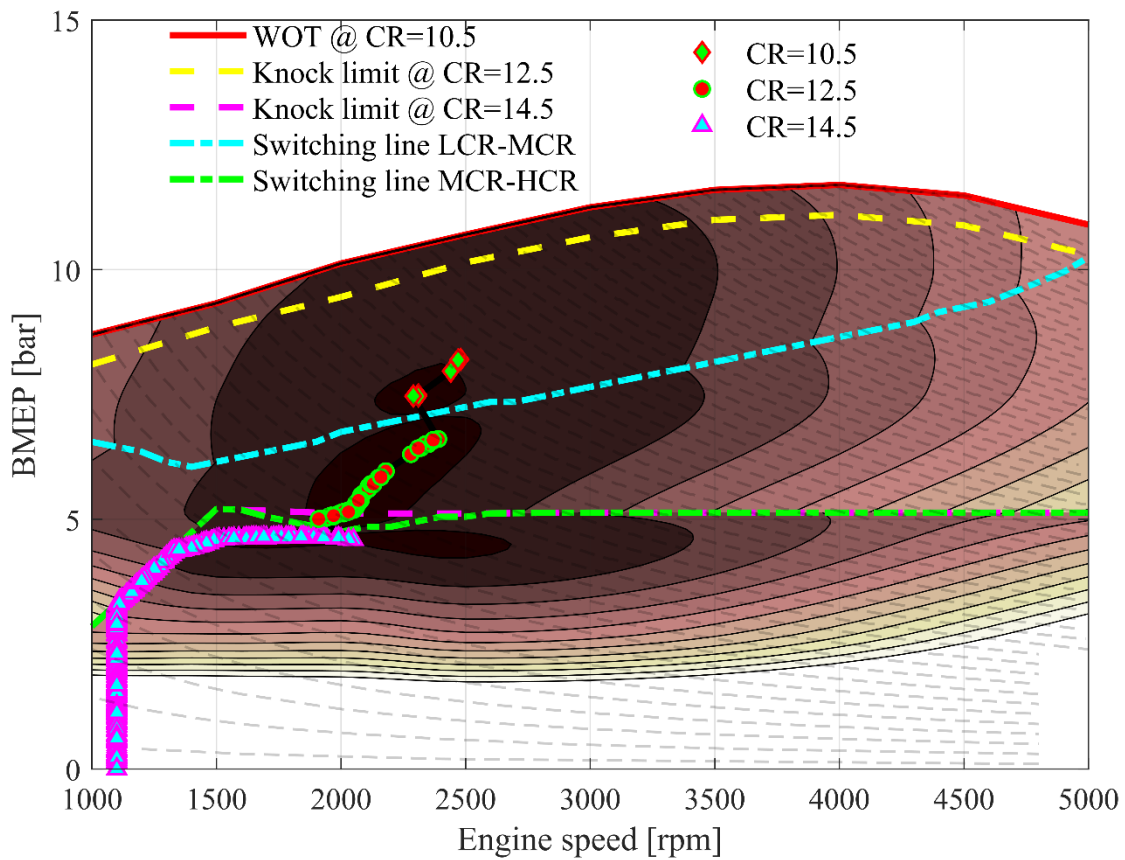


Figure 68 – Operating points of the engine over the performance map in the case of a 3-stage VCR, for a vehicle equipped with a CVT, driven along the FTP-75.

Looking at **Figure 68**, it is possible to notice immediately that most of the engine operating points are below the threshold of 2500 *rpm*. Moreover, the HCR is the most used along the drive cycle, because of its improved engine efficiency. Being the FTP-75 characterized by a low power demand and low accelerations, the HCR can be used over the majority of the cycle without the risk of knock insurgence.

3-stage VCR

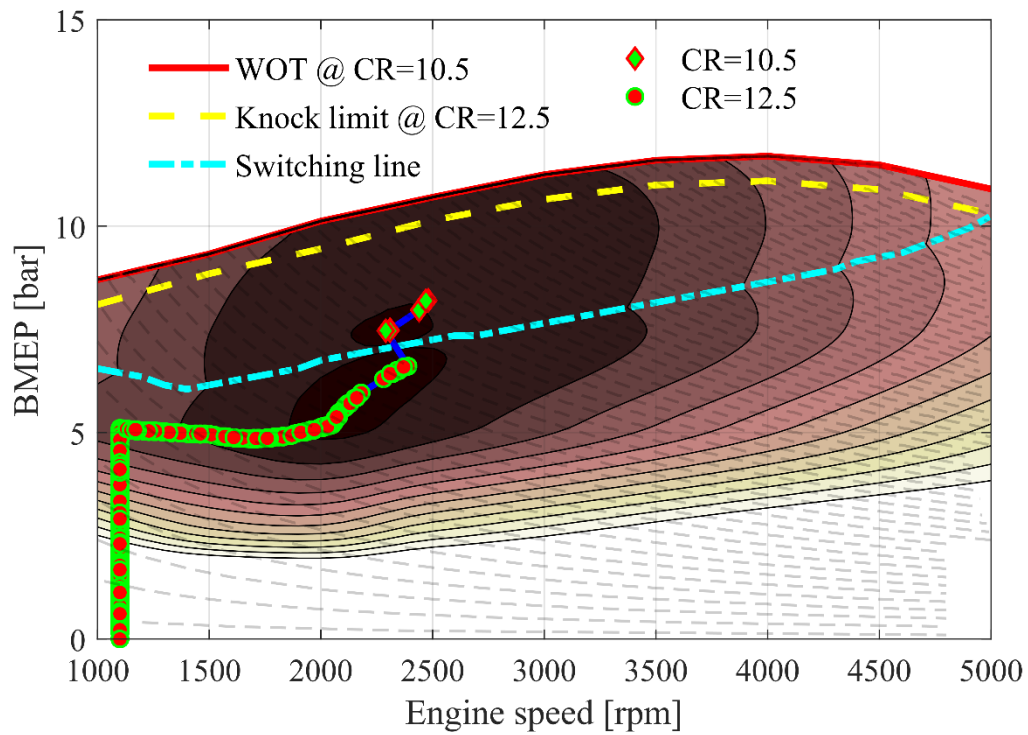


Figure 69 – Operating points of the engine over the performance map in the case of a 2-stage VCR, for a vehicle equipped with a CVT, driven along the FTP-75.

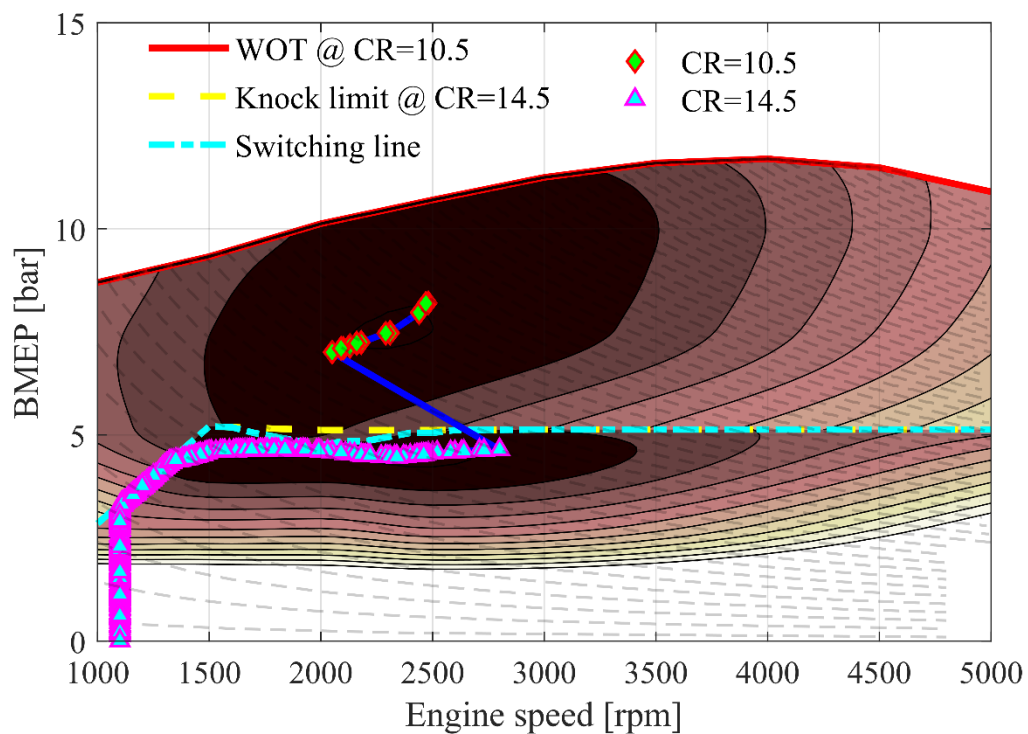


Figure 70 – Operating points of the engine over the performance map in the case of a 2-stage VCR, for a vehicle equipped with a CVT, driven along the FTP-75.

3-stage VCR

Looking instead at **Figure 69** and **Figure 70**, the same behavior can be noticed, even if only a 2-stage VCR system was exploited. Most of the engine operating points are below 2500 *rpm*, and the higher compression ratio among the two available is almost always used, for the sake of improving efficiency.

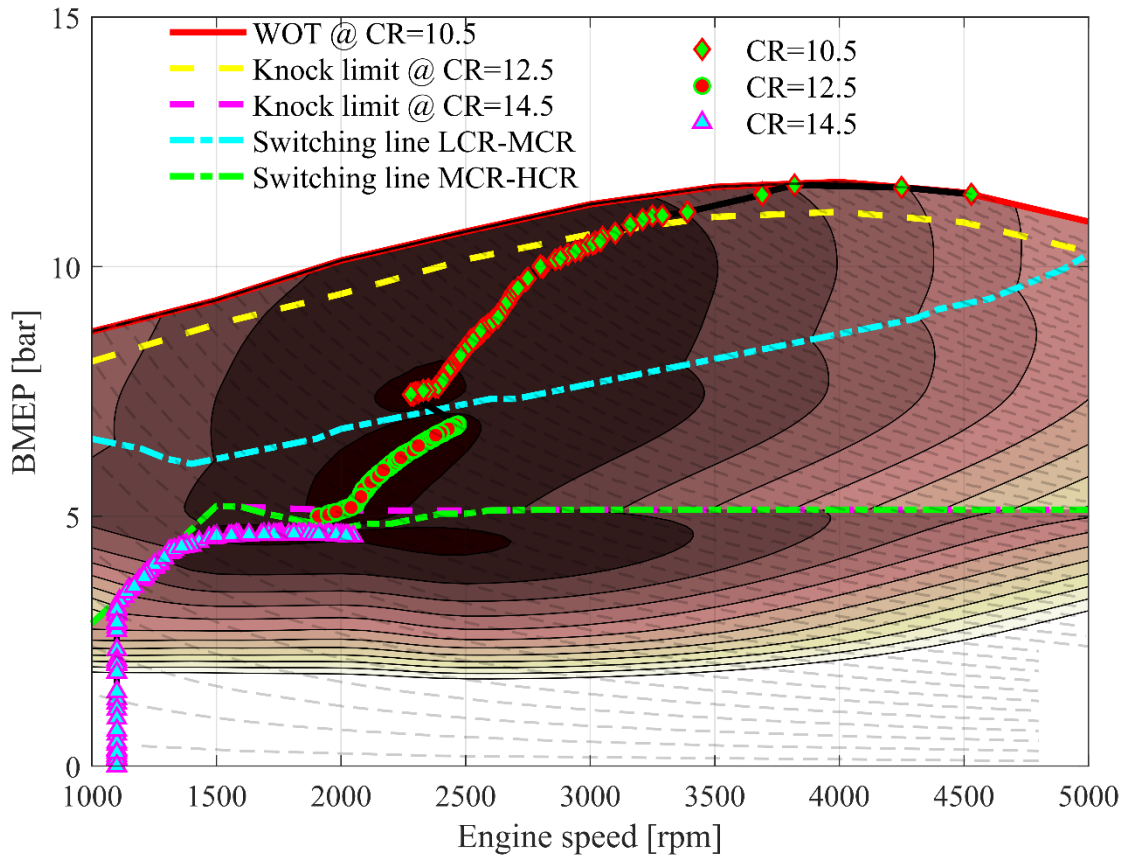


Figure 71 – Operating points of the engine over the performance map in the case of a 3-stage VCR, for a vehicle equipped with a CVT, driven along the US06.

Considering instead the US06 as drive cycle, **Figure 71** shows the engine operating points over the performance map in the case of a 3-stage VCR. Differently from the results relative to the FTP-75, many operating points are moved to speeds higher than 2500 *rpm* because of the higher power demand, those most of the operating points are still under that threshold. Moreover, the LCR is now much more frequently used because of the increased power demand, while the usage of the HCR is indeed limited by knock insurgence. The results for the two possible 2-stage VCR systems were not reported because no significant changes from the behavior just commented were observed. This same analysis was then repeated for a vehicle equipped with a DT. AT first, a run on the FTP-75 was performed. **Figure 72** shows the engine operating points on the performance map.

3-stage VCR

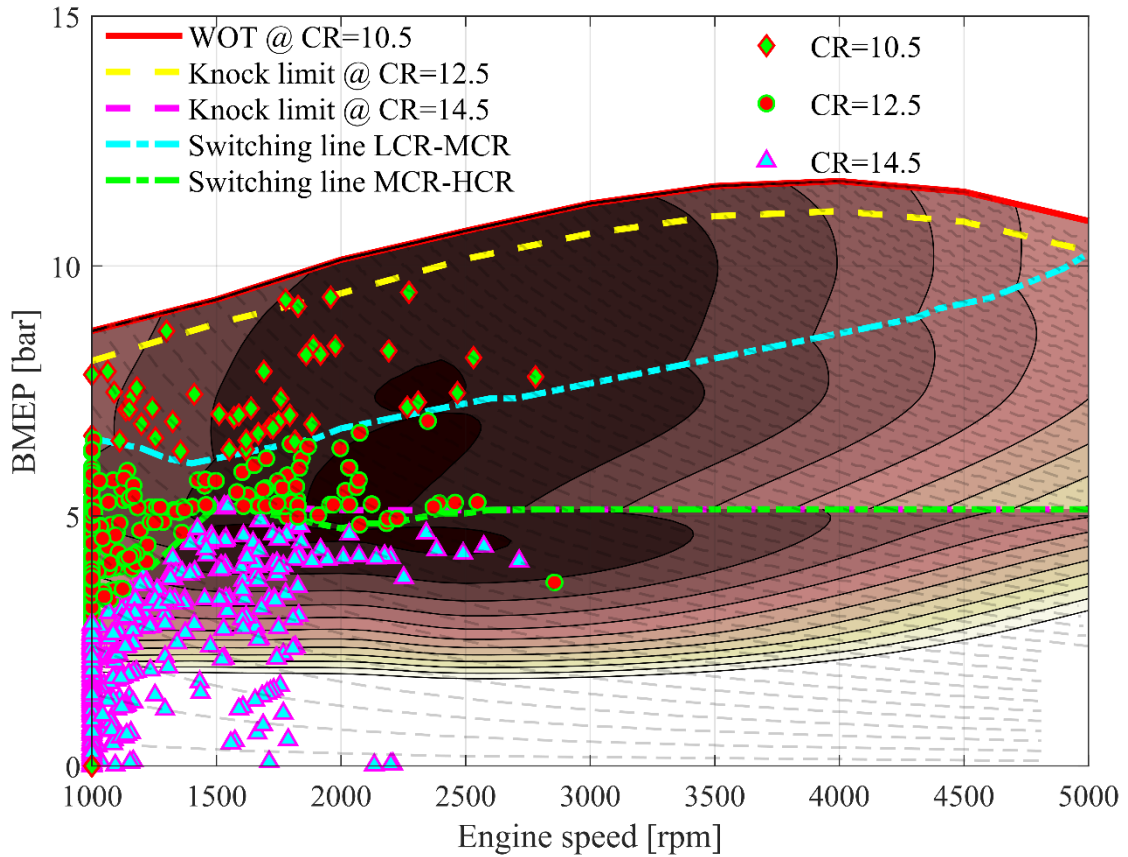


Figure 72 – Operating points of the engine over the performance map in the case of a 3-stage VCR, for a vehicle equipped with a DT, driven along the FTP-75.

As for the CVT, most of the operating points are located at engine speeds lower than 2500 *rpm* and the HCR is the one more frequently exploited. However, points are much more scattered and, in particular, several points at low loads can be noticed. As mentioned before, in this region, the maps were completed by artificial points. For this reason, the results for the DT are less reliable than those of the CVT. Furthermore, differently from the corresponding case for the CVT, the MCR and the LCR are much more frequently utilized. This is due to the discrete transmission ratios that constrain the engine speed-load points. Indeed, not having an infinite number of transmission ratios, it is not always possible to work in the optimal working point, hence the one minimizing the fuel consumptions.

3-stage VCR

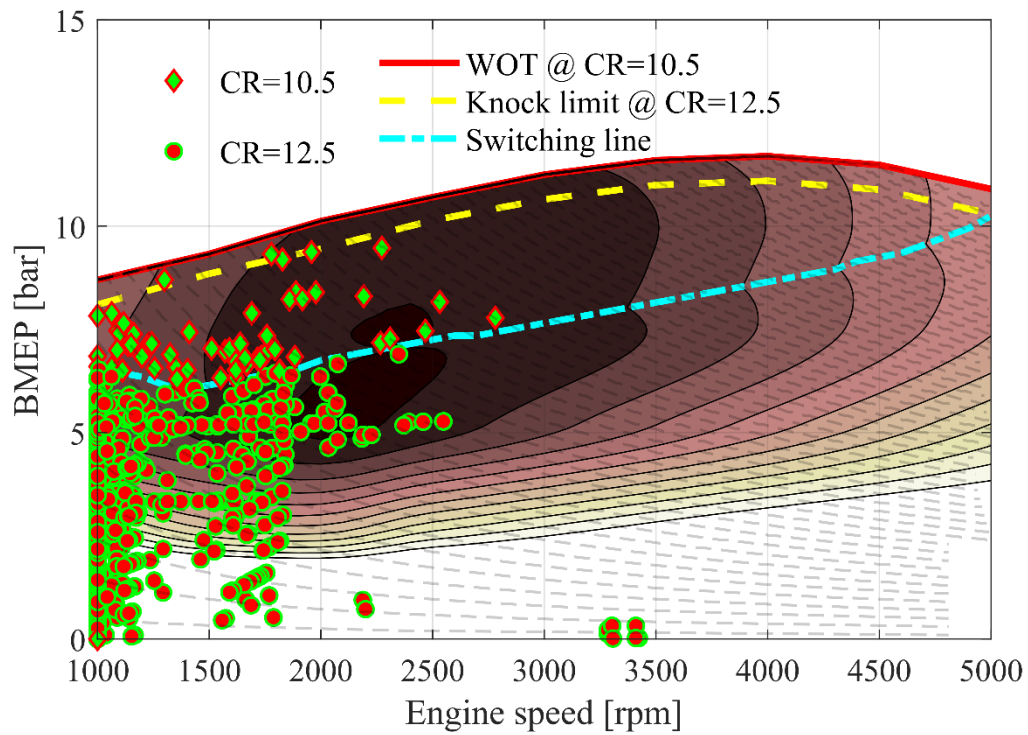


Figure 73 – Operating points of the engine over the performance map in the case of a 2-stage VCR, for a vehicle equipped with a CVT, driven along the FTP-75.

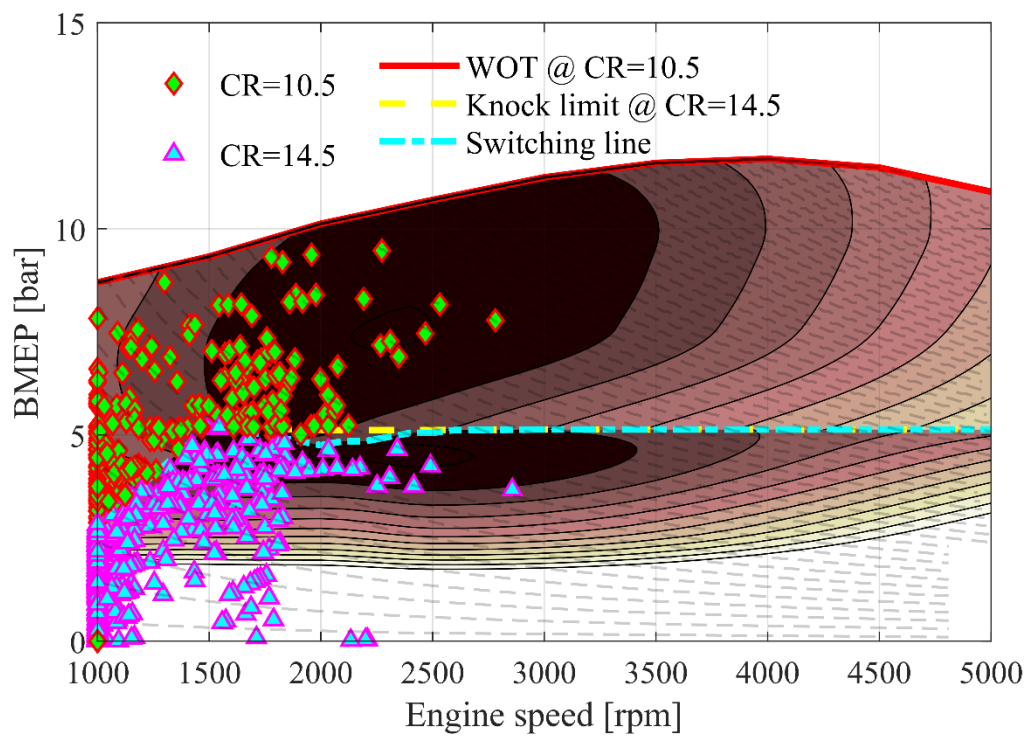


Figure 74 – Operating points of the engine over the performance map in the case of a 2-stage VCR, for a vehicle equipped with a CVT, driven along the FTP-75.

3-stage VCR

Considering the two possible 2-stage VCR systems obtainable (i.e. LCR-MCR and LCR-HCR), no significant changes can be noticed with respect to the 3-stage case. Looking at **Figure 73** and **Figure 74**, the same behavior analyzed before can be noticed. In both cases, most of the operating points are located at speeds lower than 2500 *rpm* and the higher compression ratio among the two available is more often exploited. However, also in these two cases, many of the operating points are located at low loads, affecting the reliability of the results. For the DT, no results for the US06 are presented, since, as showed in Chapter 7, the vehicle is not capable of following the drive cycle.

8.3 Fuel savings: 2-stage VCR vs. 3-stage VCR

Figure 75 and **Figure 76** show the comparison, in terms of fuel economy, between a 2-stage VCR, 3-stage VCR and different static CRs. Both plots are relative to a vehicle equipped with a CVT.

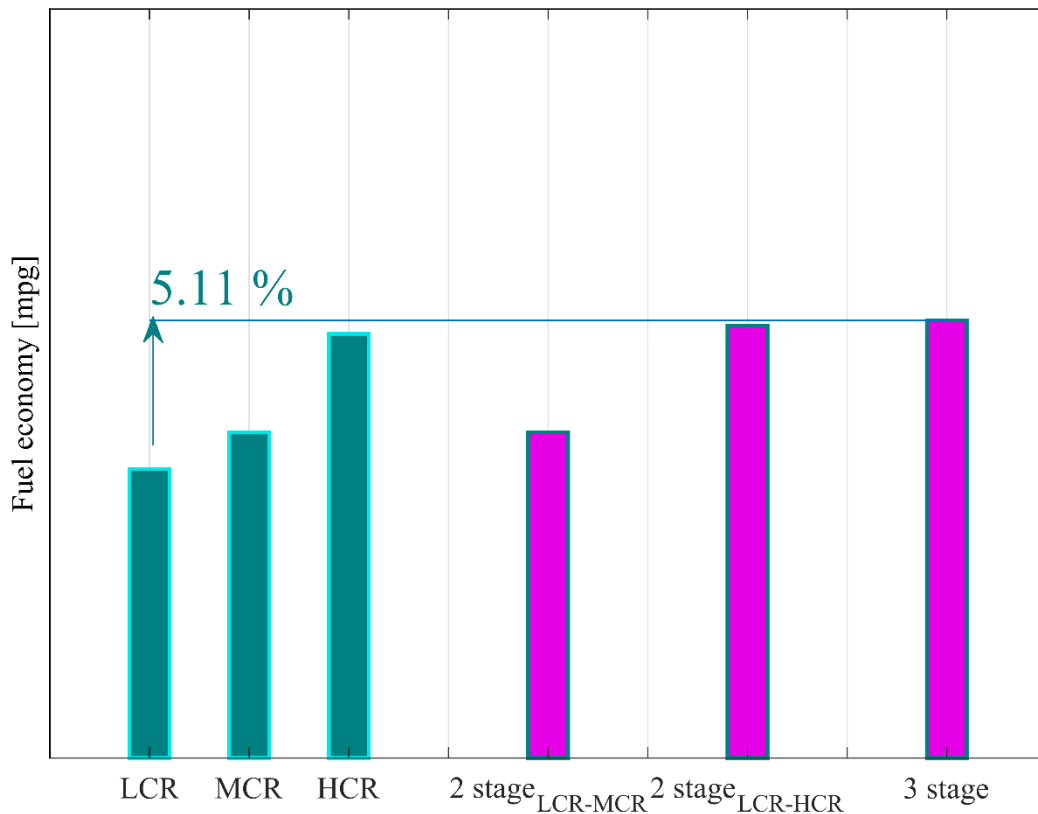


Figure 75 – Bar plot of the fuel economy for a vehicle equipped with a CVT for various VCR configurations (magenta), and three fixed CR cases (cyan) over the FTP-75

3-stage VCR

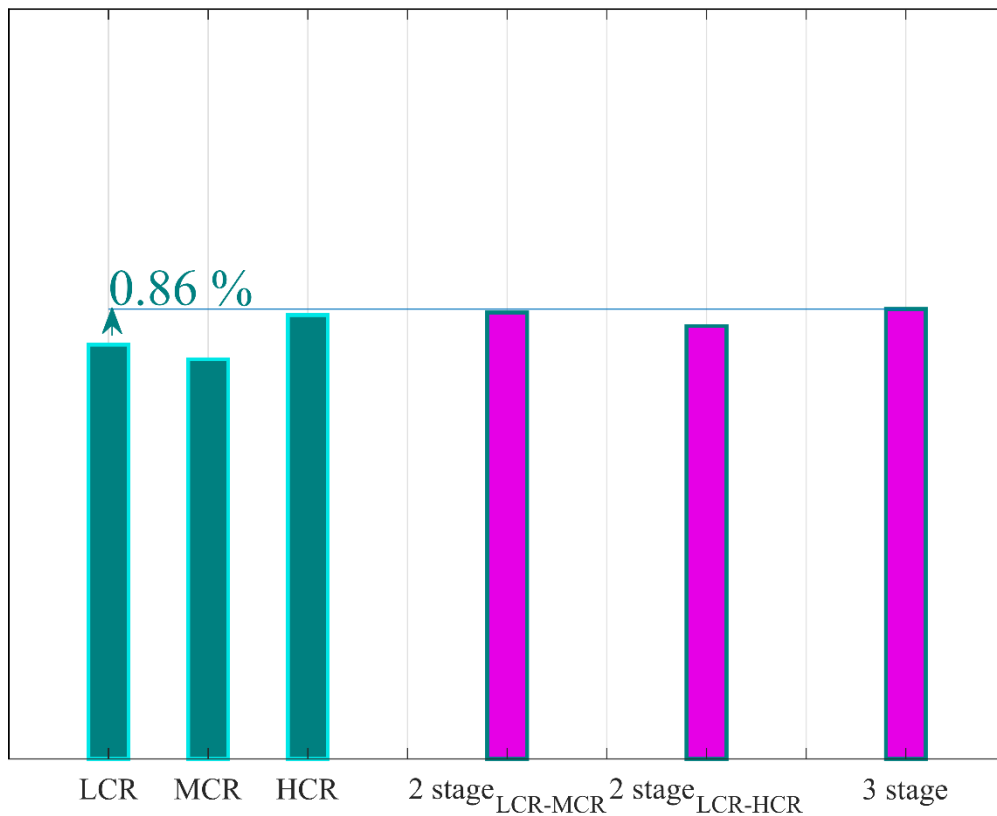


Figure 76 – Bar plot of the fuel economy for a vehicle equipped with a CVT for various VCR configurations (magenta), and three fixed CR cases (cyan) over the US06

Looking at **Figure 75**, which is for a run over the FTP-75, it is possible to notice that, not only does the adoption of a 2-stage VCR yield improvements in the vehicle fuel economy, but also that the larger the gap between the two employed CRs, the bigger the improvement. Indeed, looking at the bars relative to the two 2-stage VCR systems, the one exploiting the LCR and the HCR is capable of achieving a much higher fuel economy with respect to the other. Finally, as expected, the addition of a third compression ratio to a VCR system further improve its effectiveness. In particular, the improvement with respect to the 2 stage VCR exploiting the LCR and the HCR is very small, due to the fact that, being the FTP-75 a low power demand drive cycle, the HCR is almost always used in both cases, giving very similar results. Considering instead **Figure 76**, which is for a run over the US06, the same conclusions can be obtained. The only difference is that, since this cycle is characterized by very high accelerations and very high speeds, the HCR cannot be exploited because of knock insurgence, limiting the effectiveness of a VCR system. Considering instead a vehicle equipped with a DT, **Figure 77** show the results for a run over the FTP-75. The discrete transmission results show identical trends to the CVT case previously discussed.

3-stage VCR

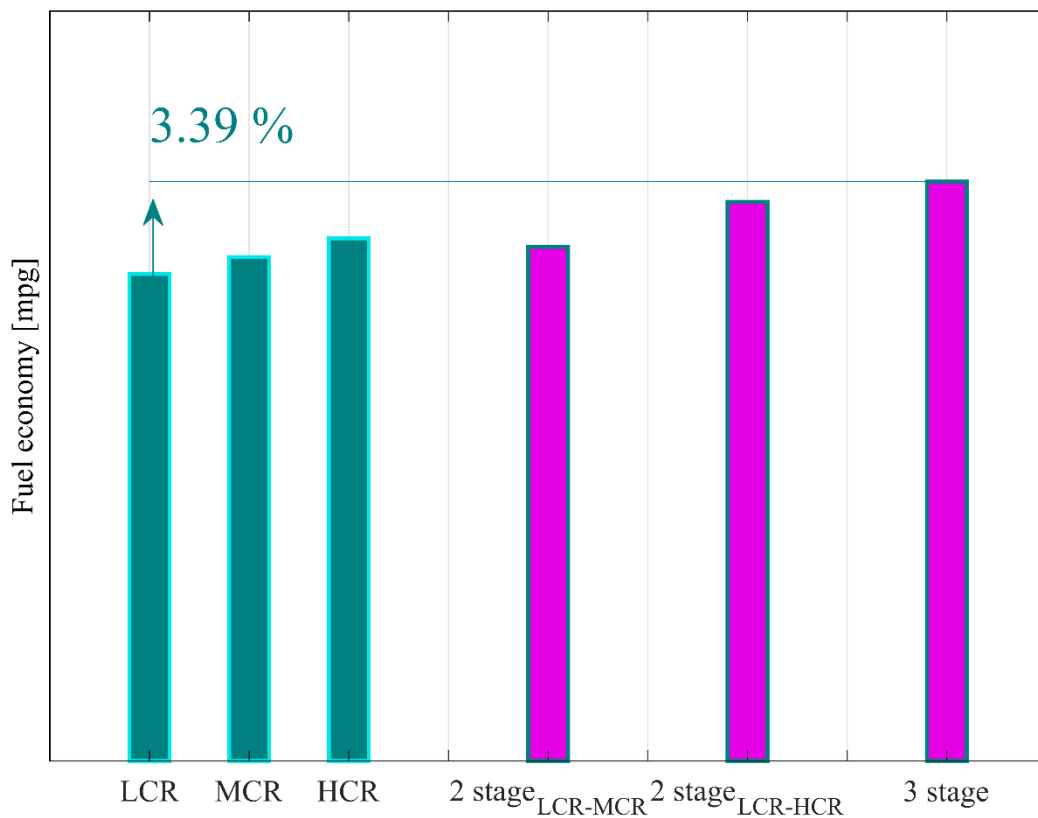


Figure 77 – Bar plot of the fuel economy for a vehicle equipped with a DT for various VCR configurations (magenta), and three fixed CR cases (cyan) over the FTP-75

These last figure shows a different behavior from the one that was highlighted during Chapter 7, the DT shows lower improvements with respect to the CVT. The reason behind this is that, in the case of the DT, the optimal CR is often not exploited because of irregularities in the maps. The mechanism is the same explained in Chapter 7 behind the strange peaks highlighted in In this case, the wrong choice of CR happens between MCR and HCR. In particular, when operating under the switch line between these two CRs, only the HCR can be exploited, however as highlighted earlier in this chapter, looking at **Figure 67** it is possible to identify a wide area in which the HCR is not the optimal one. In the case of the DT, because of the limited number of transmission ratios, several operating points end up in this area, causing this anomalous behavior.

Figure 78 represents the operating point on the differential BSFC map causing the just mentioned behavior.

3-stage VCR

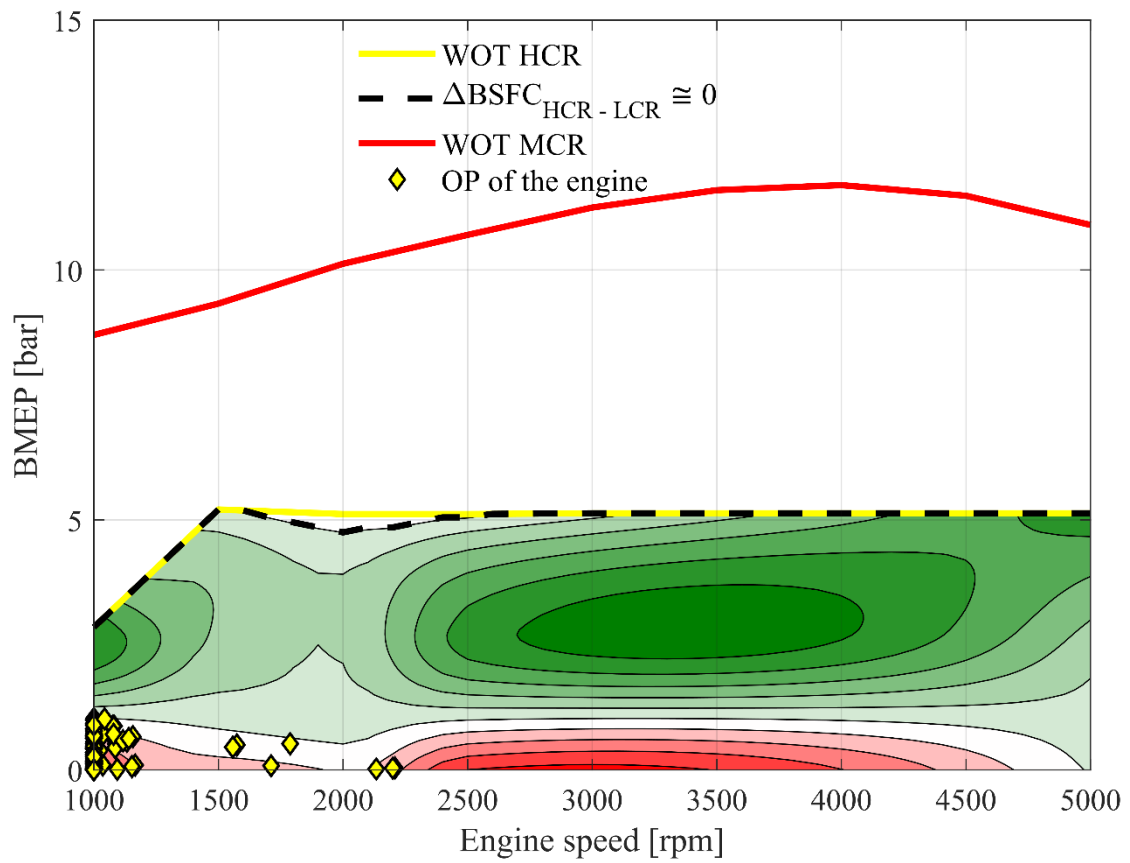


Figure 78 – Plot of the engine operating points causing a decreased efficiency for the VCR system applied to a vehicle equipped with a DT.

Conclusions

This study provides an insight into the basic working principle of a variable compression ratio engine, through the development of a simplified model for fuel consumption evaluation, and into the main parameters affecting the effectiveness of this type of systems.

Main result of this work is a model capable of evaluating the fuel consumptions for an engine provided with a VCR system. The inputs necessary to the model are simply engine performance maps, provided in tabular form, the characteristics of the selected vehicle and the speed profile of the drive cycle. The code user has only to select the desired type of transmission, Continuously Variable Transmission or Discrete Transmission, specify a switching time and a control delay. Indeed, the main target during the modelling phase was the development of a user friendly tool, usable by almost everyone and capable to be applied in different conditions, simply changing the input data.

Through runs of the model under different working conditions it was shown that longer switching times imply higher fuel consumption. Thus, the implementation of a VCR system give positive results only if the switch time is kept under a certain threshold, depending on the transmission type. Obviously, higher switching times also involve a higher number of incomplete switches, with a consequent increase of knock insurgence. It was shown that for a switch time lower than 20 – 25 engine cycles, depending on the type of transmission, no incomplete switches where present.

This two limit values were necessary to check the possibility of implementing a Load Depending Switch time. Data coming from a real VCR system were used to build a map capable of returning, for every engine operating condition, the corresponding switch time. Simulations showed not only that a LDS time is capable of staying under the two previously identified thresholds, but also that the mean switch time is very low, allowing to improve the effectiveness of the VCR system. It was shown that also doubling all the times coming from the LDS time map the conditions to avoid incomplete switches were met.

Then an approximated study about the transients was performed, showing that an increase of the 2% in the fuel injected was already sufficient to counterbalance all the advantages coming from the adoption of a VCR system.

Exerting the code on different drive cycles and with different vehicle parameters, VCR systems resulted to be better suited to light vehicle and to drive cycles characterized by mild accelerations and

Conclusions

low vehicle speed. These low power demand conditions allow the system to operate often with the high compression ratio, increasing the engine efficiency.

Finally, tests performed with new performance maps relative to different compression ratios showed that increasing the gap between the compression ratios used the effectiveness of the VCR system increases as well. Moreover, a 3-stage VCR was also modelled. Due to its higher flexibility coming from the addition of a third compression ratio, this system is capable to improve further the fuel economy of a vehicle.

In general, it was showed that results are highly affected by the available performance maps. For this study, the only map available were relative to compression ratios with a very small difference between them, reducing the advantages coming from the adoption of a VCR system.

Future developments

Due to the complexity of this systems the model is extremely simplified, hence in its future versions some refinement could be introduced:

- Relaxation of some of the assumptions made for the engine modelling, for example introducing a model for the evaluation of the transients present when the engine is changing its operating point.
- Relaxation of some of the assumptions made during the modelling of the transmission, for example introducing an efficiency map for the transmission, so that to considered the power losses in this component depending on the working conditions. Moreover a finite time and a fuel penalty due to gearshift should be implemented. Then, in the case of the CVT a limited number of transmission ratios should be considered.
- The gearshift logic for the Discrete Transmission should be redesigned to simulate the behavior of a real driver.

Moreover, in order to have reliable results, future tests should be performed with more complete experimental maps, obtained from bench tests covering most of the operating area of the engine. Furthermore, maps should be relative to compression ratios with a significant difference between them, so that to show significant improvements with respect to the baseline.

Not regarding the modelling of this type of system, it would be interesting to:

- Study the possibility to apply a VCR system in a hybrid architecture and to evaluate possible fuel savings.

Conclusions

- Study the influence of VCR system on pollutant emission. Since the compression factor is a determining factor in the pollutant production, it would be interesting to investigate the possibility to reduce pollutant emissions through a VCR system.
- Study the effectiveness of VCR systems for different engine cycles and fuels. As mentioned in this work, VCR systems could be used also on Diesel engines or on engine exploiting the Atkinson cycle.
- Produce a model also for a continuous VCR, hence a system capable of exploiting infinite compression ratios comprised between two boundaries.

Bibliography

- [1] Smith, P., Heywood, J., and Cheng, W., “Effects of Compression Ratio on Spark-Ignited Engine Efficiency”, SAE Technical Paper 2014-01-2599, 2014, doi:10.4271/2014-01-2599.
- [2] Ayala, F., Gerty, D., and Heywood, J., “Effects of Combustion Phasing, Relative Air-fuel Ratio, Compression Ratio, and Load on SI Engine Efficiency”, SAE Technical Paper 2006-01-0229, 2006, doi:10.4271/2006-01-0229.
- [3] Muranaka, S., Takagi, Y., and Ishida, T., “Factors Limiting the Improvement in Thermal Efficiency of S.I. Engine at Higher Compression Ratio,” SAE 870548, 1987, doi:10.4271/870548.
- [4] Wittek, K., Tiemann, C., and Pischinger, S., “Two-Stage Variable Compression Ratio with Eccentric Piston Pin and Exploitation of Crank Train Forces”, SAE Technical Paper 2009-01-1457, 2009, doi:10.4271/2009-01-1457.
- [5] Duleep, K., “Review to Determine the Benefits of Increasing Octane Number on Gasoline Engine Efficiency: Analysis and Recommendations - Tasks 2-5”, CRC Project No. CM-137-11-1b; 2012.
- [6] Jo, Y., Lewis, R., Bromberg, L., and Heywood, J., “Performance Maps of Turbocharged SI Engines with Gasoline-Ethanol Blends: Torque, Efficiency, Compression Ratio, Knock Limits, and Octane,” SAE Technical Paper 2014-01-1206, 2014, doi:10.4271/2014-01-1206.
- [7] Kapus, P. E.; Fuerhapter, A.; Fuchs, H.; and Fraidl, G. K., “Ethanol Direct Injection on Turbocharged SI Engines-Potential and Challenges”, SAE Technical Paper 2007-01-1408, 2007, doi:10.4271/2007-01-1408.
- [8] <http://www.iasn.net/fuel-specifications>, Worldwide fuel specification 2018.
- [9] Boretti, A., and Scalzo, J., “ Exploring the Advantages of Atkinson Effects in Variable Compression Ratio Turbo GDI Engines”, SAE Technical Paper 2011-01-0367, 2011, doi:10.4271/2011-01-0367.
- [10] Kleeberg, H., Tomazic, D., Dohmen, J., Wittek, K., and Balazs, A., “Increasing Efficiency in Gasoline Powertrains with a Two-Stage Variable Compression Ratio (VCR) System”, SAE Technical Paper 2013-01-0288, 2013, doi: 10.4271/2013-01-0288.
- [11] Saunders, R., and Abdul-Wahab, E., “Variable Valve Closure Timing for Load Control and the Otto Atkinson Cycle Engine,” SAE Technical Paper 890677, 1989, doi:10.4271/890677.
- [12] Gheorghiu, V., “CO₂-Emission Reduction by Means of Enhancing the Thermal Conversion Efficiency of Ice Cycles,” SAE Technical Paper 2010-01-1511, 2010, doi:10.4271/2010-01-1511.
- [13] “Light-Duty Automotive Technology, Carbon Dioxide Emissions, and Fuel Economy Trends: 1975 Through 2013”, Report No. EPA-420-R-13-011; U.S. Environmental Protection Agency: Washington, DC, 2013; <http://epa.gov/fueleconomy/fetrends/1975-2013/420r13011.pdf>.
- [14] Cassiani, M., Bittencourt, M., Galli, L., and Villalva, S.,” Variable Compression Ratio Engines”, SAE Technical Paper 2009-36-0245, 2009, doi:10.4271/2009-36-0245.
- [15] Moteki, K., Aoyama, S., Ushijima, K., Hiyoshi, R., Takemura, S., Fujimoto, H., and Arai, T., “A Study of a Variable Compression Ratio System with a Multi-Link Mechanism”, SAE Technical Paper 2003-01-0921, 2003, doi:10.4271/2003-01-0921.

- [16] Tomita, M., Aoyama, S., Ushijima, K., Tanaka, Y., Takahashi, N., Moteki, K., and Takaba, T., “Compact and Long-Stroke Multiple-Link VCR Engine Mechanism”, SAE Technical Paper 2007-01-3991, 2007, doi:10.4271/2007-01-3991.
- [17] Sluder, S., Smith, D., West, B., “An Engine and Modeling Study on Potential Fuel Efficiency Benefits of a High-Octane E25 Gasoline Blend”, Oak Ridge National Laboratories, Report No. ORNL/TM-2017/357, 2017.
- [18] <https://www.epa.gov/vehicles-and-engines>, Vehicles and Engines data, US EPA.
- [19] Barlow, T., Latham, S., McCrae, I., Boulter, P., “A reference book of driving cycles for use in the measurement of road vehicle emissions”, TRL limited, Report No. PPR354, 2009.
- [20] Huettner, T.F., Millward, P., Loesch, S., and Wolfgang, S., “The Dual Mode VCS Conrod System – Functional Development and Oil Investigations,” SAE Technical Paper 2018-01-0878, 2018, doi:10.4271/2018-01-0878.
- [21] Königstein, A., Grebe, U., Wu, K., Larrson, P., “Differentiated Analysis of Downsizing Concepts”, MTZ Worldwide Magazine 06|2008 Volume 69, 2008.